Ministry of Education and Science of Ukraine

Kharkiv Naional Automobile and Highway Universit
Ukrainian State University of Science and Technology
Educational and scientific institute
“Prydniprovska State Academy of Civil Engineernig and Architecture”

Hlushkova D. B.,
Volchuk V. M.

OPTIMIZATION OF THE STRUCTURE AND PROPERTIES OF MATERIALS FOR DOUBLE-BINDING MACHINES APPOINTMENT

Monograph

Dnipro
NNI PDABA
2024 year

UDC 669.017:519.21

G 12

Recommended for publication by the decision of the Academic Council
Educational and scientific institute
“Prydniprovska State Academy of Civil Engineernig and Architecture”
(protocol No. 3 dated October 24, 2024).

Reviewers: V.I. Bolshakov, Honored Worker of Science and Technology of Ukraine, Doctor of Technical Sciences, Professor of the Department of Materials Science and Materials Processing of the Dnipro State Academy of Construction and Architecture;

O.P. Haponova, doctor of technical sciences, professor, head of the department of applied materials science and construction materials technology of Sumy State University;

V.V. Subbotina, Doctor of Technical Sciences, Professor, Head of the Materials Science Department of the National Technical University "Kharkiv Polytechnic Institute".

Authors: D.B. Glushkova, doctor of technical sciences, professor, head of the department of metal technology and materials science named after O.M. Petrichenko;
V.M. Volchuk, Doctor of Technical Sciences, Professor, Head of the Department of Materials Science and Materials Processing of the Dnipro State Academy of Construction and Architecture

Hlushkova D.B.
G 12 Application of fractal theory for modeling structure and properties: monograph / D.B. Hlushkova, V.M. Volchuk – Dnipro: 2024. – 204 p.
ISBN

The monograph "Optimization of the structure and properties of materials for dual-purpose machines" is devoted to solving the scientific problem of assessing the properties of dual-purpose metal materials based on the analysis of the spectrum of fractal dimensions of their structural components and improving the efficiency of friction pairs of parts of a volumetric hydraulic drive by choosing the material for their manufacture and its modes heat treatment. The scientifically proven effectiveness of using the ion-plasma method for coating the working surfaces of dual-purpose parts. Special software has been created that allows you to estimate the spectrum of statistical dimensions of heterogeneous structures with a complex geometric configuration of their elements. The results of theoretical and experimental research are implemented in production.
The monograph is recommended for researchers, engineers, teachers of institutions of higher education, graduate students and students of institutions of higher education who specialize in the field of materials science and mechanical engineering.

CONTENT

LIST OF CONVENTIONAL ABBREVIATIONS

РВ	Working area
ЗРО	Workspace area
ОК	Area of compromise
ЕС	Expert system
БЗ	Knowledge base
БД	Database
ЛПР	Decision maker (expert)
$D_{0\ г}$	The fractal dimension of graphite
$D_{1\ г}$	Information dimension of graphite
$D_{2\ г}$	The correlation dimension of graphite
$D_{0\ к}$	Fractal dimension of carbides
$D_{1\ к}$	Information dimension of carbides
$D_{2\ к}$	Correlation dimension of carbides
D_{200}	Statistical dimension characterizing the most rarefied space of the object of observation (bright areas of structural elements)
D_{-200}	Statistical dimension characterizing the most concentrated space in the object of observation (dark areas of structural elements)
HSD	Shore hardness
HB	Brinell hardness
$\sigma_В$	Ultimate tensile strength (MPa)
$\sigma_{изг}$	Bending strength limit (MPa)
KC	Impact viscosity (kJ / m2)

ОУ	General level
ІВ	Інтервал варіювання
НУ	Нижній рівень
ВУ	Upper level
$K_{\sigma в}$	The coefficient of sensitivity of the tensile strength limit to dimensional characteristics
$K_{згин}$	The coefficient of sensitivity of the bending strength limit to dimensional characteristics
K_{KC}	The coefficient of sensitivity of impact viscosity to dimensional characteristics
K_{HSD}	Coefficient of sensitivity of hardness to dimensional characteristics

INTRODUCTION

The leading role of accelerating the scientific and technological progress of Ukraine is played by mechanical engineering. The pace of its development largely depends on the achievements of science and technology in the development of high-tech processes, improving the reliability of various types of machine parts. An important link in the work in this area is the further improvement of the technology for the manufacture of dual-use parts.

Analysis of the operating experience of these machines [1, 2] has shown that the main reason for their failure is the wear of the working surfaces of the counterbodies of precision friction units, and this entails an increase in the cost of maintenance and current repairs.

Modern volumetric hydraulic machines operate under conditions of high speeds, pressures and temperature changes. For example, in axial piston hydraulic machines, the speed of rotation of the output shaft reaches 10000 rpm and more, the pressure of the working fluid reaches 50 MPa, and its temperature varies from -50°C to +135°C.

In friction units (or tribocombinations) of technical systems, the wear of friction surfaces depends on the following factors: the nature of the friction surface, the material, its processing and structure, the nature of the friction surface, load modes, and wear intensity. In this regard, much attention is paid to the problem of increasing wear resistance and corrosion resistance of friction pairs surfaces.

The choice of friction pair materials that ensure an increase in their resource above the achieved level is an important task. Its decisions depend on the design and purpose of the unit, production technology, operating conditions, requirements for the properties of parts, their service life and reliability, taking into account the cost of materials and their scarcity, the cost of manufacturing parts from the selected material and operating costs.

In the arsenal of materials science, there is a high-tech method of changing the properties of surfaces – applying coatings that meet the requirements of operational properties and characteristics.

Therefore, the study of the regularities of changes in the structure and properties of the materials of the tribosystem in the process of its operation and the development of methods for increasing the durability of the parts of the volumetric hydraulic drive is an urgent task. But significant money and time are spent on the study of these properties and characteristics. Therefore, in order to reduce the material and time costs for conducting full-scale experiments, the paper describes the authors' studies that allow assessing the operational properties and characteristics of coatings of materials using the theory of fractals. This theory makes it possible to describe real structures of varying complexity using fractional dimensions to model structure and properties. By studying the sensitivity coefficients of the fractal dimension of the structural elements with the properties of the studied parts of the volumetric hydraulic drive, hydraulic hammer, models for assessing these properties were obtained.

The monograph also discusses the main stages of identification of the technology for the production of cast iron rolls in order to model their properties and structure. In the metallurgical industry, the quality of technological processes can be influenced, for example, by the quality of raw materials, blanks, controlled variables, quality of tools, processing modes, etc. The quality management system of the target product, which is organized at each technological operation, is at best operational and works in real time. Based on the above, the paper reveals the basics of the influence of the fractal dimension of the structure of cast iron rolls on their mechanical properties, This will allow you to control the properties of rolls in the process of their manufacture through the use of the obtained mathematical models.

CHAPTER 1
STATUS OF THE ISSUE AND OBJECTIVES OF THE STUDY

1.1. Working conditions of dual-use parts

During operation, positive displacement hydraulic drives provide a stepless wide range of speed control of hydraulic cylinders, the ability to implement flexible communication between the pump motor and the hydraulic motor through the use of high-pressure hoses, a minimum weight-to-power and torque ratio [1].

Examples of successful use of a positive displacement hydraulic drive are [1, 2]:

– lifting a nuclear submarine from the bottom of the Barents Sea using 26 hydraulic cylinders with a force of 9000 kN each;

– operation of the ship carrier chamber at the Krasnoyarsk Hydroelectric Power Station, which, with the help of a volumetric hydraulic drive, ensures the passage of vessels through a dam with a height of 124 m. Hydraulic drive consists of 156 hydraulic motors with a total capacity of 14400 kW;

– Modern harvesters are equipped with volumetric hydraulic drives based on axial piston hydraulic machines.

In Ukraine, volumetric hydraulic drives of the widest orientation are produced: for road construction machines, agricultural machinery, for machine tool building of forging and pressing production, aviation, ship hydraulic systems, mining and mine developments. A number of enterprises are engaged in the repair of hydraulic equipment due to the high cost of new ones.

The development of volumetric hydraulic drives in Ukraine is carried out by the design bureaus of plants [3–5] that produce serial hydraulic equipment specialized in their wide use (Dnipropress, Dnipropetrovsk, Novokramatorsk Machine-Building Plant), Kharkov Design Bureau for Mechanical Engineering named after A.A. Morozov (hydraulic drive for ground military equipment and the national economy), Promgidroprivod LLC (Kharkiv) – design of hydraulic drives for metallurgy and heavy engineering, etc.

Regardless of the purpose, reliability, operability, sensitivity and other important parameters of hydraulic drives depend not only on the choice of the schematic diagram, its design, but, as noted by most developers [6–9], on the material, method of surface treatment, and the degree of their geometric accuracy. When analyzing hydraulic drive units, it is advisable to note the categories of parts similar in purpose and many general technical requirements to structures (the shape of work surfaces). They are divided as follows:

– casing parts of pumps;

– open clutches and torque converters;

– hydraulic cylinder liners;

– body parts of spool distributors;

– plungers, spools, pistons;

– distributors and support rings of axial piston pumps;

– impellers of hydrodynamic gears.

To solve the problems of increasing the service life of parts of a volumetric hydraulic drive, scientists pay a lot of attention to the study of changes in the structure and surface properties of parts in the process of mutual friction (sliding).

As indicated in [9], the wear resistance of a metal is determined by a combination of structure and a number of properties:

Greater resistance, compression, tension, bending, shear, high hardness and ductility in the absence of brittleness; stability of mechanical properties at high temperatures and pressures under wear conditions.

High thermal and thermal conductivity; thermodynamic stability of phases in a wide range of temperatures and pressures.

Resistance to corrosion, high saturation and uniformity of distribution of alloying elements.

Such properties can be created with a favorable combination of viscous and hardening phases – a solid matrix solution and a dispersed variable phase.

The authors [3] emphasize the need for close orientation of the matrix crystals and the variable dispersed phase, which is the minimum value of the interfacial surface energy. It is known [4, 5] that small values of interfacial surface energy sharply increase the rate of dissolution and release of highly dispersed particles.

The creation of a whole complex of different physical, mechanical and other properties in one material (for example, high hardness combined with high ductility) is practically impossible in a one-component or multicomponent alloy, but it is real in a heterogeneous alloy [4]. In this, not only a favorable combination of the properties of the existing phases can be achieved, but also their improvement due to the interaction of different crystal lattices.

Phase transformations in the process of friction were studied using the method of continuous radiographic examination. The essence of the method lies in the fact that in the process of friction, a continuous X-ray examination of one of the elements of the pair is carried out at a point that is at a certain distance from the point of exit from the contact [5].

The method used is effective for studying the friction dynamics of any metal pairs, since the thickness of X-ray penetration is comparable to the thickness of the active surface layer. The method of continuous X-ray examination makes it possible to trace the kinetics of structural transformations that take place under given operating conditions.

In all experiments, the external conditions (sliding speed, media) were the same, and the load changed [7, 9]. In the surface layer, during friction, the content of austenite increased at low loads, and decreased at high loads. In the process of friction, a stable austenite content was established above or below the original content. Under these friction conditions, there is a critical specific pressure, which is the stable content of austenite Magnitude. This critical pressure corresponds to a load of 250 MPa. At the same time, the content of austenite in the surface layer remained practically constant during the long friction process.

The formation of the secondary structure during friction occurs under conditions of impulsive load, rapid temperature changes in the working microvolumes of the metal [10, 11], is also determined by the duration of being in contact and overheating of the surface – relative to the martensitic point Mn and the critical region Ac. The authors examined cemented steel 20X2NCHA, structurep martensite and austenitic-carbide mixture. In the future, depending on the temperature and rates of heating and cooling, various transformations occur in the process of friction. With slow heating, a range of transformations occurs that correspond to tempering processes. At a temperature of 200–300°C, austenite decays, martensite and austenite decay products are released. An increase in temperature leads to the development of tempering processes. When the temperature of Ac_1–Ac_3 is reached, austenization of the heated layer and dissolution of carbides in it begins. As the heating rate increases, the duration of austenite decay decreases.

The limiting values of the time and heating rate required to complete the decay of austenite of a given steel are determined by the decay curves of austenite.

In the process of friction, after leaving the contact, all samples are covered with an oxide film, at low loads the film is thin and easy to remove even with light etching. With an increase in friction pressure, the film thickens, its thickness increases, and the color becomes brownish-black. The resistance of austenite to oxidation is higher than that of its decay products. The authors found that heating the surface during friction causes its oxidation, after which the surface temperature decreases, but the metal is heated to a great depth. The accumulation of heat in the surface layer contributes to the decomposition of austenite.

Since ferrite, martensite, and carbides oxidize more easily than austenite, the surface is additionally oxidized and the entire cycle is repeated [5].

In [7] it is shown that at different sliding speeds, as the number of contact cycles increases, the amount of residual austenite decreases. Starting from a certain point, a stable austenite content is established for each friction mode.

The process of decomposition of austenite in a vacuum is more intense than with friction in air. At a load of 20 MPa under the same experimental conditions, complete decomposition of austenite in vacuum is observed at a sliding velocity of 0.6 m/s after 40 minutes of frictional operation, and at a sliding velocity of 0.9 m/s – at 13 minutes. At low sliding velocities, both in vacuum and in the atmosphere, there is a period when there is no decay of austenite. This period in the atmosphere is longer than in a vacuum, since the temperature of the surface layer does not immediately reach the value necessary for disintegration. Changing the load value from 20 to 30 MPa at low sliding speeds does not have a very noticeable effect on the course of the decay curves. When the sliding velocity increases above 0.45 m/s, the change in load greatly affects the growth of the decay curves, here the effect of the load in creating a high temperature of the friction surface is affected.

Studies carried out using the method of continuous X-ray make it possible to establish the interval of friction conditions, which is characterized by changes in the processes of hardening and hardening [5]. The hardening of metals and alloys is determined by the force of all bonds between atoms or the weakest bonds that limit the strength of crystalline bodies.

Much attention is paid to research related to the study of the relationship between physical and mechanical properties and the structure of materials with their tribotechnical characteristics. As a result of the study of the conducted studies, it became obvious that the processes of friction and wear cannot be described using the existing mechanisms of macrodeformation and fracture [9, 12–15].

In addition, these studies practically do not take into account the phenomena with the relaxation properties of tribosystem materials. The intensity of relaxation processes determines the ability of the material structure to increase or decrease the level of internal loads, which should significantly affect wear resistance [16–18].

The relaxation properties of materials in contact have also been studied in works [7, 18–21]. It has been experimentally established that the rate of pressure drop during the introduction of a rigid sphere into a viscoplastic medium is a step function

of the stress acting at a given point in time. The disadvantage of conducting studies is that they do not take into account the influence of sliding speed and temperature.

In the works [22, 23] it is shown that the wear resistance and antifriction of steel under conditions of ultimate friction depends on its ability to cyclic stress relaxation, which is closely related to dynamic microplasticity.

The authors of the papers [24, 25] note that the relaxation ability of the near-surface layers of the contacting materials determines such tribotechnical characteristics as the wearability and the ability of the load-bearing combinations. It is proposed to assess the relaxation ability by the X-ray method, which allows to assess the nature of the evolution of the dislocation structure is a dynamic process, the quantitative characteristic of the relaxation properties of the surface layers is internal friction.

Having no functional connection with traditional mechanical characteristics, internal friction is an independent physical and mechanical characteristic of the material [21, 22].

However, the relationship between the energy parameters of friction and the relaxation properties of materials has not been studied at all.

At present, it is expedient for us to solve the issue of choosing a material for the parts under study, as well as methods for improving their performance.

1.2. Materials for dual purpose parts

Parts of hydraulic drives are made mainly of high-alloyed and high-quality tool, cemented, nitrided, which are characterized by increased wear resistance, a small coefficient of linear expansion, minimal deformation during heat treatment and operation [19, **Ошибка! Источник ссылки не найден.**].

The material of spool pairs must retain its primary dimensions during operation. The high hardness of the working surfaces is necessary to prevent the impact of solid inclusions in the working fluid. The selection of material for

hydraulic drive parts should also take into account the influence of high working pressures, water, high specific and contact loads.

Institute carried out work on the selection of materials for several groups of parts according to the type and state of their load , as well as according to some other specific requirements. The properties and purpose of these steels in accordance with State Standards 5632-92 and 5949-85 are listed in the table. 1.1.

Of the given steels for highly loaded parts, the most high-strength steels (with a strength limit value of at least 1000 MPa) were selected for consideration [22]. For less loaded parts and parts with special properties , steels 30X13, 40X13, 36HXTЮ are proposed in [19

The corrosion resistance of all the above steels depends on the carbon content and the number of alloying elements. Chromium additives increase the corrosion resistance of steel most effectively. Chromium forms a stable protective film of oxides on the steel surface, which, despite its small amount, protects the metal from corrosion [23].

As the carbon content increases, the corrosion resistance of chromium steel decreases [23]. This is explained by the fact that corrosion resistance is determined - by the amount of chromium in the solid solution. Carbon forms carbides with chromium , impoverishes the solid solution, which leads to a decrease in the concentration of chromium in the solid solution.

The higher the carbon content in steel, the more chromium is needed to maintain corrosion resistance, and conversely, the lower the carbon concentration, the higher the corrosion resistance of steel at a constant chromium content [23].

Table 1.1

Properties and purpose of steels in accordance with GOSTs 5632-92 and 5949-85

Steel brand	Recommended modes of heat treatment of blanks for making samples	σin	σt	δ5.%	ψ, %	KSU J / cm 2 (kHz m/cm2)	Appointment	Note
		N/mm 2	kHz / mm 2					
		no less						
1	2	3	4	5	6	7	8	9
14X17H2	And an option Hardening from 975-1040°C, cooling in oil, quenching at 275-350°C, cooling in air Option II Hardening from 1000-1030°C, cooling in oil, quenching at 620-660°C, cooling in air	1080 (IO)	835 (85)	10	30	49 (5)	It is used as a corrosion-resistant high-strength steel with quite satisfactory technological properties in chemical, aviation, etc. industries; as heat-resistant steel (up to 400°C), as heat-resistant steel (up to 800°C) - for working blades, discs, shafts, bushings	It has the highest corrosion resistance after quenching with a low vacation. The term of work is long. The recommended application temperature is up to 400°C

Continuation of table 1.1

1	2	3	4	5	6	7	8	9
25X13H2	*	–	–	–	–	–	Corrosion-resistant steel for parts with increased plasticity, subjected to shock loads, as well as products exposed to weakly aggressive environments (atmospheric precipitation, aqueous solutions of salts of organic acids at room temperature, etc.)	The highest corrosion resistance is achieved after heat treatment (hardening with relaxation) and polishing; has good machinability by cutting
20X17H2	By agreement	–	–	–	–	–	Corrosion-resistant high-strength steel for heavy-duty parts working on abrasion and impact in mildly aggressive environments	Has high hardness (up to NKS 45)

Continuation of table 1.1

1	2	3	4	5	6	7	8	9
09X16N4B	Option I Heating from 1140-1160°C, holding for 5-5.5 hours, cooling in air, resting at 600-620°C, cooling in air Hardening at 1030-1050°C, cooling in air or in oil, quenching at 600-620°C, cooling in air (twice)	980 (1000)	835 (85)	8	45	59 (6)	It is used as a corrosion-resistant steel for high-strength stamped -welded structures and parts working in contact with aggressive environments	It has the greatest corrosion resistance after quenching with low tempering (up to 400°C)
	Option II 1. Heating from 1140-1160°C, holding for 5-5.5 hours, cooling in air, resting at 600-620°C, cooling in air	1180 (120)	930 (95)	8	40	59 (6)	As heat-resistant steel (up to 850°C) for superheater pipes and pipelines - ultra-high pressure installations, rolled sheet	Recommended temperature up to 650°C. The term of work is very long

Continuation of table 1.1

1	2	3	4	5	6	7	8	9
09X16N4B	2. Hardening at 1030-1050°C, cooling in air or in oil, quenching at 600-620°C, cooling in air 3. Hardening at 970-980°C, cooling in air or in oil, quenching at 300-370°C, cooling in air	1180 (120)	930 (95)	8	40	59 (6)	As heat-resistant steel (up to 850°C) for superheater pipes and pipelines - ultra-high pressure installations, rolled sheet	Recommended temperature up to 650°C. The term of work is very long
30X13H7C2	Quenching at 1040-1060°C, cooling in water, annealing at 860-880°C, cooling to 700°C for 2 hours and then with a furnace, annealing at 660-680°C – 30 min, cooling in air, hardening	1180 (120)	785 (80)	8	25	20 (2)	Heat-resistant steel (up to 950°C), used for valves of automobile engines	Stable in sulfur-containing environments

Continuation of table 1.1

1	2	3	4	5	6	7	8	9
	790-810°C, cooling in oil							
13X14NZV2FR	And an option Hardening from 1040-1060°C, cooling in air or in oil, quenching at 640-680°C, cooling in air	930 (95)	735 (75)	14	55	88 (9)	Heat-resistant steel (up to 750°C) for highly loaded parts - disks, shafts, tension bolts, vanes, etc. parts operating in conditions of high humidity	The recommended temperature of use is up to 550°C, the service life is long
	Option II Hardening from 1040-1060°C, cooling in air or in oil, quenching at 540-580°C, cooling in air	ISO (115)	885 (90)	12	50	69 (7)		
07X16H6	Hardening from 975-1000°C, cooling in water, in air or in oil, further cold treatment at – 70°C, holding for 2 hours or	1080 (110)	880 (90)	12	50	69 (7)	High-strength steel for products operating in atmospheric conditions, acetic acid and other saline	Increased strength is achieved by applying tempering at

Continuation of table 1.1

1	2	3	4	5	6	7	8	9
	at - 50, aging for 4 hours, aging at 350-400°C, aging for 1 hour, cooling in air						environments and for elastic elements. Does not have delta - ferrite	temperatures of 750°C and 850°C
95X18	Hardening from 1000-1050°C, cooling in oil, quenching at 200-300°C, cooling in air or in oil	Hardness - not less than 55 NES	Ball-bearing steel of high hardness is also used for parts subject to heavy wear	It is used after tempering with low relaxation				
30X13	Hardening at 950-1050°C, cooling in oil, quenching at 200-300°C, cooling in air or in oil	Hardness - not less than 48 ICS					Steel for cutting, measuring and surgical instruments, springs, etc. parts and products	It is used after tempering and low leave with ground and polished surface, has

Continuation of table 1.1

1	2	3	4	5	6	7	8	9
								increased hardness. The recommended application temperature is up to 400-450°C
40X13	Hardening from 1000-1050°C, cooling in oil, quenching at 200-300°C, cooling in air or in oil	Hardness - not less than 50 NKR					Steel for cutting, measuring and surgical instruments, springs, etc. parts and products	It is used after tempering and low tempering with a ground and polished surface, it has increased hardness. The recommended application temperature is up to 400-450°C

Continuation of table 1.1

1	2	3	4	5	6	7	8	9
13X11H2B2MP	Option I Hardening from 1000-1020°C, cooling in air or in oil, quenching at 600-710°C, cooling in air	880 (90)	735 (75)	15	55	88 (9)	Heat-resistant steel (up to 750°C) for loaded parts - compressor discs, vanes, etc.	Recommended for application temperature up to 600°C, long service life
	Option II Hardening from 1000-1020°C, cooling in oil or in air, quenching at 540-590°C, cooling in air	1080 (NO)	930 (95)	13	55	88 (9)		
11X11H2B2MF	And an option Normalizing from 1000-1020°C, hardening from 1000-1020°C, cooling in oil or in air, quenching at 540-	980 (Y0)	835 (85)	10	50	59 (6)	Heat-resistant steel (up to 750°C) for loaded parts - compressor discs, vanes, etc.	Recommended for application temperature up to 600°C, long service life

Continuation of table 1.1

1	2	3	4	5	6	7	8	9
11X11H2B2MF	590°C, cooling in air						Heat-resistant steel (up to 750°C) for loaded parts - compressor discs, vanes, etc.	Recommended for application temperature up to 600°C, long service life
	Option II Normalizing from 1000-1020°C, hardening from 1000-1020°C, cooling in oil or in air. Vacation at 640-680°C, cooling in air	835 (85)	735 (75)	12	55	69 (7)		
16X11H2B2MF	And an option Normalizing from 1000-1020°C, quenching from 1000-1020°C, cooling in oil, quenching at 660-710°C, cooling in air	By agreement					Heat-resistant steel (up to 750°C) for loaded parts - compressor discs, vanes, etc.	Recommended application temperature - up to 600°C; The term of work is long
16X11H2B2MF	Option II Normalizing from 1000-1020°C, hardening from 900-1020°C, cooling in oil, quenching at 550-590°C, cooling in air	By agreement						

Heat treatment of chromium-containing steels negatively affects corrosion resistance, especially for steels with a high chromium content. After improvement in steels, there is an intensive diffusion of carbon outside the grain boundaries and the formation of chromium carbides [**Ошибка! Источник ссылки не найден.**]. Due to the high diffusion rate of carbon and the low diffusion rate of chromium, its content outside the grain boundaries decreases, which leads to intergranular corrosion [26].

Intercrystalline corrosion is a special type of corrosion, when under the influence of an aggressive environment, the corrosion process proceeds only along grain boundaries . As a result of the connection between the grains, they weaken and cracks appear. Intercrystalline corrosion in the initial stage causes a decrease in plasticity and viscosity of the alloy, and then its destruction [25]. To eliminate unwanted intercrystalline corrosion, additional alloying is used while simultaneously reducing the carbon content in steel [26].In the table 1.2 shows the materials used for the manufacture of the main parts of hydraulic drives [**Ошибка! Источник ссылки не найден.**, 27, 28]. At a working pressure of up to 103 n/cm ^{2,} gray structural cast iron СЧ-20 [11] is used.

A number of enterprises use steel 45 for the manufacture of spool pairs, which after improvement is carbonitrated [**Ошибка! Источник ссылки не найден.**]. In terms of wear and corrosion resistance, it does not meet the demands of enterprises. We were faced with the task of choosing a steel brand that surpasses steel 45 in terms of the main indicators necessary for the successful operation of the parts under study, and to choose a coating that will increase wear resistance, corrosion resistance, and eliminate dimensional changes.

Considering that in the process of processing (the process of changing the geometry of the friction surfaces and the physical and chemical properties of the surface layers of the material in the initial period of friction, which usually manifests itself under constant external conditions in the reduction of friction force, temperature and intensity of wear) of the tribosystem , as well as in the process of its in further work, the formation of near-surface and surface layers occurs , it can be concluded that a change in the

relaxation ability of the tribosystem will also occur [30]. Knowing the laws of this change can be the basis for choosing compatible materials in the tribosystem.

Table 1. 2

Materials and modes of operation of sliding friction pairs of volumetric hydraulic machines

Type hydraulic machines	Couple friction	Counterbody materials	Characteristics of the couple friction			Ra , Mk m	Heat treatment/ HRC (HV)
			p	v	p×v		
1	2	3	4	5	6	7	8
HP -1250/200	Piston - sleeve	Steel 20X – Br. AZH9-4	15 0	2	300	0.32	Chm / 59-62
NAR - 63/200	Saddle pad - inclined disc	Br. AZH9-4 Steel X12F1	17	7	119	0.32	O.Z/ 59-62
	Cylinder block - distribution disc	Bro . OSH10-2-3 Steel X12F1	29	10	290	0.16	O.Z.
	Bloc cylinders	Br. AZH9-4 Steel 18 KhHT	30 0	0.3	102	0.32	Chm
RMNA-250/320	Saddle pad - inclined disc	BrAZHN 10-4-4 Steel 38X2MUA	19	12	220	0.32/0.1 6	Abstract HV900
	Rotor - distribution . Disc	Steel 38X2MUA Bro OSN 10-2-3	7	17, 5	122.5	0.32/0.1 6	Abstract HV900
	Plunger Rotor	Steel 382MUA BrAZHMts11-6.5-1	31 0	2.1	651	0.32/0.6 3	Abstract HV900
UNA- 125/320	A plunger is a plunger	BrAZHN10-4-4 Steel 18 KhHT	48 5	0.5	242.5	0.32/0.2 5	Chm / 53-57
UNA- 450/200	Plunger - Rotor	Steel 18KHGT BrAZHN10-4-4	33 0	2.5	825	0.25/0.1 6	Chm /57-6 3
	The heel is inclined disc	BrAZHN10-4-4 Steel 382MUA	15	12	180	0.32	HV900

End of table 1.2

1	2	3	4	5	6	7	8
MRF -400/25M1	Piston - Connecting rod	Cast iron A4B- 1 Steel 18 KhHT	45 0	0.0 5	22.5	0.32	Chm / 56-62
	Piston - Sleeve	Cast iron A4B-1 Steel 18 KhHT	20 0	0.4 5	90	0.63/0.1 6	Chm / 56-62
AT 74-90 /320	Saddle pad - Inclined disc	BrAZH9-4 Steel X12F1	15	11	165	0.32	O.Z/ 59-62
ON 74- 224/90	Saddle pad - Inclined disc	BrAOSN 10-2-3 Steel X12F1	15	15	225	0.32	O.Z/ 59-62
ON 32/320	Saddle pad - Inclined disc	BrAZH9-4 Steel SHX15	15	9	135	0.32	O.Z/ 59-62
G15-25R	Rotor - distribution. disc	BrOF 10-1 Steel 20X	7	9	56	0.16	Chm / 58-63
	Drum - Tractor	Cast iron SC 32-52 Steel 18 KhVH	12 5	1.5	187.5	0.63/0.1 6	O.Z/ 59-63
	Tractor – Bearing ring .	Steel 18KHVG Steel SHX15	3400 0	0.0 2	680	0.63	O.Z/ 59-63
NRF = 25/50 0	Piston - sleeve	Steel 40X Cast iron SC32-52	12 7	1,2	152.4	0.32	O.Z/ 45-48
H- 400U	Piston - Sleeve	Steel 40X Cast iron SC32-52	11 6	1	116	0.32	O.Z/ 45-48
G12-2	Plate - Stator	Steel R6M5 Steel SHX15	7000	6	42000	0.2	O.Z/ 60-64
G12-3	Plate - Stator	Steel R6M5 Metal-ceramic a Zh420X3	7000	3	21000	0.1	O.Z/ 60-64

1.3. Methods for increasing the wear and corrosion resistance of parts

In practice, enterprises engaged in the manufacture and repair of positive displacement hydraulic drive parts use chemical-thermal treatment, diffusion saturation and surface alloying [33–38] to improve their performance.

Chemical and thermal treatment is carried out in order to increase fatigue strength, hardness, corrosion resistance, wear resistance. One of the most widely used methods of chemical and thermal treatment is carburization. Steels with a carbon content of no more than 0.2% are subject to carburization. When using a solid carburetor (saturated medium), heating is carried out in furnaces, when using a gas carburetor - in shaft sealed furnaces.

The process time is determined by the composition of the steel, the required layer depth (0.15–2.5 mm), and the method of carburization. The growth rate of the cemented layer is 0.1 mm/h at a layer depth of 1.0 mm and 0.15 mm/h at a shallower depth [33].

The final operation is always tempering at 160–180°C for 2–3 hours, which relieves stress and increases the viscosity of the material. The properties and areas of use of cemented steels are shown in Table. 1.3 [33].

Table 1.3

Areas of use of cemented parts

Steel grade	HRC	Use
20X	58 – 62	Plungers, pins, throttles
18HGT	58 – 62	Sleeves, bushing, gears
12KHNZA	57 – 61	
18HNVA	57 – 61	Connecting rods, gears, spools, valves
H17N2	60 – 64	

The hardness of the core is HRC28-42.

The hardness of the cemented layer decreases at temperatures above 250°C. Practice shows that nitriding is more effective than carburization. Nitriding is carried out after mechanical and heat treatment in an atmosphere of dissociation of ammonia NH3 when heated to 500–700°C in sealed shaft furnaces (Table 1.4) [33]. The nitriding hardness of the layer is 1.5–2 times higher than the hardness of the cemented layer. The nitriding layer has great corrosion resistance. Warping of parts in the nitriding process is almost Missing.

There are known literature data on the combination of several processes of chemical-thermal treatment. The paper [33] describes the sequential carburization and nitriding of chromium steels in order to increase fatigue strength. The paper [39] describes a new method of chemical and thermal treatment of steels, which leads to the formation of chromium nitrides and carbonitrides in the surface layer.

Table 1.4

Areas of application of some nitriding steels

Steel grade	Nitriding mode			Nitriding result		Applied
	T, °C	duration, hours	Degree of dis.	hardness HV	layer depth, mm	
40KhNMA	500	50	15-30	550	0,45-0,50	sleeves, bushings, spools, valves, seats
2X13	580	20	25-35	800	0,25-0,27	
End of Table 1.4						
38HMUA	510	35-55	20-40	950	0,30-0,35 0,50-0,55	connecting rods, pistons, shafts, spherical parts

The process is carried out in 2 stages: at the 1st stage, nitriding or carbonitration of the surface layer is carried out, then chromium plating in powders, including chromium, ammonium chloride salts. Chromium plating is carried out at low temperatures (700°C). The resulting layer has good adhesion and high density, but low wear resistance.

The paper [33] describes a method consisting of nitrocarburization and laser boring. The depth of the layer doubles compared to laser boring with high microhardness.

In works [27, 40, 41] describes the processes of diffusion-surface alloying of carbon steels, including vacuum-diffusion chromium saturation, heat treatment with heating to Ac_3 + (30–50 ° C) and cooling. In order to increase the operational stability of products, heat treatment is carried out repeatedly, heated at a rate of 80–120°C/min, hold for 1.5–2 minutes per 1 mm, cool in water to 200–400°C.

All methods of chemical and thermal treatment are labor-intensive, differ in the duration of the processes, and the results do not always justify the costs.

An analysis of the experience of a number of machine-building enterprises shows the effectiveness of the use of ion-plasma technology [35, 42].

By setting the properties of coatings by changing their chemical structure and composition, it is possible to directly influence wear resistance, corrosion resistance, the formation of stable characteristics of the coating, which contributes to increasing the durability of machine parts and mechanisms.

1.4. Conclusions and objectives of the study

From the review it follows:

– the main reasons for the failure of parts of volumetric hydraulic drives are wear and corrosion, and these processes develop in the coupling units,

– A review of theoretical and experimental studies has shown that in the field of compatibility of friction pairs of the parts under consideration, a large role is given to the material.

It is shown that during the working out period the main property is scuff resistance, and after running-in – wear resistance. In this regard, it is important to disclose the mechanism of these processes and develop the compatibility of materials at different stages of work.

– it is shown that the impact on the surface of the coupling (sliding) of parts by chemical-thermal treatment, diffusion metallization, complex methods of surface treatment can be solved only by particular problems.

– the study of the experience of using ion-plasma technology allows us to assume the feasibility of its use to increase the service life of hydraulic drives.

To solve the problem, research was carried out in the following areas:

– choice of material for the manufacture of spools;

– selection of plasma coating composition and optimal modes of its application;

– study of the effect of plasma coating on wear resistance, corrosion resistance of the selected steel;

– development of special-purpose coatings, optimization of its composition;

– bench and industrial tests.

SECTION 2. RETROSPECTIVE ANALYSIS RESULTS OF FUNCTIONING PERIODIC TECHNOLOGIES

2.1. Identification of technological processes

According to the nature of the course, **technological processes** are divided into continuous, periodic and discrete [43].

Continuous technological processes are those , processes in which the final products are produced as long as raw materials, energy, catalysts that control the effects are supplied. Such processes include, for example, oil refining processes.

Periodic processes are those in which a certain, limited amount is produced in a relatively short period of time (hours or days). final product. In this, for the allotted period of time, the periodic process is continuous. An example of a batch process would be the technological process of smelting metal in a blast furnace, the production of massive metal castings, etc.

Discrete processes are those in which the final product is produced in a certain period of time, and this process can be stopped, as well as continued from any technological operation without reducing the specified one level of quality. At the same time, we can give such examples as the process of assembling products on a conveyor (machines, household appliances), testing finished products on special stands, candy production technologies, etc.

Most technological processes require their breakdown into interdependent subsystems. The need to control technological processes is dictated by the following factors :

- Maintaining the composition and number of input components at a given level to ensure the required quality of the finished product;

- continuous change (adjustment) of the parameters of the technological process, which is associated with constant wear of tools and variable composition of raw materials;

- starting and stopping some components of the technological process that require the performance of specific precisely synchronized operations, etc.

The methodological _ for the management of periodic technological processes is a systematic approach, which provides a comprehensive solution to the problems of managing the components of its technologies. Such management, as a rule, is ensured by the use of a systematic approach, where the periodic technological process itself from its beginning to The ending is treated as a whole.

The need to apply a systematic approach in the management of periodic technological processes is determined by the complexity of their identification. Such technological processes include a relatively large number of input and output variables, some of which can change randomly or unpredictably. For example, the quality of the charge during the production of coke varies by a relative Coal from horizon to horizon also changes its quality in a wide range, the width of which is determined both by the place of coal extraction and by the method of its extraction.

Thus, nonlinear relationships between the input parameters and the insufficiency of a priori information about the regularities of the processes create significant difficulties in obtaining models adequate for predicting the course of these processesIt should be noted that the implementation of periodic multi-parameter technological processes should meet several often contradictory requirements for their quality criteria (for example, hardness-

plasticity, etc.), which are determined by both the quality of the target product and the technology of its production.

The quality management system of the target product, organized for each technological operation, in this case is operational and in real time.

In our opinion, in order to confirm the paradigm presented in the book, it is enough to give an example of its application. In this regard, the authors provide an example of identification of a specific technological batch process – technology for the production of cast iron section rolls. It should be noted that most of the periodic technological processes are multi-criteria [43, 44], and in this regard, there is a need for a permanent choice of the criterion, since "it is impossible to run all trams at the same time."

The above initiates the scheme of possible identification of periodic multiparameter technologies, presented in Fig. 1.1.

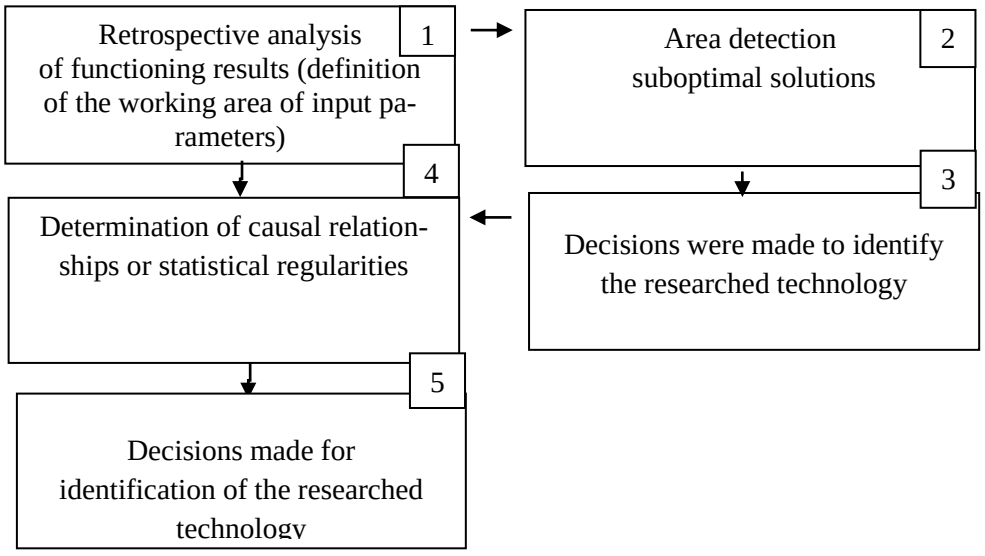

Fig. 1.1. Scheme of possible identification of periodic multiparameter technologies

2.2. Prerequisites, goals and objectives of research

Ferrous metallurgy today is an important branch of the national economy of many countries of the world with ore deposits. Competition in many industries initiates the production of high-quality products with specified properties and competitive price indicators. At the same time, the main share of rolled metal is made from cast iron, a significant part of which is accounted for by multi-tonnage castings, in particular rolling rolls. In order to withstand competition in the world market of finished metal products, metallurgical enterprises are switching to the production of rolls from economically alloyed cast iron grades, which leads to a significant economic effect on an industrial scale. In connection with the expansion of the range of metal products, the modern customer is interested, first of all, in the quality of the rolling rolls themselves, including their physical and mechanical properties. Assessment of these characteristics directly at the facility leads to large material and time costs within the limits of their mass production and is not always technically implemented, as it can lead to a violation of the integrity of the roll. Therefore, non-destructive testing methods and mathematical modeling methods have recently been widely used to assess the quality characteristics of rolls.

Despite the fact that over the past decades, many methods and models have been introduced in production to assess the quality characteristics of multi-tonnage metal castings (see, e.g., multi-tonnage metal castings). [43]), their development is relevant. The study of the above works shows that today such methods give a satisfactory forecast of properties, which partially diverges from the requirements of the customer. Thus, this problem is one of the main ones in modern materials science, which is associated with a number of objective and subjective reasons considered in the literature review.

The paper shows that it is impossible to implement the most obvious, deterministic approach used to assess the quality characteristics of long rolled cast iron rolls, in particular their mechanical properties, based on the analysis of cause-and-effect relationships and relationships. This is due to the fact that it is impossible to implement the most obvious, deterministic approach used to assess the mechanical properties of rolls, based on the analysis of cause-and-effect relationships and relationships, since it is impossible to implement the most obvious, deterministic approach used to assess the mechanical properties of rolls, since The technology for the production of rolling rolls is end-to-end, which characterizes a complex multi-parameter process. Therefore, the quality of cast iron is largely influenced by a large number of technology parameters (chemical composition, alloying elements and modifiers, cooling conditions, thickness of the casting mold spread, casting method, etc.), which determine the formation of the structure and are interrelated [45]. Even a slight change in the parameters of the technology can lead to(a) To the extent permitted by the provisions of this Convention, the Secretary-General shall ensure that the Secretary-General of the Council of Europe and the Member States of the Member States of the Republic of Moldova and the Member States of the Republic However, the current regulatory and technical industry documentation regulates only the level of hardness of rolling rolls, the requirements for strength, viscous properties and wear resistance are not specified. There are sampling methods to determine only the hardness that the standard assumes and is provided by the cast sample and the sample from the end of the barrel, as they differ in crystallization conditions. Given that the technology for the production of rolling rolls is a multi-parameter process [48], this also seriously complicates its identification. Therefore, an important aspect is

to ensure stable quality indicators of roll iron, especially its wear resistance, without additional tests and with minimal material and time costs.

It is likely that one of the possible solutions to this problem would be to obtain the necessary information by conducting full-scale tests on a finished multi-tonnage object. However, this task is not always feasible, since its implementation requires large material and time costs, which often exceed the permissible limits. Application of methods of non-destructive quality control of massive metal castings (magnetic, ultrasonic, thermal, optical, radiation, etc.) for These technologies are ineffective, as they are usually based on methods, for the most part, aimed at reliable detection of dangerous defects, which, as a rule, are evaluated by experts in industrial settings based on their experience. These assessments are poorly amenable to deterministic analysis and formalization. As a rule, they are not based on a regularFor the most part, they are justified by normative documents, experience and statistics (see, for example, [47]). The use of classical methods of metallography in assessing the structure of cast iron, by which it would be possible to judge its mechanical properties, for example, determining the content of graphite or carbides in it, does not always allow their quantitative assessment with a degree of accuracy that can be sufficient to solve practical problems.

Prompt obtaining of the necessary information about the quality characteristics of cast iron rolls, obtained in the process of their manufacture and operation, is also complicated by the fact that the target product, which is a multi-tonnage product, obtained as a result of its casting in the temperature range T 1310 1350 0 ≈C ÷, ^{occurs} only at the end of the main cycle of the technological process. Thus, only after casting the main product and its cooling, the completion of the main cycle of the technological process can occur, and this happens with a period of several hours to

several days, depending on the size of the roll [48]. In this regard, obtaining the necessary information is possible only after this period. All control influences that can make some adjustments to the technological process can be made only after the end of the main cycle, therefore, they can be taken into account by the user only in the next cycle, ie. when casting the next product. However, at the same time, there is no guarantee that the required reserve of materials required for casting the next product will remain the same, and it will be possible to adequately adjust the quality characteristics of cast iron and steel rolling rolls.

The listed shortcomings substantiate the basic requirements for the search and development of new scientific approaches aimed at assessing the qualitative characteristics of rolling rolls.

Analysis of the fundamental works of domestic and foreign scientists over the past 70 years, who initiated and developed in their works the theoretical and practical scientific foundations for the formation of the structure and obtaining high-quality castings from cast iron: M.G. Oknov, I.M. Bogachev, A.E. Krivosheev, K.P. Bunin, Y.M. Taran-Zhovnir, T.S. Skoblo, L.S. Rudnytsky, N.A. Budagyants, A. Inoue, T. Hashimoto and others. (see, for example, [47-63]), showed that one of the solutions aimed at solving the problem of operational, necessary for practical purposes, assessment of the qualitative characteristics of massive iron castings, in particular rolling rolls, with minimal costs, is a method based on the creation of mathematical models for predicting these characteristics depending on the chemical composition of the casting, structural parameters.

In order to obtain acceptable results, the developed methodology should include the use of both classical and modern methods for assessing the structure and properties of the manufactured product. Thus, in order to establish the relationship between the mechanical properties and structural

elements of roll cast iron, it is planned to use the theory of multifractals [64]. Proposed methodology is the most acceptable for the quantitative assessment of most real structures, the approximation of which by whole Euclidean figures introduces a certain error, and therefore is not always acceptable in the practical problems of modern materials science. According to the proposed methodology, each inhomogeneous object, which is the structures of most metals, can be characterized by a spectrum of statistical Rainyi dimensions [65]. Thespectrum of dimensions of multifractals is interpreted as some physical regularities that have separate statistical properties that make their material representation possible. For example, in the works of B. Mandelbrot, F. Ens, S.V. Svechnikov, V.S. Ivanova, V.I. Bolshakov, Y.I. Dubrov, B.M. Smirnov, I.Zh. Bunin, A.G. Kolmakov, G.V. Vstovsky, V.F. Terentyev e. In this regard, it is planned to conduct special experiments, the analysis of which allows to develop a qualitative and quantitative assessment of the following mechanical properties of cast iron: tensile strength; bending strength limits; impact strength and hardness. As a result of the analysis of the work of the technology for the production of rolls and research work aimed at solving the problem of assessing mechanical properties, the formulation of the task of operational forecast of these properties and The main ways of its solution are defined.

Taking into account the above, improving the quality characteristics of rolled cast iron rolls is an urgent and important scientific and practical problem that can be solved by applying a systematic approach based on the development and implementation of mathematical models for assessing quality criteria depending on the chemical composition and structure parameters. This approach allows not only to predict and adjust the quality indicators of rolls in the production process, but also to achieve their im-

provement by optimizing the composition, which will lead to an increase in their operational characteristics.

Section rolls of the SPHN design, containing 2.8...3.5% carbon by weight, alloyed with chromium (0.5...0.8%), nickel (0.9...1.3%), copper (0.2 ... 0,3%); rolls containing 2.9...3.25% carbon, alloyed with chromium (0.5...0.8%), nickel (0.9...1.3%) and modified with magnesium (0.038...0.054%). Modifiers were used in the manufacture of rolls (Foundrisil , Elmag-600, Elmag-900, Vl 57 (M), Barinoc, Elgraf).

The microstructure and mechanical properties of industrial roll irons made by SPHN and SSHN were investigated by standard methods of optical microscopy and mechanical tests on standardized equipment. Specimens for mechanical testing and metallographic studies were cut in the tangential direction from the surface layer of the castings to the cast iron rolls.

2.3. Requirements for quality indicators of the target product

Rolls are the main working tool in rolling production, with the help of which metal deformation is carried out - crimping and drawing ingots and billets [94-123]. These rolls provide an increase in the productivity of rolling mills, an improvement in the quality of rolled products, a decrease in metal losses due to defects, and a decrease in roll metal consumption.

Rolling rolls are different in design, differ from each other in shape, size, depending on the type of product to be obtained. Accordingly, different types of steel and cast iron rolls have different physical and mechanical properties. In the rolls of sheet mills, the barrel is smooth, in the case of high-quality mills, there are streams corresponding to the profile of the processed metal on the surface, which affect the heterogeneity of the distribution of mechanical properties in the working layer.

In turn, the quality criteria of rolls, in particular mechanical and service properties, largely depend on their chemical composition, taking into account alloying and modifying elements, crystallization rate and heat treatment modes [94, 107, 122]. These factors determine the type and nature of the structure roll material (steel – pre-eutectoidal, eutectoid, trans-eutectoid or cast iron – white, gray or intermediate). The structure is the main characteristic of the quality of rolls, since it determines their mechanical (strength and ductility), physical (melting point, viscosity, density, permittivity, heat capacity, thermal conductivity, electrical conductivity, etc., and service properties, thermal and wear resistance, etc. [118].

Based on the different operating conditions of rolled steel and cast iron rolls, their purpose is determined by a set of physical and mechanical properties used for the manufacture of rolls, their chemical composition, technological modes and subsequent processing methods. The qualitative characteristics of the rolls have a significant impact on the following technical and economic indicators of the mills' operation: the utilization rate of the mills and all auxiliary equipment, the duration of continuous operation of the mills between transshipments, metal losses in the form of defects at the settings after transshipment of rolls, product quality and relative consumption of roll material [100-120].

The service life of the rolls is determined by the compliance of the wear resistance and strength of the roll, the profile of the rolled products and the type of mill, the temperature factors of heating and cooling of the rolls during operation, the smoothness of the metal grip by the rolls and the exclusion of slipping, the rhythm of the rolling process.

A number of publications devoted to the issue of increasing the strength and increasing the service life of rolls, for example, T.S. Skoblo

and others. [51] show that research is currently being conducted in the following main areas:

–creation of new and modernization of existing technological processes;

–optimization of the chemical composition of materials and development of new ones;

–search for effective methods of heat treatment that increase the complex of physical and mechanical properties of rolls;

–improvement of operating conditions;

–restoration of the working surface of metal barrels of rolling rolls;

–development and research of reliable quality control methods and basic evaluation criteria.

Improving the quality of roll metal properties is achieved through the use of the following technological operations: out-of-furnace refining, treatment with desulphurizing additives, slags, vacuum disagation, blowing with inert gases. The use of these types of processing affects the structure, which is reflected in the change in the ratio of its components, the number, shape and distribution of non-metallic inclusions, the shape of graphite. For example, out-of-furnace refining is particularly effective for metal subject to plastic deformation.

Relatively new and proven developments in the field of rolling roll manufacturing technology include: centrifugal casting method; various methods of manufacturing multilayer rolls that provide the required set of properties; methods of doping and modification. The structure of the rolls of the centrifugal casting is characterized by smaller inclusions of the carbide phase, which are evenly distributed in the matrix. For roll steel, the use of this method allows to increase the density from 7.68 to 7.86 g/cm^3

and the tensile strength from 480 to 637 MPa. Alloying and modifying elements (chromium, nickel, molybdenum, magnesium, etc.) have a significant impact on the complex of physical and mechanical properties of roll iron and steel, the presence of which, however, does not guarantee the production of rolls with the required macro- and microstructure. The most important characteristics of rolling rolls are the following properties: hardness, wear resistance, toughness, strength, coefficient of friction, thermal and wear resistance of roll material.

Based on the above, the following requirements are imposed on rolled steel and cast iron rolls:

1). High hardness and strength of the working layer of roll barrels.

2). Increased heat and wear resistance of the bleached layer.

3). Impact strength to meet customer requirements.

4). High gripping ability of the roll material (coefficient of friction).

5). Minimum cost.

2.4. Existing methods for assessing the quality of the target product

To study the structure of metals and alloys and its influence on their properties, traditional methods of macro- and microanalysis, X-ray, spectral, thermal, as well as flaw detection (X-ray, magnetic, ultrasonic) are widely used [102-106]. They have their own sensitivity threshold, most often a narrow focus and are used directly depending on the purpose of the object of study (pipes, rolling rolls, metal structures, etc.). The existing mathematical models for predicting the qualitative characteristics of metal products, based only on the analysis of statistical data, give a very approximate physicochemical interpretation of the processes that occur during the formation of the structure or unambiguously take into account

the influence of the chemical composition and other parameters of the technology. As a result, the results of the forecast may not always meet the requirements.

We will consider some aspects of the development of classical methods and models for assessing the quality of metal castings, in particular cast iron and steel rolls, theoretical prerequisites for obtaining rolls with improved properties, which can be used in the development and study of new methods for operational assessment of their quality characteristics.

Their structure is characterized by the type of metal matrix, the number and complex shape of the excess phase, but, in addition, it varies in the cross-section and length of the barrel, which is determined by the influence of the chemical composition of the rolls, the thermal resistance of the casting mold and the heat treatment mode. Due to the multiparametric nature of the technology, it is impossible to take into account the contribution of all parameters influencing the formation of the structure and properties.

Therefore, it is not always possible to establish the relationship between the material structure of metal castings, in particular steel and cast iron rolling rolls, and the quality characteristics unambiguously and with a certain amount of error [111].

To evaluate and predict the service characteristics of castings using non-destructive testing methods, special structural diagrams and nomograms are widely used, which are based on the analysis of the initial parameters of the technology and provide the obtained structure in the finished product.

2.5. Prerequisites for the development of a methodology for operational assessment of the quality of the target product

A literature review of the considered existing traditional and new methods for assessing the physical and mechanical properties of metal castings indicates that all of them have a narrow specificity of use, take into account the impact on the properties of only certain parameters of the technology, based mainly on statistical data. To date, they give a satisfactory prognosis of properties, which partially diverges from the requirements of the customer, and apply them directly for express assessment of mechanical properties cast iron and steel rolling rolls are not advisable. Improving the complex of mechanical properties of rolls due to their prompt determination in the production process – a laborious, time-consuming and expensive task, the improvement of which, according to the authors, should go through the creation of an express method for their determination. This is evidenced by a number of fundamental works on the theory and practice of obtaining high-quality castings.

In this regard, the prerequisite for the development is the study of new methods, taking into account the influence of the most significant parameters influencing the formation of the structure. Obviously, the parameters are strongly interrelated, and some of them can vary over a wide range, which leads to a change in quality criteria. Taking into account the multi-criteria and multi-parameter nature of the technology, research should be based on the analysis of cause-and-effect relationships and parameter relations, which makes it possible to obtain results consistent with full-scale experiments. This approach makes it possible to predict and adjust the mechanical properties of rolled cast iron rolls in the process of their production.

In this regard, the paper examines the possibility of applying the theory of multifractals [98-112] to quantify the structure and mechanical properties of metals in general and cast iron in particular. At the same time, it is impossible to implement a deterministic method for assessing the mechanical properties of rolls, based on the analysis of parameters, due to the multicriteria nature of the technology.

These reasons are triggered by the following conditions:

–the impossibility of conducting full-scale tests on the finished product, as this leads to a violation of its integrity;

–due to the multiparametric nature of the production technology, it is not possible to implement a deterministic method for assessing the mechanical properties of rolls;

–difficulties associated with operational information on mechanical properties due to the duration of the main cycle of the technological process of their production (from several hours to three days);

–operating conditions of rolls· dictate increased requirements from the customer to a set of service characteristics;

–expansion of the range of rolled steel and cast iron rolls produced;

–improvement of the production technology of rolls.

A number of subjective reasons dictating the creation of an operational methodology include:

–the need for expensive equipment[3] to study the structure and mechanical properties of most metallurgical enterprises due to economic reasons;

–the customer's requirements for obtaining rolls with an improved set of physical and mechanical properties, which leads to additional material and time costs necessary for the practical implementation of this task;

–absence of normative documents on the mechanical properties of rolled steel and cast iron rolls, with the exception of the tolerance for the hardness of the roll barrel;

–discrepancy in statistical data on the mechanical properties of rolls of different designs, which is explained by the lack of a single statistical base;

–low correlation coefficient of formal equations in the considered models, which are included in the methods.

Existing models and methods for evaluating the mechanical properties of cast iron make a forecast that practically satisfies the requirements of production.

2.6. Substantiation of the method of operational assessment of the qualitative characteristics of the target product under development

In the process of improving the technological process, as a rule, the requirements for the quality of the target product are constantly increasing, which leads to partial changes in the technology of its production. Part of these changes is initiated by the developer's desire to overcome the difficulties associated with the adequate identification of the target product's quality indicators. For example, for batch technological processes, the quality of the target product (in particular, the quality of massive metal castings), as a rule, is determined by the methods of full-scale tests, which are carried out only after the completion of the main technological cycle, which can take place for a long time. In this regard, obtaining acceptably accurate information about the quality of the target product is possible only after the end of the main technological cycle, which is why adequate control actions can be

made only after its completion. At the same time, there is a possibility that the quality of the raw materials spent on the manufacture of the next product number, for example, due to their new arrivals, will differ significantly from the previous quality to such an extent that the user will have to constantly, anew, determine the control influences adequate to these changes.

This, and similar situations, initiate the formulation of the task of forecasting the quality indicators of the target product obtained during the implementation of the periodic technological process.

For the periodic technological process, taking into account possible temporary permanent changes in the quality of the source material, at the beginning of the implementation of its main technological cycle, it is necessary to develop a method for predicting the permissibly accurate values of the quality indicators of the target product.

In this regard, we will consider the currently existing method for predicting the quality of the target product, which is obtained during the implementation of the batch technological process, on the example of the production of cast iron rolling rolls [43].

The periodicity of the rolling roll production process is primarily due to the time of preparation of the roll shape, the time of metal smelting, the time of pouring metal into molds, and the cooling of the roll. All these processes take place for a long time (up to 3 ÷4 days, and in some cases even more), depending on the weight of the product.

As a rule, only after the end of the main technological cycle, the quality of the received product is determined and checked for compliance with the established regulatory documents. Most of these methods do not provide a solution to the problem, since they, in addition to statistical methods, are implemented only after the completion of the main technological cycle.

At present, in the implementation of periodic technologies and the impossibility of creating an effective, deterministic method for predicting the quality of the target product, statistical regularities are often used, created on the basis of the analysis of the background of the object of study for the entire period of its existence.

In the case when it is impossible to conduct a direct experiment on a real object, for example, due to the multi-tonnage of technology, it is rational to use heuristic procedures along with a statistical forecast [50].

Fig. 2.1 shows the scheme of implementation of the proposed method.

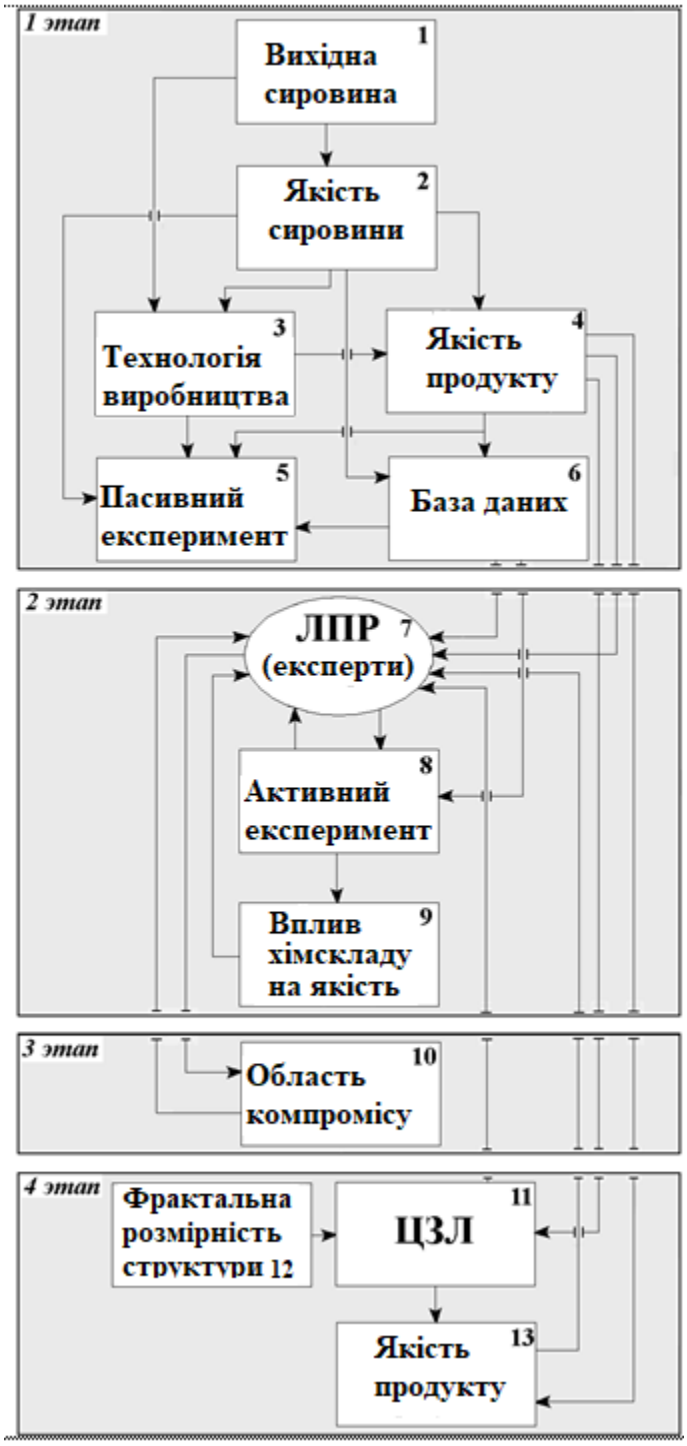

Fig. 2.2. Scheme of implementation of the developed method

At *the first stage*, the assessment of the quality of cast iron rolling rolls is carried out only after the completion of the main technological cycle, taking into account the quality of the feedstock, including the quality of the

charge material (Fig. 2.1, blocks 1, 2), compliance with all technological parameters during their casting (Fig. 2.1, block 3). Carrying out full-scale tests on the laneAt the same stage (Fig. 2.1, block 4) it is possible to supplement the database according to the mechanical properties of the rolls and provides a reliable assessment of the results obtained, which is necessary to control their further forecast using the methods of mathematical statistics. Only after these operations is a passive experiment carried out (Fig. 2.1, block 5). The passive experiment is based on a representative amount of statistical information that characterizes the operation of this technology over a long period of operation (in this particular case, from 1945 to 2014). [64-93]. As a result of its implementation, equations are formed in the form of a database for the rolls of the studied versions (Fig. 2.1, block 6), describing the quality of the target product as a function of the chemical composition of the starting material and structure parameters.

The obtained equations of the passive experiment are created based on the analysis of the influence of parameters describing the working area (RO) of the technology. RV is all the numerical values of the chemical composition, the elements of the structure of the initial product, and the indicators of the selected mechanical properties obtained in this case. By defining the RV, the user thereby assigns the permissible values of the variables, the range of their changes and the quality criteria of the target product. This, as a rule, is produced in the process of production of goods and, in the future, serves as a guide for the formation of regulatory documentation.

After conducting a passive experiment, the *second stage* of research is implemented. Its implementation was initiated by the search for ways to improve the quality of the produced rolls. Having analyzed the technology of roll production, a hypothesis was put forward that in the RV parameters of the technology there are such RRO in which the mechanical properties

are improved. That is, it was assumed that it was possible to select such a range of numerical values of the selected parameters, in which the mechanical properties were improved. The difficulty of determining a previously unknown ZRO by direct experiment often lies in the difficulty or impossibility of its implementation at the object of identification (massive metal rolls).

The use of simulation or other modeling methods in order to assess the mechanical properties of rolling rolls is excluded from the unacceptable accuracy of the results, since the regularities formed as mathematical models are needed mainly in order to predict the results. These forecast data can probably be reasonably accurate provided that the object's metrics are isomorphized and its mathematical model, which is practically impossible when modeling multiparameter technologies.

In this case, methods of mathematical design of experiments are often used, including the use of matrices for planning an active experiment. An active experiment, as a rule, is carried out in laboratory conditions, but there are options for its implementation in production – evolutionary planning. Taking into account the astronomically large number n of all possible variants of the selected variables - 2^n, which cannot be reproduced with the help of direct experiments, since this will entail enormous material and time costs for the manufacturer, it was decided to conduct a special experiment.

To solve this problem, a modification of the active experiment has been developed, which allows to conduct an experiment on a real object in industrial conditions. Therefore, at the second stage (Fig. 2.1, blocks 7-9), it is proposed to experts (persons who have worked for a long time in the field of operation of this technology, hereinafter we call them decision-makers (decision makers, Fig. 2.1, block 7)) to appoint the RRO in which

the quality indicators of the target product, in their opinion, can acquire suboptimal values. At the same time, the matrix for planning an active experiment, which is a kind of database that implements the range of values of the goal function specified by the constraints (see Fig. 2.1, block 8), is divided into three parts.

The first part is the lines of the planning matrix, in which it is allowed to conduct direct experiments on a real object, in the case of cast-iron rolls.

The second part of the planning matrix – the part in which direct experiments cannot be carried out. The implementation of this part of the matrix is based on the data obtained by heuristic procedures, which, in this case, consist in the fact that previously appointed experts in the specified lines of the planning matrix give numerical estimates of the quality indicators of the target product, which are initiated by the lines of this matrix. For the reliability of the results obtained from the decision-maker (Fig. 2.1 Block 7) the data of the passive experiment are used (Fig. 2.1 Block 6).

The third part of the planning matrix includes lines in which experts (for some reason) will not be able to make a reliable assessment of the quality indicators of the target product. In this case, it is proposed, in order to predict the results, which are dictated by the relevant lines of the planning matrix, to use the existing theoretical prerequisites and ideas about the technology under study, which make it possible to make the necessary forecast of the mechanical properties of section rolled iron rolls.

As a result of the implementation of the active experiment (Fig. 2.1, block 8), the obtained equations make it possible to determine the mechanical properties of rolls with changed (improved) indicators.

At the same time, the coefficients for variable equations estimate the influence of each variable on the goal function (Fig. 2.1, block 9). In addi-

tion, the implementation of the second stage made it possible to determine the chemical composition and ratio of the structural components of the rolls with changed quality indicators. During the implementation of the second stage, it may be necessary to adjust the projected results. In this case, experts can conduct repeated studies, as indicated by the links between blocks 7, 8 and 9.

In addition, it should be noted that many of the multi-parameter technologies are aimed, for example, at the implementation of the process of obtaining a material with predetermined properties. Some of these properties may contradict each other in their physical nature, for example, an increase in the strength of cast iron or steel is contrary to an increase in ductility and a decrease in brittleness. In this regard, the task of defining the area arises, which will hereinafter be called the compromise area (OC) (Fig. 2.1, block 10). Within the OK, the contradictions between the criteria are within the limits acceptable to the user.

With regard to *the implementation of the third stage,* aimed at determining the QA properties of the material of the studied rolls (Fig. 2.1, block 10), it should be noted that most of the criteria that characterize the efficiency and efficiency of the technology are set by the standard technology and other regulatory documents within the permissible limits. Probably, this is dictated by the fact that the developers of regulatory documents strive to maintain the technological process, as far as possible, in a specifically selected part of the RV.

Fig. Figure 2.2 shows an example of determining the OK for the selected mechanical properties of the working area of the barrels of cast iron rolls of the SPHN performance (SPHN-41, SPHN-43, SPHN-45, SPHN-49, SPHN-51, SPHN-60 and SPHN-65). This area was determined by the graphic-analytical method, which consists in the normalized representation

of variables, the value of which is given as a percentage [36, 37]. These criteria describe the mechanical properties of cast iron rolls, their chemical composition according to TU U 14-2-1188-97. The assessment of the mechanical properties of the barrels of the rolls of the SPCP performance was carried out according to the average results of full-scale tests of samples cut in the tangential direction (sampling was carried out on 320 heats with a total weight of ~900 tons) [19, 22, 23, 27, 33, 45, 47].

On the graph of Fig. 2.2 The RO of mechanical properties has the following limitations: $Y_1 \approx 220...380$ MPa, $Y_2 \approx 390...840$ MPa, $Y_3 \approx 8...25$ kJ/^{m2}, $Y_4 \approx 40...70$ HSD (taking into account the entire range of cooling conditions used in metallic form) , where Y_1 is the tensile strength; Y_2 is the ultimate flexural strength; Y_3 - impact strength; Y_4 is Shore hardness.

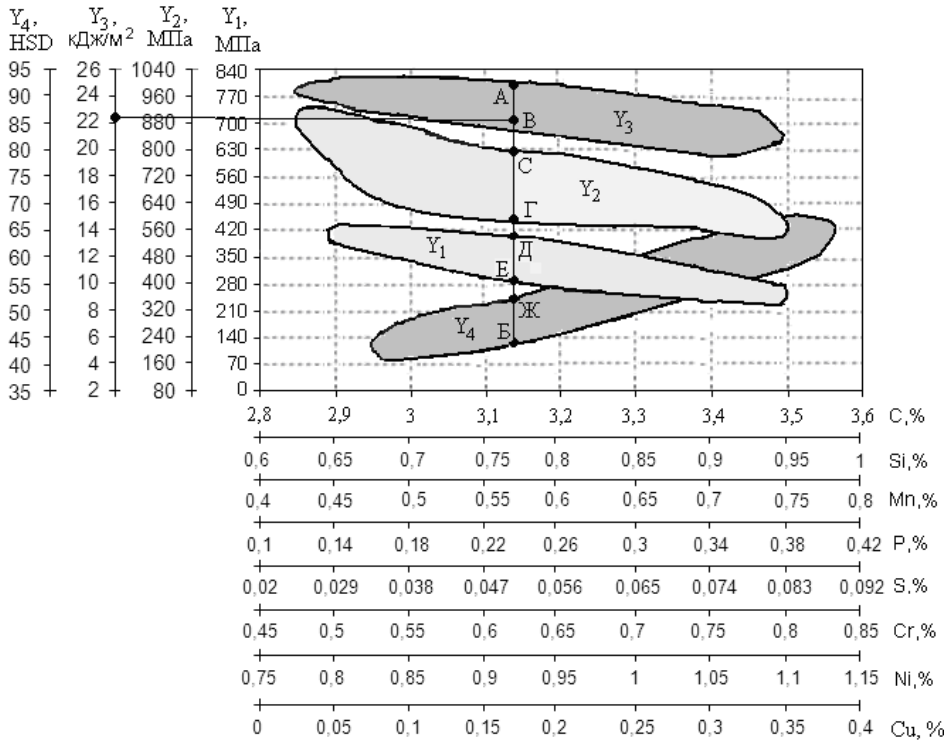

Fig. 2.2. OK of mechanical properties of barrels of cast iron rolls performance of SPCP depending on the chemical composition

The graph in Fig. Figure 2.2 makes it possible to select the preference value of a particular mechanical property. If there is a preference for one of the properties of the roll, for example, the impact strength Y_3 (see the position of point C in Fig. 2.2), then by drawing the vertical AB, it is possible to predict the chemical composition of the product and the interval of existence of its mechanical properties. In this case, criterion Y_2 varies from 580 to 800 MPa (segment SG); Y_1 – no more than 290... 410 MPa (segment DE); Y_4 – no more than 43... 51 HSD (ZB segment). The chemical composition of the roll is determined from Fig. 2.2 and takes the following values: 3.14% C, 0.77% Si, 0.57% Mn, 0.236% P, 0.051% S, 0.62% Cr, 0.92% Ni, 0.17% Cu.

The area of existence of the values of mechanical properties is regulated by the following parameters of the technology: the rate of heat dissipation during cooling of the rolls, which is reflected by the contribution of structural elements and other parameters of the technology (manufacturing method – sand casting, metal, centrifugal casting), etc.

Thus, in the formulation of the task of predicting the quality of the target product (rolling rolls), the conditions of existence of the QA are taken into account, it is more correct to call this area, the area of compromise, since it, this area, may change depending on the changes that the requirements for the criteria are undergoing. OK – the area in which the criteria that determine the performance and efficiency of a particular technology are best combined with each other because possible contradictions among them are acceptable. minimal, "opposites interact with each other only in the midst of compromise."

At *the fourth stage* (Fig. 2.2, blocks 11, 12), it is proposed to evaluate the elements of the structure of roll cast iron and steel using the language of the theory of multifractals. This choice is due to the fact that the

approximation of structural elements with a complex geometric configuration of their shape, if it is made by whole Euclidean figures, then this introduces a certain error in assessing the characteristics of the quality of the material on the basis of the analysis of the elements of its structure at different scale levels.

This initiates the replacement of the geometric characteristics of the structural elements (length, area, volume) with a more differentiated dimensional estimate, which is supposed to partially compensate for the incompleteness of the existing formal axiomatics used in the identification of the structure. To partially compensate for the incompleteness of formal axiomatics, it is proposed to use the language of a higher level [64] – the language of fractal geometry.

The feasibility of using fractal geometry will be considered from the example of determining the structure of barrels of three rolls of SPHN-49 (Fig. 2.3). As can be seen from the figure, the structure of the considered sections of rolls *a*, *b*, does not differ from each other in composition (perlite + carbides + lamellar graphite), but is different in the geometric shape of the elements. The results of the metallographic analysis for cementite in accordance with GOST 3443-87 are identical to all three rolls: C15 →CP6000.

The fractal dimension of the cementite of the ledeburite eutectic calculated by the cell method for roll 1 is 1.857; for roll 2 – 1,972 and for roll 3 – 1,768.

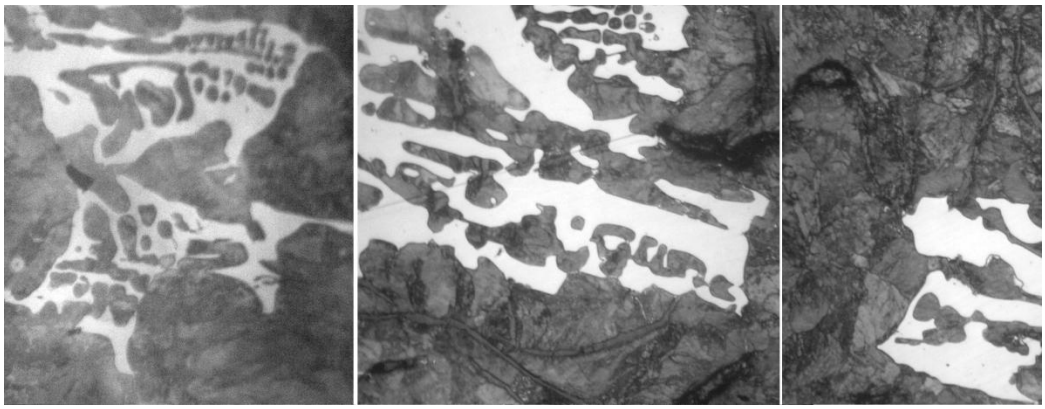

a *b* *c*

Roll 1 Roll 2 Roll 3

Fig. 2.3. Structure of barrels of rolls of SPHN-49 cast state at a distance of 20 mm from the surface: colonies of ledeburite, graphite eutectics, pearlitic matrix (a, b, c), etching HNO3, ´500

Table. 2.1 There are no indicators of the hardness of the rolls, calculated by area according to Euclidean geometry, since they are not sensitive to the geometric characteristics of cementite, presented in GOST 4387.

Table 2.1

Results of calculations and tests

p/n	Characteristic	Roll 1	Roll 2	Roll 3
1	Hardness determined by full-scale tests	52 HSD	54 HSD	51 HSD
2	Hardness Calculated Considering the Fractal Dimension of Cementite	51 HSD	54 HSD	49 HSD

According to GOST 3443-87, the area occupied by cementite is 15% and the area of its largest inclusions (6000 μm^2) is the same for all three rolls. Therefore, hardness cannot be determined using these indicators. In this case, the error in the assessment of hardness by geometric dimensions determined by Euclidean geometry is beyond the sensitivity of direct tests

according to this GOST. As follows from Table. 2.1 hardness indicators, calculated by full-scale tests and analytically, using fractal dimensions, differ slightly (relative error is ~4%). This fact indicates that the fractal dimension of the structure elements can act as an indicator of the hardness of the working area of the barrels of rolling rolls of the SPHN performance.

In order to minimize the costs and efficiency of the planned research, the implementation of the fourth stage is carried out in the central plant laboratory (CPL, Fig. 2.2, block 11) with reference to industrial conditions. Together with the metallographic analysis of the roll structure, a multifractal analysis of its elements was carried out in parallel (Fig. 2.2, block 12) at the same scale of its increase with the help of a specialized program "Multifractal" developed for this purpose. Preliminary analysis of dimensional evaluation of the structural elements of the studied roll iron (lamellar and spherical graphite, cementite, ledeburite) in the scale range from ×200 to ×1000 showed that these estimates varied within the error of the experiment, which does not exceed 5 ÷7%. This emphasizes the fractal nature of the metal structure (self-similarity), and indicatesreliability of numerical values of dimensional estimates of the elements of the structure of rolling rolls, which in turn makes their further use rational in the forecast of qualitative characteristics, in particular mechanical properties. From an economic point of view, it is also advisable to apply this approach when the factory laboratories are not sufficiently equipped with high-resolution metallographic microscopes (electron and scanning electron microscopes). The elements of the structure of the roll material obtained in their statistical dimensions can be used to predict its mechanical characteristics (Fig. 2.1, block 13).

The implementation of the fourth stage makes it possible to adjust the results of the prediction of the mechanical properties of the studied rolls.

2.7. Selection of variables and justification of quality criteria

Determination of the full range of physical and mechanical properties from the example of rolling rolls– $Y_i(i=1,...,n)$, which are formed in the production of these products, is one of the urgent tasks of modern materials science [44]. We assume that each property, out of the set of known properties, corresponds to a certain criterion- $Y^*_{i,r}(r=1,...,s) \in \mathrm{Y_i}$, which evaluates a particular quality of the rolling roll, and even the manufacturability or economy of its production. We accept that there are many qualitatively heterogeneous criteria – $Y^*_i(i=1,...,n)$, including a subset of $\{Y^*_{i,r}(r=1,...,s)\}$ qualitatively homogeneous criteria [1]. As a rule, the value of the criterion is interpreted as an assessment of the degree of achievement of a particular goal. The user, when defining the PB of the technology, assigns the boundary values of the controlled variables $X_k(k=1,...,m)$ and those quality criteria $Y_i(i=1,...,n)$, which he identified as the main ones in the implementation of this technology.

Naturally, the choice of quality criteria and variables of rolling roll production technology should be based on a detailed analysis of the operation of this technology and fundamental research. As shown in many works of well-known domestic researchers-practitioners A.E. Krivosheev, N.A. Budagyants, T.S. Skoblo and others [93-123], the most significant parameters influencing the properties of roll iron and steel are their chemical composition and structure. Their choice is due to the fact that the chemical com-

position of the roller material is formed on the basis of the composition of charge materials, scrap, various harmful impurities, additives and additives of individual alloying elements, modifiers. The structure of cast iron and steel rolls at different scale levels, which serves as an indicator of many of their quality characteristics, see Figure 1. technological operations (cooling conditions of rolls, casting method, heat treatment, etc.) for quality characteristics.

Figure 2.4 shows the results of the selection of X variables (elements of chemical composition and structure parameters) and mechanical properties for cast iron section rolls with a lamellar graphite structure. As can be seen from the above diagram, the number of controlled variables is 11, and the number of quality criteria selected by experts is 4 [36, 37].

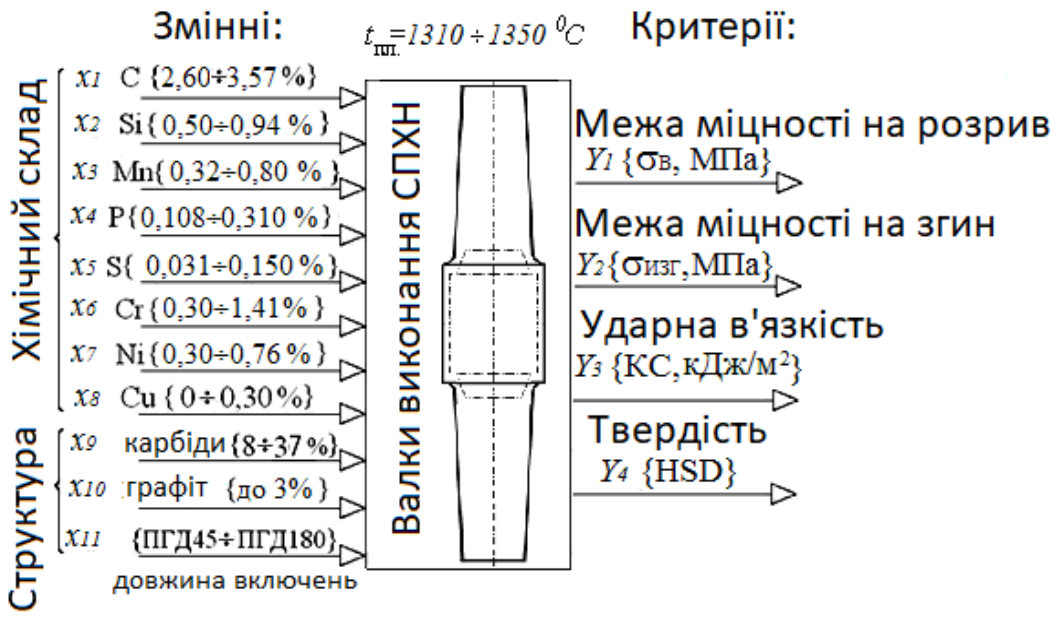

Fig. 2.4. Schematic diagram of multiparameter technology production of rolling rolls

The approximate degree of influence of elements of chemical composition and structure parameters on the mechanical properties of cast iron

in the RV and beyond was determined on the basis of an analysis of the background of this technology and those theoretical provisions that are set forth in the following literature sources [94-123].

2.7. Chemical composition and structure

As a material for this study, four cast iron rolls of the SPHN (SPHN-43, SPHN-45 (after two meltings), SPHN-49) and SSHN (SSHN-50 after three meltings) manufactured by PJSC DZPV (Dnipropetrovsk) were accepted.). Section rolls (C) cast iron rolls with lamellar graphite (P) and spherical graphite (W) are alloyed with chromium (X) and nickel (H) to improve their performance characteristics, in particular hardness and wear resistance.

Cast iron rolls of all types are cast in a combined mold – a chill, in which there is an accelerated crystallization of the working layer of the roll barrel, and flasks with necks, clubs and a profit part molded in them. Stationary combined casting molds are designed for casting cast iron rolls weighing from 100 kg to 20 tons with the required hardness of the working layer of barrels and satisfactory mechanical properties of the drive elements.

The molds for casting the studied rolls were assembled in a special casting pit, the surface of which is lined with refractory bricks (Fig. 2.5 *a*). The rolls were cast vertically, with a tangential feeder installation at the bottom of the mold (Fig. 2.5 *b*). This method of two feeders ensures a clean swath surface. In the process of rotation, lighter and lighter particles (slag, non-metallic inclusions) and gases are moved to the center of the roll and transferred to profit. Siphon The installation of the feeder, with all its advantages, has a common drawback, which is that after pouring the metal, the hottest part of the roll is at the bottom, which disrupts the directional

hardening of the metal – the bottom up. [47, 54]. The molds of the molds for casting the roll blanks were smooth. The dimensions and configuration of the chills are determined by the size and configuration of the rolls. When designing chills, it is necessary to take into account the shrinkage of the roll blank and the allowance for their processing. The wall thickness of the molds for small and medium-sized rolls is to be kept in the range of 120...180 mm and for large ones - 180...260 mm. As many years of experience have shown, with thinner walls, chills crack quite quickly and become unusable.

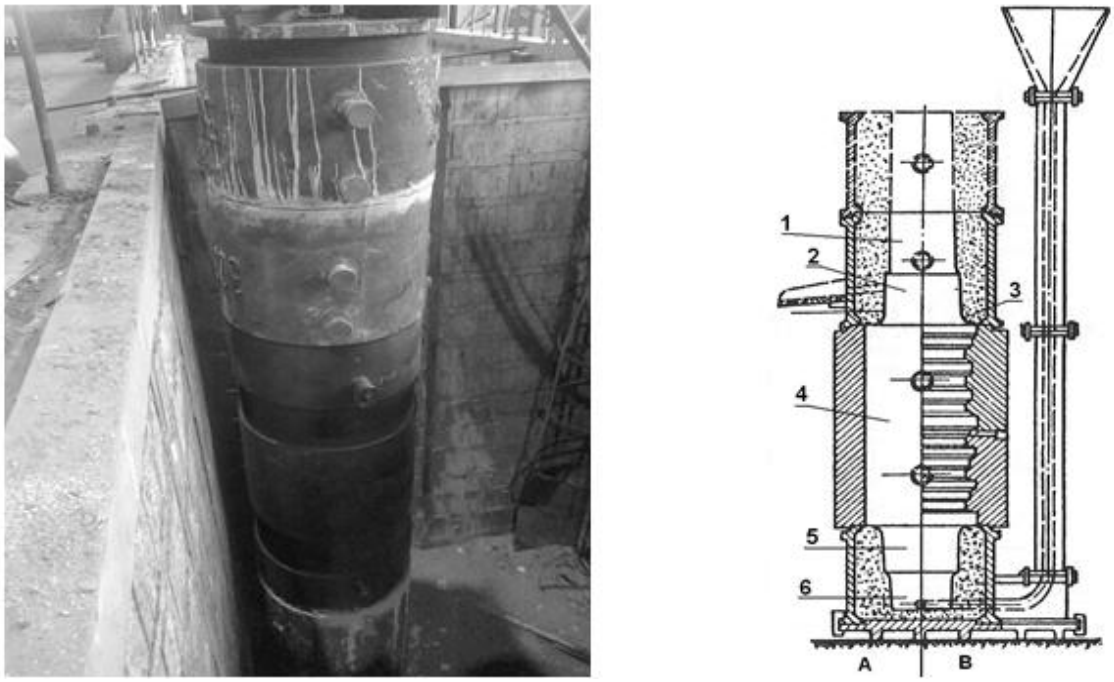

а *б*

Fig. 2.5. *а* – appearance of the casting mold for casting cast iron rolls manufactured by PJSC DZPV; b – chill with a smooth inner surface (A); chill with a calibrated inner surface (B). 1 – upper club; 2 – upper neck; 3 –dumbbell; 4 –barrel; 5 – lower neck; 6 – lower club

For casting rolls with perlite-graphite and perlite-cementite-graphite structure of the working layer, depending on their purpose, the inner surface of the molds is covered in some cases with a layer of casting paint with a thickness of 0.75...3.00 mm, and in other cases with a layer of spread –. thickness 6...12 mm. For chills with a smooth inner surface, the thickness of the chills and the thickness of the headlamp layerSpreads also have a great impact on the quality of the rolls, especially on the distribution of properties across the cross-section. The thickness of the paint layer or spread is of great importance in the manufacture of unprofiled rolls with a perlite-cementite-graphite structure made of alloy cast iron. The use of a thick layer of chill coating contributes to significant zonal lication of carbon, phosphorus, sulfur, as well as non-metallic inclusions. This increases the fragility of the rolls, which leads to the formation of cracks and breakages. In this regard, in the production of rolls of this type, it is important to coordinate the thickness of the layer of heat-insulating coating of the roll with the operating conditions of the rolls, as well as with the distribution of structural components and the hardness of the metal along their cross-section [47]. Pouring of liquid metal was carried out in the temperature range of 1310÷1350 ^{0} C after slag purification and sampling for marking chemical analysis. Cupola melts were used for casting chills weighing up to 12 tons, and furnace melts were used for casting chills weighing more than 12 tons. The duration of cooling of chills in the mold is as follows: with a roll weight of up to 3 tons – 12 hours; With a mass of 3... 6 tons – 24 hours; with a mass of 6... 10 tons – 40 hours; with a mass of 10... 13 tons – 60 hours and for a weight of more than 13 tons – 72 hours. Knocking out of the rolls of the SPHN was carried out after cooling to 250... 300 ^{0} C, and chills of the rolls of the SSHN – after cooling to 100...150 ^{0} C.

Technological parameters for obtaining rolls are given in Table. 2.1.

Table 2.1

Parameters of cast billets of cast iron section rolls,
produced by the foundry of PJSC DZPV

Roll manufacturing technology					Parameters of roll barrels		
№ Fins	Furnace ILT-6, ILT-20	Die casting	Cast iron pouring temperature, ^{0}C	Coating thickness of the mold, mm	Diameter, mm	Length, mm	Weight, kg
1-173	SPHN-43		1310÷1350	4÷12	520	1000	1600
2-134	SPHN-49				940	1200	6450
1-233	SPHN-45				1000	1900	9500
2-130	SPHN-45				920	1900	8200
1-120	SSHN-50				376	600	500
3-203	SSHN-50				350	500	362
2-33	SSHN-50				400	600	568

The composition and structure of cast iron rolls are the main factors determining their physical and mechanical properties. Cast iron rolls of SPHN performance containing 2.8...3.5% carbon by weight, alloyed with chromium (0.5...0.8%), nickel (0.9...1.3%), copper (0.2...0.3%) were studied; rolls containing 2.9...3.25% carbon, alloyed with chromium (0.5...0.8%), nickel (0.9...1.3%) and modified with magnesium (0.038...0.054%) (Table 2.2).

The chemical composition of the rolls was established in strict accordance with the required structure and their service purpose, and was regulated by the regulatory requirements of TU U 27.5-24608640-002:2008 "Cast iron rolls".

Table. 2.3 shows the main characteristics of the rolls.

Table 2.2

Chemical composition of the investigated graded rolled rolls of SPKHN and SSHKHN versions, % by mass

3	Si	Mn	P	S	Cr	Ni	Cu- SPHN; Mg - SSHN
3,25…3,50	0,75 ... 1,10	0,44 ... 0,70	0,070 ... 0,085	0,009…0,026	0,60 ... 0,75	1,05 ... 1,29	0,20 ... 0,29
2,92 ... 3,34	0,60 ... 0,80	0,66 ... 0,90	0,100 ... 0,190	0,035 ... 0,066	0,66 ... 0,80	0,89 ... 1,15	0,22 ... 0,26
2,90 ... 3,12	0,75 ... 0,93	0,63 ... 0,84	0,096 ... 0,115	0,025…0,058	0,62 ... 0,77	1,11 ... 1,20	0,25 ... 0,32
2,80 ... 2,95	0,65 ... 0,90	0,50 ... 0,76	0,090 ... 0,108	0,020 ... 0,051	0,65 ... 0,79	1,08 ... 1,15	0,23 ... 0,29
2,90 ... 3,17	1,60 ... 1,97	0,49 ... 0,68	0,045…0,070	0,011…0,019	0,43 ... 0,61	1,00 ... 1,17	0,048…0,052
3,00…3,30	1,49 ... 1,85	0,48 ... 0,72	0,042…0,066	0,008…0,020	0,35 ... 0,45	1,03 ... 1,27	0,046…0,054
3,14 ... 3,38	1,43 ... 1,88	0,47 ... 0,60	0,053…0,074	0,010…0,034	0,46 ... 0,54	1,01 ... 1,30	0,050…0,057

Table 2.3

The main nomenclature of rolls for the production of small-grade, medium-grade and large-grade rental

Cast iron marking	Hardness of the working layer, NSD	The structure of the worker layer of rolls	The rough weight of the swath, kg	Barrel sizes rolls, mm	Purpose of rolls	Making rolls
2	3	4	5	6	7	
SPHN -43	43-53	Chromium-nickel alloyed pearlite cast iron with lamellar graphite and medium carbide content.	3255	520 ×1000	Rolls of draft cages of small-, medium-grade wire and pipe rolling mills.	SPHN -43 SPHN -49 SPHN -45
SPHN -49	49-59		12080	940 ×1200	Rolls of finishing cages of large-grade, rail milking and continuous-procurement mills	SPHN -45 SSHN -50
SPHN -45	45-55		15100 16730	920 ×1900 1000 ×1900	Rolls of pre-cleaning cages of high-grade, rail milking and continuous-procurement conditions	SSHN -50 SSHN -50

End of table 2.3

1	2	3	4	5	6	7	Melting No. roll
№13217, №13218, №13191 від 05.09.11 р.	SSHN -50	50-62	Chromium-nickel alloyed pearlitic cast iron with spheroidal graphite and medium carbide content	1660 1660 1100	376 ×700 376 ×700 326 ×600	Rolls of rough, pre-cleaning and crimping cages of grade rolling mills	1
3-203 №13247, №13248, №13185, №13186 від 02.08.11 р.	SSHN -50	50-62		1000 1000 1100 1100	350 ×500 350 ×500 326 ×600 326 ×600		№14093 від 18.10.11 р. 2-134 №11212 від 26.02.11 р.
№13281, №13282, №13194, №13195 від	SSHN -5 0	50-62		1145 1145 1110	400 ×600 400 ×600 326 ×600		№11208 від 24.02.11 р. 1-233 №11218 від

Section rolls with smooth barrels were studied (Fig. 2.6).

Fig. 2.6. Cast iron rolls manufactured by PJSC DZPV (Dnipro)

To improve the quality of roll metal, the following modifiers were used: - Foundrisil for rolls of SPHN execution; Elmag -600, Elmag -900, Vl 57 (M), Barinoc, Elgraf - for rolls of SPHN. The Foundrisil modifier, which is based on ferrosilicon containing the optimal amount of calcium and barium, is designed to provide effective control over the level of bleaching in gray and high-strength cast irons. Its use is especially effective in the processing of gray cast iron with low sulfur content, when the use of other modifiers is ineffective. Spherodising modifiers Elmag -600, Elmag -900, Vl 57 (M), Barinoc, Elgra are designed to produce castings from high-strength cast iron and modify steel.

To study the influence of the chemical composition and structural parameters of the selected cast iron on its mechanical properties, the following research methods were used: metallographic, using the optical microscope Neophot-2; full-scale tests – determination of mechanical properties; multifractal analysis of structural components; planning and modeling methods, expert assessments, described in the following sections.

As samples for structural analysis and full-scale tests, chips of the working area of metal barrels of rolls and witness samples were selected. After grinding the samples on abrasive paper with a dispersion of 200 to 1200 μm and polishing on paper with a layer of diamond paste with a dispersion of 25 to 3 μm, etching the sections were carried out in a 4% solution of nitric acid in ethyl alcohol (4 cm^3 HNO_3 and 96 cm^3 of alcohol). Grinding of samples was carried out under water cooling to prevent structural changes in the surface layers of the metal due to its heating.

Fig. 2.7 –Fig. 2.9 shows the structure of roll barrels.

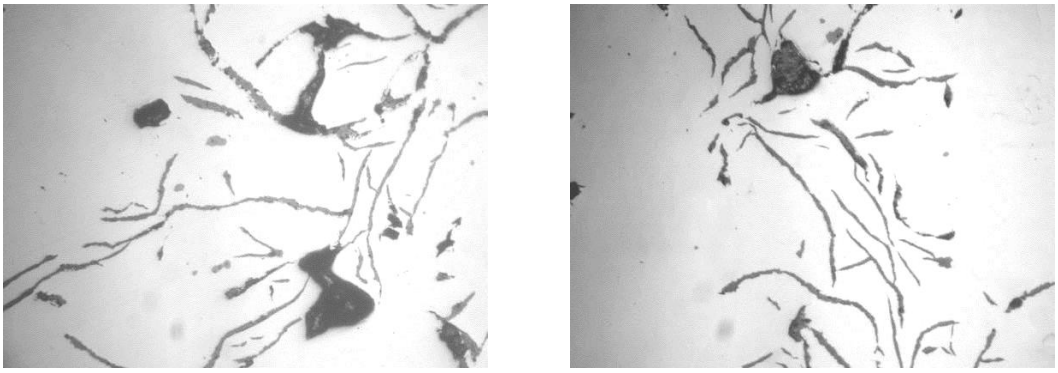

а *б*

Fig. 2.7. Microstructure of barrels of rolls of SPHN-45 (*a*) and SPHN-49 (*b*) at a distance of 10 mm from the surface in the cast state: form of graphite inclusions, without etching, ×200

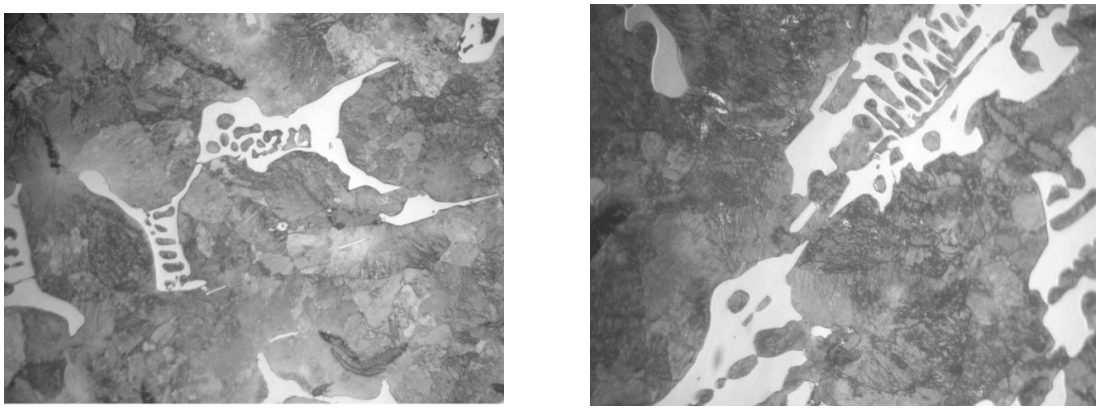

а *б*

Fig. 2.8. Microstructure of barrels of rolls of SPHN-45 (*a*) and SPHN-49 (*b*) at a distance of 10 mm from the surface in the cast state: form of graphite inclusions, etching HNO_3, ×200

In the working area of the barrels of the rolls of the SPHN performance, the amount of carbides in the form of cementite of ledeburite eutectic varied from 8 to 37%; corresponding to the standard C25. The content of lamellar graphite, which should be considered as a structural component and a non-metallic inclusion at the same time, varied ~~from 0 to 3%, which corresponds to the PG2 score, with the length of the plates estimated by the PGD45÷PGD180 scores according to GOST 3443. Analysis of the microstructure made it possible to record the change in the shape of graphite inclusions within narrow limits - PGF1, PGF2; distribution of graphite inclusions - PGr1, PGr2. The area occupied by lamellar perlite was 60-85%, which corresponds to the P70 and P85 standards, respectively.

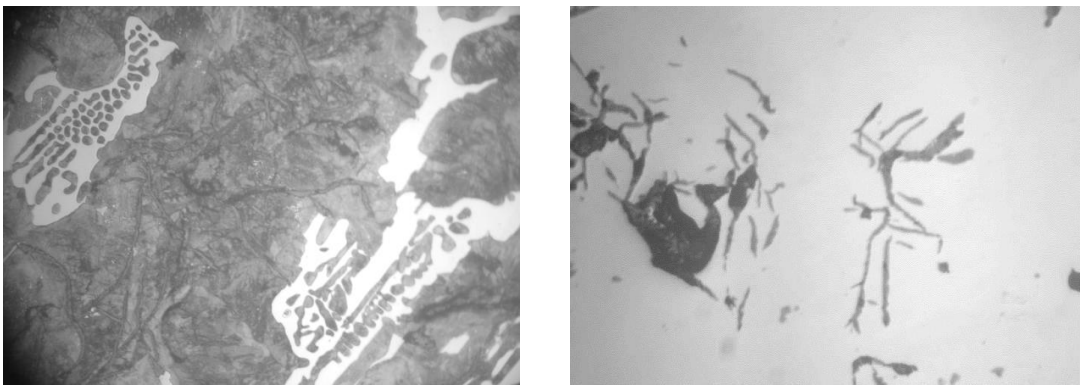

a *b*

Fig. 2.9. Structure of barrels of cast iron rolls of SPHN-43 version cast at a distance of 30 mm from the surface: colonies ledeburite, graphite eutectics, pearlite matrix (*a*); form graphite inclusions (*b*); *a* - etching HNO_3 b - not etched ×, 200

For the rolls of the SSHN design, the size of spherical graphite inclusions (their diameter) on the surface of the section varied from 35 to 59 μm, which according to this GOST corresponds to the standard SHGd45

or score 6 ISO 945-75 (Fig. 2.10). Spherical graphite in the working layer of the barrel (SHGf5 in shape) at a depth of ~5 ÷15 mm is much less common than carbides, including ledeburite, which is explained by its content ~up to 3% (standard SHG4). The spherical shape of graphite is caused by the addition of a small amount of magnesium - up to 0.054% by weight.

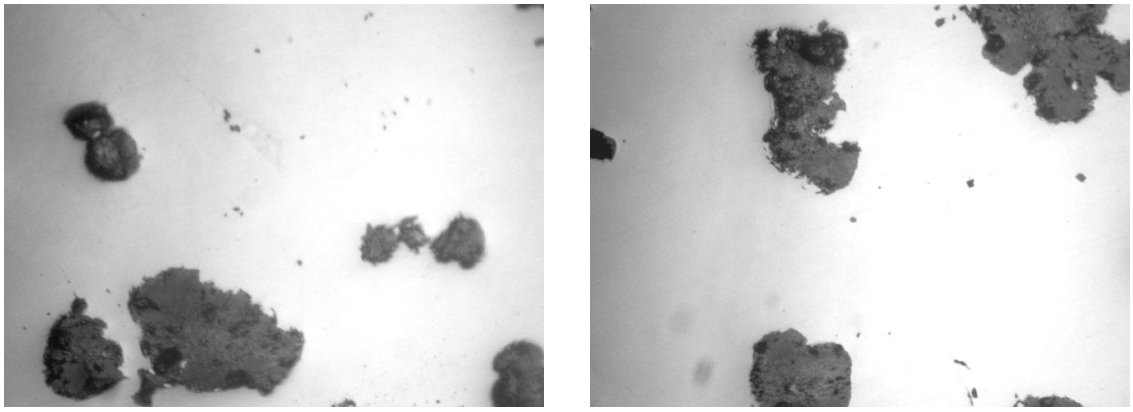

a *b*

Fig. 2.10. Microstructure of the working area of roll cast iron of SSHN-50 at a distance of 40 mm from the surface: inclusion of spherical graphite (*a, b*), ×400 without etching (melting 1-120)

Perlite has different dispersion of PD (average distance between two adjacent cementite plates): from 0.79 μm (PD0.5 according to the standard) to 2.2 μm (PD1.6), which was determined with an increase in the structure of × 1000. The area occupied by perlite is 60-70%, which corresponds to the P70 standard.

Fig. 2.11 shows the microstructure of roll cast iron with spherical graphite shape after etching HNO_3 (melting 3-203 and melting 2-33).

The area occupied by cementite for theperformance of SSHN-50 after three heats was generally 20-30% according to calculations using the linear method of A. Rozival corresponds to the score of C25.

a

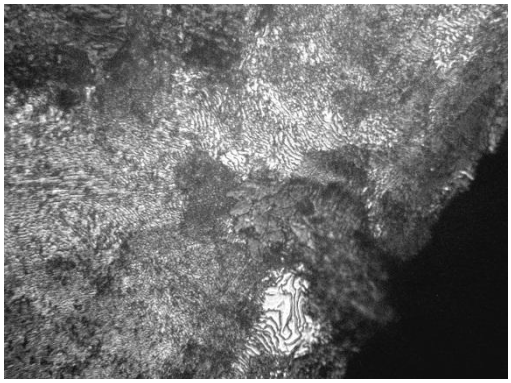

b

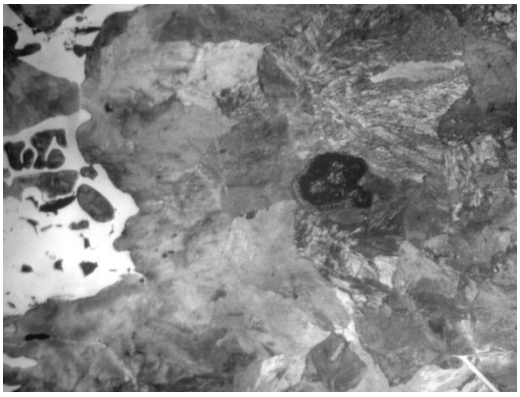

c

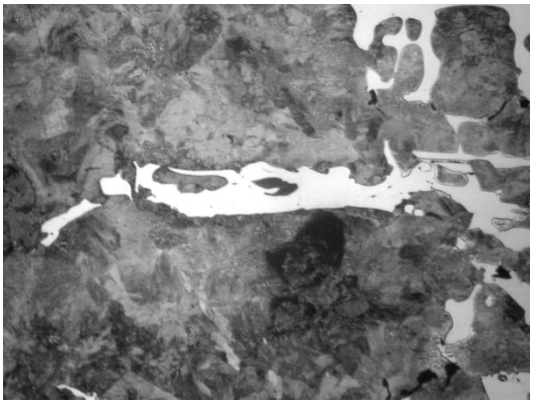

d

Fig. 2.11. Microstructure of the working area of the rolls of SSHN-50 at a distance of 40 mm from the surface: pearlitic matrix (*a, b*), ×800; ledeburite colony (*c, d*), ×300 after *a, b* - melting 3-203*;* *c, d* Heats 2-33

2.7 Results of experiments and their analysis

The material of the rolls is almost never subjected to mechanical strength tests. When testing cast iron rolls, they are limited to measuring the hardness on the surface of the barrel in accordance with TU U 14-2-1188, and the mechanical strength of steel rolls is estimated based on the test results of only samples cast separately or in the form of tides to the rolls. Such tests do not give a sufficiently complete picture of the mechani-

cal strength of the material of the rolls themselves. As mentioned above, the mechanical strength of the same material, in particular a cast iron roll, is different in its cross-section, so it is impossible to make an accurate judgment about the strength of the roll by a separate sample. In addition, the direction of the fracture-causing force in relation to the direction of columnar crystals in the roll structure has a significant impact on the test results [46-52].

To obtain satisfactory data on the mechanical strength of the roll material, it is advisable to test samples cut from different places of the roll body in the radial *and* tangential *directions*. Such samples can be cut from rolls during their initial machining and subsequent calibration. Under the conditions of sampling these samples, it is advisable to accept small samples for mechanical strength testing. Bending resistance and impact strength were determined on samples 10 ×10 ×6 mm, tensile strength – on specimens with a diameter of 6 mm and an effective length of 36 mm.

One of the main indicators of rolls is the hardness of the working layer, regulated by the technical conditions for the supply of rolls. Hardness is determined on the surface of the barrel and in the depth of the working layer. To test the hardness and check the microstructure for the depth of the working layer, the barrel was cast 50 mm longer than the specified size. Rings were cut from this allowance during the processing of rolls on the machine, from which templates were selected for laboratory tests. In order to eliminate irregularities and dashes, the tested surface is subjected to grinding.

The mechanical properties of rolled iron were determined on standard certified equipment using modern methods and measuring equipment: the INSTRON testing machine, the PSV 5 pendulum impact tester, the CD-40 testing machine, the Shor hardness tester. Blanks were selected from cast samples, from which samples for full-scale tests were made. Specimens

were cut from the working area of smooth metal roll barrels in the tangential direction, and were also made from separately cast samples in witness sample castings–. The mechanical properties of roll iron were determined in accordance with GOST 27208-87 "Castings of cast iron. Mechanical test methods. The impact strength of cast iron was determined without notching on samples measuring 101055 ×mm ×. To assess the level of flexural strength, samples of 10 ×10 ×90 mm were used, and in tensile tests – samples with a diameter of 25 mm, with an effective length of 50 mm. Below, in Table. Figure 3.4 shows the mechanical properties of the studied rolls.

Table 2.4

Mechanical Properties of Rolling Rolls of SPHN and SSHN Versions

№ p/n	Smelting No.	Execution Felling	σ_V, MPa	σ_{sg}, MPa	DC, kJ/m^2	HSD
1	2	3	4	5	6	7
1	1-173	SPHN-43	330	670	14	45
3	2-134	SPHN-49	320	440	15	51
4	1-233	SPHN-45	370	480	17	46
5	2-130	SPHN-45	420	600	19	47
6	1-120	SSHN-50	410	720	20	51
6	3-203	SSHN-50	390	630	23	54
7	2-33	SSHN-50	400	700	21	56

2.9. Conclusions and objectives of the study

From the review conducted in this section, it follows:

– the main reasons for the failure of parts of volumetric hydraulic drives are wear and corrosion, and these processes develop in the coupling units;

– A review of theoretical and experimental studies has shown that in the field of compatibility of friction pairs of the parts under consideration, a large role is given to the material.

It is shown that during the working out period the main property is scuff resistance, and in the post-running-in period – wear resistance. In this regard, it is important to disclose the mechanism of these processes and develop the compatibility of materials at different stages of work.

– it is shown that the impact on the surface of the coupling (sliding) of parts by chemical-thermal treatment, diffusion metallization, complex methods of surface treatment can be solved only by particular problems;

– the study of the experience of using ion-plasma technology allows us to assume the feasibility of its use to increase the service life of hydraulic drives.

To solve the problem, research was carried out in the following areas:

– choice of material for the manufacture of spools;

– selection of plasma coating composition and optimal modes of its application;

– study of the effect of plasma coating on wear resistance, corrosion resistance of the selected steel;

– development of special-purpose coatings, optimization of its composition;

– bench and industrial tests.

SECTION 3.
EFFECTS OF PLASMA COATINGS ON THE SERVICE PROPERTIES OF PARTS DUAL-USE

The experience of tool production and some branches of mechanical engineering has shown the prospects for the use of ion-plasma coatings to improve the performance characteristics of machine parts and tools [57]. The development of plasma coating technology is far ahead of the understanding of the reason for the increase in their performance [58].

At present, the relationship between the properties of the applied coatings and the performance characteristics of the machine parts and tools on which they are applied has not been established, there are no rules for choosing the optimal technological parameters of coating to obtain certain properties. The use of the ion-plasma method in specific production conditions requires the selection of technological modes of its application and optimization of its parameters [59].

3.1 Justification for the choice of plasma coating composition

When choosing plasma coatings and the technology of their application, first of all, the properties of refractory compounds are analyzed, from the comparison of which it is possible to come to the disappointing conclusion that titanium nitride (Table 3.1) [57]:

– has high strength properties (microhardness, modulus of elasticity) in a wide range of temperatures;

– low thermal conductivity;

– resistant to high-temperature corrosion and oxidation;

– the coefficient of thermal expansion ($9.35 \cdot 10^{-6}$ deg^{-1}) is close in value to the coefficient of thermal expansion of steel used as a substrate, which is important for good adhesion;

– Titanium and nitrogen are not acutely scarce materials and are widely used in industry.

Taking into account the above, titanium nitride was chosen as the coating material.

Table 3.1

Properties of refractory joints used as a coating

Connection characteristics	Ti–N	TiC	ZrN	Mo_2N	CrN
Nitrogen content , carbon, masses, %	22,63	20,05	13,2	–	–
Cage Type	FCC	FCC	FCC	Cube	–
Cage period , nM	4,249	4,324	4,567	4,167	–
Density, $kg/^{m3}$	5430	4930	7090	–	–
Melting point, °C	–	–	–	It decomposes at 600°C	Decomposes at 1500°C
Modulus of elasticity, $x10^7$ N/m	25600	46000	–	–	–
Microhardness, MPa	20500	31700	29500	–	10800
Coefficient of thermal expansion, $1/deg \cdot 10^6$	9,35	7,95	7,24	4,5	2,3

4.2 Search for optimal technological parameters for deposition of plasma coatings of parts

The optimal parameters for applying plasma coatings to the working surfaces of parts in this work varied: the value of the negative potential applied to the product during ion bombardment; heating temperature of products; the pressure of the reaction gas fed into the chamber and the deposition time of the coating. The first stage of coating is ionic cleaning. It is

carried out to obtain an atomically clean surface of the product immediately before the deposition of the coating by bombarding the surface with accelerated ions of the evaporating material. At the same time, a negative potential is applied to the product, which accelerates ions, which, bombarding the surface, completely disperse the neutral atoms to be precipitated, as well as partially the atoms of the surface layer, producing high-quality cleaning of the surface.

At the same time, accelerated ions are introduced into the surface layer, saturate it and thereby create the prerequisites for good adhesion of the coating to the substrate. During ion cleaning, the parts are heated. Temperature control is mandatory to avoid vacations. It was carried out by an optical parameter. Temperature control is carried out by periodically switching the electric arc evaporator on and off. During ion bombardment, a negative potential of 1000 was applied to the parts. According to technical data [43, 44] of the Bulat-3T installation, the temperature of the substrate can vary from 300 to 800°C. Ion bombardment performed at the temperature of the substrate 500°C, made of 38X2MFUA steel, corresponds to the best adhesion of the coating and the highest wear resistance (Table 3.2). At lower temperatures, there is a decrease in adhesion, which leads to peeling of the coating during operation and, as a result, to scuffing, a decrease in wear resistance. These phenomena are also observed when the heating temperature of the sprayed surface exceeds the tempering temperature of steel due to the hardening of the latter.

At the end of ion purification, the potential supplied to the product is reduced to 150-250 V and a dosed amount of nitrogen is supplied to the chamber. At the same time, the energy of the ions becomes insufficient for sputtering. A coating is formed, which is a combination of the evaporated material with nitrogen entering the chamber. In the work, for the produc-

tion of nitridotitanium coatings in the evaporator, the following was installed.

Table 3.2

Effect of Titanium Ion Bombardment Temperature on Coating Adhesion lined and wear-resistant in operation

Steel grade	Adhesion K_α (in the numeral) and wear resistance (in the denominator) at temperatures, °C				
	Uncoated	300	400	500	700
38X2MUA	$\frac{-}{3\cdot10^{-4}}$	$\frac{0,60}{2,8\cdot10^{-4}}$	$\frac{0,75}{2,5\cdot10^{-4}}$	$\frac{1}{2,0\cdot10^{-4}}$	$\frac{0,50}{2,3\cdot10^{-4}}$

an electrode made of titanium VT1-00 (GOST 19807−94), and gaseous nitrogen of the OSCh brand (GOST 9293−94) was used as a gas reagent. The amount of gas supplied to the chamber is regulated by a pusher and a decrease in vacuum is recorded, which is recorded by a vacuum gauge.

The gas supply is kept constant throughout the spraying cycle. The optimal nitrogen pressure should be determined on a case-by-case basis and depends on the composition of the cathode, the model of the vacuum-plasma installation on which the coating is applied [45, 49]. To determine the optimal value of nitrogen pressure, which ensures the production of a high-quality coating on the working surfaces, titanium nitride was applied at different partial pressures of nitrogen – from $5\cdot10^{-3}$ Pa to 1 Pa.

This pressure range was selected on the basis of literature data on the performance of the plasma-coated product [45, 49]. Coatings obtained with different nitrogen vises differ in the number and size of the droplet phase and color. The largest amount of droplet phase is observed in coatings ob-

tained at a nitrogen pressure of $3 \cdot 10^{-2}$ Pa. They are gray and yellowish-gray in color. With an increase in nitrogen pressure to 1 Pa, the coatings acquire a golden-yellow color with a small amount of droplet phase without traces of peeling.

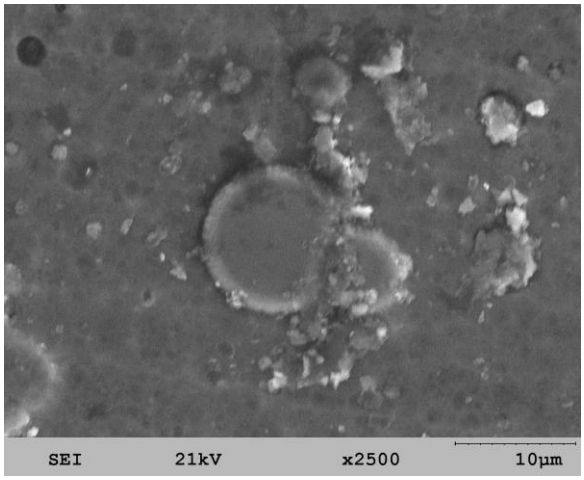

a

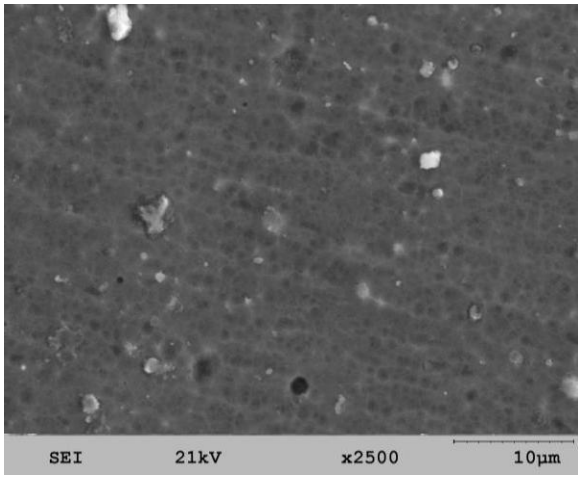

b

a – $3 \cdot 10^{-2}$ Pa; b – 1 Pa

Fig. 3.1 – Microstructure of surfaces of titanium nitride coatings obtained at different partial pressures of nitrogen

Table 3.3

Effect of Nitrogen Partial Pressure on Performance

Titanium Nitride Coating

Nitrogen pressure , Pa	$3 \cdot 10^{-3}$ Pa	$3 \cdot 10^{-2}$ Pa	1 Pa
Microhardness, GPa	23,0	25,0	20,0
Coating color	grey	yellow-gray	golden yellow

At nitrogen pressures of $3 \cdot 10^{-3}$ Pa, $3 \cdot 10^{-2}$ Pa, the microhardness of the coating increases.

Radiographic studies showed an increase in the width of the diffraction maxima β (333), which indicates a microdistortion of the crystal lattice of the chemical compounds that make up the coating [60]. It can be assumed that this phenomenon is explained by the use of nitrogen atoms, the diameter of which is larger than the diameter of the sphere inscribed in the titanium lattice. High hardness and high level of microdistortion leads to an increase in the brittleness of the coating. When the pressure is increased to 1 Pa microhardness is reduced to 20 hPa. With a decrease in the level of microdistortion of the crystal lattice in the coating, its plasticity increases. The brittleness of the coating decreases with a sufficiently high hardness. Experiments have shown that titanium nitride coating obtained at a pressure of 1 Pa of nitrogen effectively increases the wear resistance of parts made of 38X2MUA steel.

A very important parameter is the thickness of the coating to be applied. This is due to the fact that with large thicknesses, the coatings are brittle and become prone to cracking and peeling.

The thickness of the coating to be applied is proportional to the arc discharge current and the deposition time. At an arc current of 80 A, the growth rate of titanium nitride coating is 10–12 μm/h [59]. We studied coatings with a thickness of 2 to 7 microns applied to 38X2MFUA steel.

The results of the studies showed that the coating of titanium nitride with a thickness of 6 microns has the greatest adhesion activity to the substrate and the effect on increasing the wear resistance of steel. At greater thicknesses, peeling of the coating is observed (Fig. 3.2) [61, 62].

Table 3.4

Influence of Nitrogen Partial Pressure on Wear Resistance of Coated Parts

Steel grade	Wear resistance, $g \cdot 10^{-4}$ at partial pressure			
	Uncoated	$3 \cdot 10^{-3}$ Pa	$3 \cdot 10^{-2}$ Pa	1 Pa
38X2MFUA	3,0	2,8	2,5	2,0

Table 3.5

Effect of Thickness of Applied Titanium Nitride Coating
on the wear resistance of parts

Steel grade	Wear resistance, $g \cdot 10^{-4}$ at a partial pressure of 1 Pa						
	Uncoated	Coating thickness, μm					
		2	3	4	5	6	7
38X2MFUA	3,0	2,9	2,5	2,2	2,0	1,9	2,7

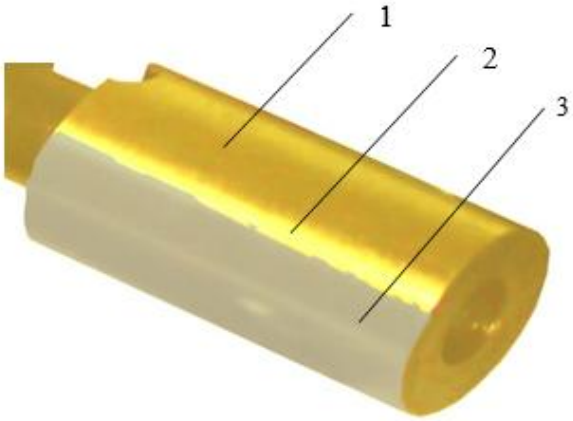

1 – coverage; 2 – detachment boundary ; 3 – Substrate

Fig 3.2 – Initial stage of peeling of a coating with a thickness of 7 μm

Corrosion resistance tests were carried out on samples made of 38Cr2MFUA steel with titanium nitride coating and uncoated. The tests were carried out in water at a temperature of 20°C for 1000 hours. The corrosion rate at the beginning of exposure to an aqueous environment (24 hours) is high, although it is noticeable that the corrosion rate index increases more slowly in plasma-coated samples. Such dependence takes place in the first 24 hours. Then there is a significant decrease in the corrosion rate indicator. The value of the corrosion rate indicator stabilizes and subsequently decreases only slowly.

Thus, in order to obtain a high-quality coating on parts of a volumetric hydraulic drive made of 38X2MUA steel, it is necessary to carry out ion bombardment of the surface at a voltage of 1000 V at an operating vacuum of $6 \cdot 10^{-3}$ Pa. The heating temperature of the surface of the parts should not exceed 500 ° C. The subsequent condensation of the coating should be carried out at a partial pressure of nitrogen of 1 Pa. The optimal coating thickness is 6 microns. The choice of these parameters is justified by the

achievement of the best adhesion of the coating and substrate, increasing wear resistance, corrosion resistance.

4.3 Structure and phase composition of applied plasma coatings of dual purpose parts

To reveal the physical essence of the optimal coating, it was necessary to investigate its structure and phase composition. A significant amount of droplet phase is observed on the surface of the studied samples, made of 38X2MЮA steel, heated by ion bombardment to a temperature of 500°C (Fig. 3.4).

X-ray microspectral analysis established that this is precipitation (Fig. 3.5).

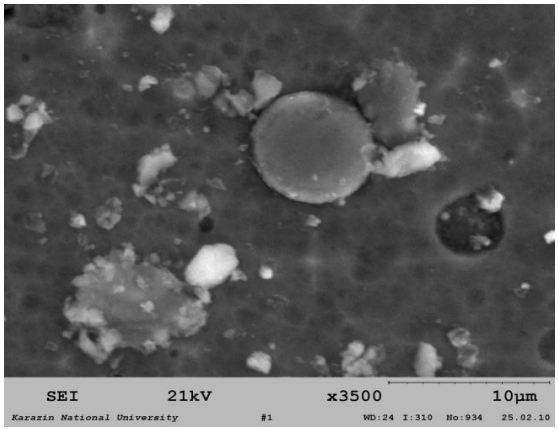

Fig 3.4 – Surface became after bombing ions titanium

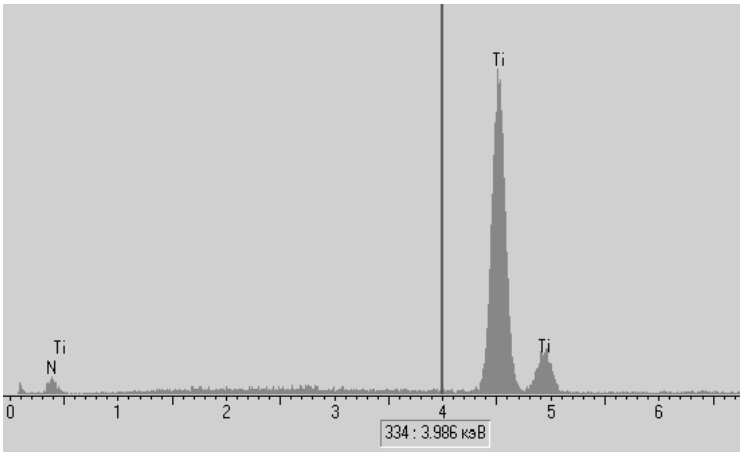

Fig 3.5 – Microdistribution titanium on surface after ion bombardment

The presence of titanium in the substrate was not detected. The hardness of the surface layer after ion bombardment increased from 400–450 MPa to 1050–1100 MPa. The next step after bombardment is coating deposition. When comparing the microstructure of the steel surface after heat treatment and preparation of the surface for coating (Fig. 3.6, a) with the microstructure of the same surface after coating (Fig. 3.6, b), it is noticeable that the applied titanium nitride coating smooths out the irregularities that can play the role of stress concentrates, as well as some geometric defects.

Fig. 3.6, a – Appearance goldsmith with became 38X2MUA after heat treatment and grinding

Fig. 3.6, b – External appearance goldsmith from coating nitride titanium

This comparison allows you to determine the surface preparation requirements for coating. The surface prepared for plasma coating must be

mechanically clean, free of foreign inclusions, have a high level of surface cleanliness, and must not contain any defects. Micro -X-ray spectral studies have shown that the coating contains titanium, nitrogen and carbon (Fig. 3.7). Titanium and nitrogen were not detected in the matrix of the studied samples. The applied coating does not significantly change the composition and structure of the base metal. The distribution of elements from the surface of the coated part, presented in Fig. 3.7 shows that the titanium content reaches its maximum value directly on the surface, then the amount of titanium decreases and a second spike (2 times smaller than on the surface itself) is observed at a depth of ~ 3 μm , followed by a sharp decrease in titanium.

This is explained by the fact that in the α– Ti coating , it gradually decreases from the substrate to the outer surface of the coating, as it is deposited on the surface during the bombardment, and in the condensing coating, the minimum amount of the droplet phase is observed. As for carbon, the maximum value is at a depth of ~ 3 μm . The nitrogen content is greatest at a depth of ~ 3 μm and then sharply decreases with increasing depth.

The content of other elements, starting from 4 μm , is almost the same. Obviously, carbon diffuses from the matrix towards the coating when the surface is heated during ion bombardment. At the same time, high adhesion of the coating to the substrate and low adhesion to the material being processed is achieved, which is one of the main requirements for the coating to ensure high wear resistance of parts. X-ray structural studies showed that residual compressive stresses of 1800 MPa were found in the near-surface layer of the coating. This fact is of great importance for increasing wear resistance. Due to the fact that tensile stresses are

responsible for the destruction, the presence of compressive stresses strengthens the working surface more strongly, the greater their value.

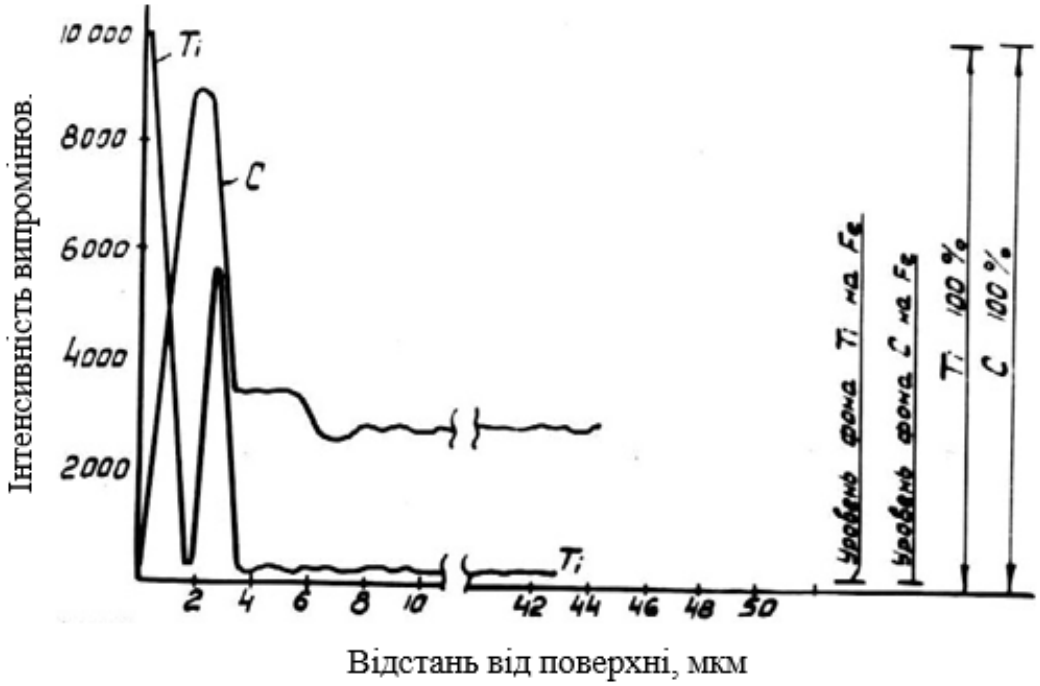

Fig. 3.7 – Distribution elements along coating, transitional zones and matrices sample

Compressive stresses occur if the coefficient of thermal expansion of the base material is much smaller than the coating. When cooling a part with a coating, the diameter of the cylindrical part will decrease faster than the diameter of the coating and due to the contact forces acting between the coating and the surface of the part, the coating will compress, that is, compressive stresses will arise in it. As the coating thickness increases, the force required to compress the coating must increase, while the bond strength between the surface of the part and the coating remains constant. Therefore, with an increase in the thickness of the coating, when it reaches a critical value, peeling of the coating should occur.

3.4 The influence of plasma coatings on tribotechnical characteristics of the studied materials

Tribotechnical tests were carried out to assess the feasibility of using ion-plasma technology for parts of a volumetric hydraulic drive . Research on wear resistance was carried out by the SMC-2 machine. The duration of the tests was 10 hours with a total load of 200 N.

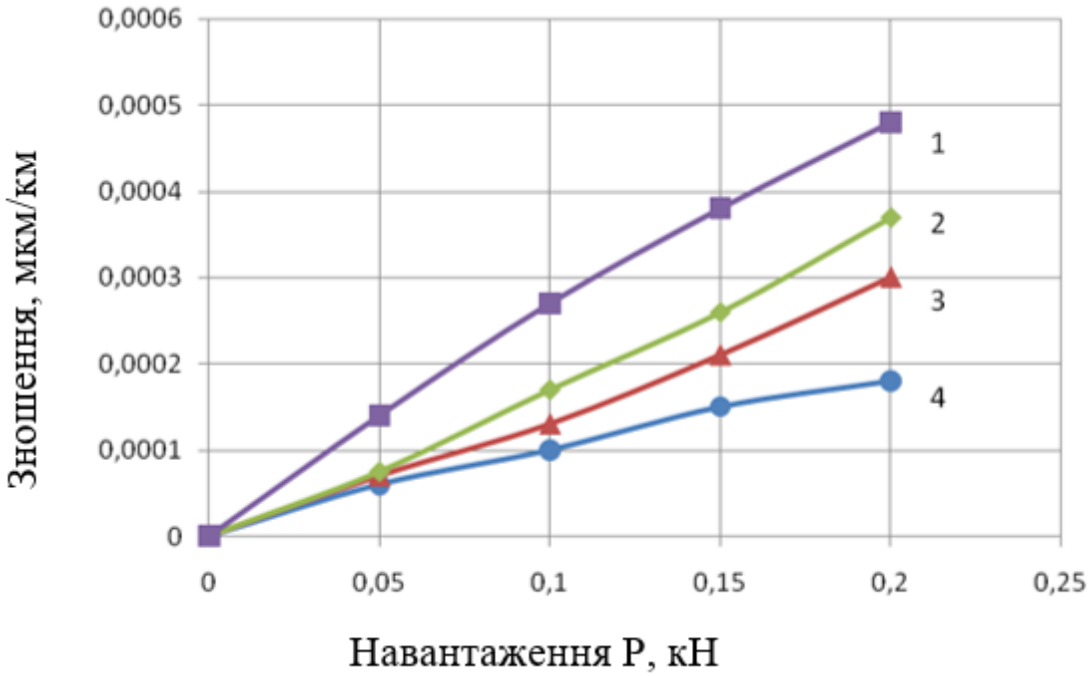

1, 2 – steel 38 Kh2MUA after nitriding;

3, 4 – steel 38 X2MUA with Ti -N coating

Fig 3.8 – Influence superficial processing on value wear and tear

The rollers were made of 38X2MUA steel. A total of 10 samples were tested. Five were nitrided, and the others were plasma coated with titanium nitride at the installation. "Bulat 3T" with the same technological parameters. The pads are made of graphite cast iron, the chemical composition of which is given in the table. 3.6.

Table 3.6

Chemical composition of the counterbody material

Sample No	Contents elements, %							
	C	Mn	Si	P	Cr	No	Mo	Cu
1–10	–	0.9-1.0	1.8	0.1-0.12	0.35	0.9-1.0	0.45-0.55	0.35-0.4

The results of wear resistance tests showed that titanium nitride coating reduces the wear of 38X2MUA steel by more than 2 times compared to nitriding.

In table 3.7 given average the results wearable tests everyone researched materials.

Table 3.7

The results wearable tests

Material disc	Pad material	Wear and tear reel, Mr. 10^{-4}, (average of three tests)	Wear and tear pads, $g \cdot 10^{-4}$, (average of three tests)
steel 45	SC20	46.0	26
steel 45 with carbonation	SC20	40.0	18
steel 38X2MUA	SC20	25.0	15
steel 38X2MUA with nitriding	SC20	19	12
steel 38X2MUA with coating TI–N	SC20	9	6

According to the results of the wear resistance tests, it can be concluded that the titanium nitride coating contributes to an increase in wear resistance compared to nitrided steel (by 48%), as well as a reduction in the wear of the gray cast iron mating material (by 27%) in the tested sliding conditions.

4.5 Determination of friction coefficients of a part with a plasma coating

Friction coefficients show the resistance of a part with a plasma coating to burr formation . Friction coefficients were calculated taking into account the diagram of the moment of friction. In fig. 3.9 shows the dependence of friction coefficients on load.

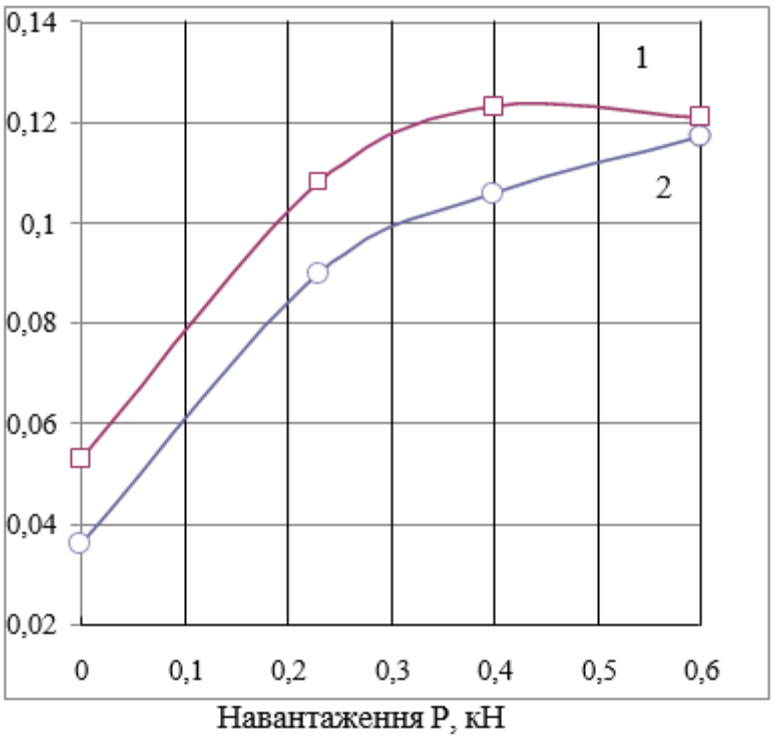

1 – steel sample 38X2MЮA without Ti -N coating;

2 – sample of steel 38X2MЮA with Ti -N coating

Fig 3.9 – Dependence of friction coefficients on load

As can be seen from the graphs in fig. 3.9, under almost all loads, the coefficient of friction of the 38X2MUA steel sample with coating ~is 30% less than without coating.

4.6 Characteristics of the strength of a part with a plasma coating

A set of studies was conducted to determine the strength characteristics of the studied steels after heat treatment and after applying the appropriate coatings.

The results of the research are given in table. 3.8.

Table 3.8

Results of studies of strength characteristics

Sample No	Brand became	Type of strengthening treatment	Presence of surface defects	Hardness in friction zone HV_5	Final stresses, σ_{ost}, MPa	End hardness
1	Steel 45	Hardening + high leave	not detected	271-283	210	180-192
2	Steel 45	Carbonitration	not detected	396-450	250	320-340
3	38X2MUA	Hardening + high leave	not detected	300-320	240	315-320
4	38X2MUA	Improvement + nitriding	not detected	349-362	260	329
5	38X2MUA	Enhancement + coverage Ti-N	not detected	550-570	490	410-430

Sample No. 1 hardening by quenching followed by high relaxation. Changes in hardness on the surface of this sample were not detected as a result of the tests.

Sample No. 2 has a slight increase in H_v *hardness* friction surfaces in comparison with the hardness of the core. Which can be explained by two possible reasons: an increase in the content of carbon and nitrogen in the surface layer as a result of carbonization after heat treatment; strengthening of the surface layer during the tests.

Sample No. 3, which after improvement was strengthened by nitriding, has a natural increase in hardness.

In sample No. 5, the coating is not detected during metallographic examination of the cross section due to its small thickness (less than 5 μm). Slightly, however, the increase in the hardness of this sample compared to the core is explained by the effect of Ti –N plasma coating. X-ray structural studies showed that residual radial compressive stresses are present in the near-surface layers of all samples.

For samples No. 1, 2, 3, the value of these stresses is almost at the same level (–210...260 MPa).

In sample No. 5 with Ti -N coating, the maximum level of residual compressive stress (–490 MPa) was found in the near-surface layers, which can be attributed to the effect of Ti -N plasma coatings.

4.7 Determination of nanohardness and modulus of elasticity

The value of nanohardness was determined by the method of Oliver and Far by the depth of the impression at the maximum load on the indenter . The modulus of elasticity was determined by the unloading curve of the indenter using the device " Nano Indenter II".

In the table 3.8–3.9 show the obtained values of nanohardness and modulus of elasticity under different loads at different depths of indenter insertion.

An analysis of the results of the obtained values of nanohardness was carried out . In fig. 3.12 presents histograms, from which it follows that the nanohardness of the 38X2MUA steel with a plasma coating is 2 times higher than the nanohardness of the 45 steel with a carbonitride coating.

The conducted studies showed that increasing the load by 5 times from 10 mN to 50 mN does not significantly affect the value of nanohardness (Fig. 3.13).

Table 3.9

Nanoindentation results for steel 45

View processing of steel 45	Embossing depth Indian (nm)	Load, mH	Modulus of elasticity, E(F), GPa	Nanosolid H(F), GPa
polished without coating	307.3	10.0	226	4.2
	325.0	10.0	199	3.8
	292.7	10.0	217	4.7
	294.7	10.0	208	4.6
	341.0	10.0	223	3.5
	312.1	10.0	214	4.2
stand deviation	20.6	0.0	11	0.5
after carbonitration	252.0	10.0	205	6.4
	240.2	10.0	198	7.1
	238.2	10.0	216	7.1
	236.1	10.0	220	7.2
	244.2	10.0	213	6.8
Average	242.1	10.0	210	6.9
stand deviation	6.2	0.0	9	0.3

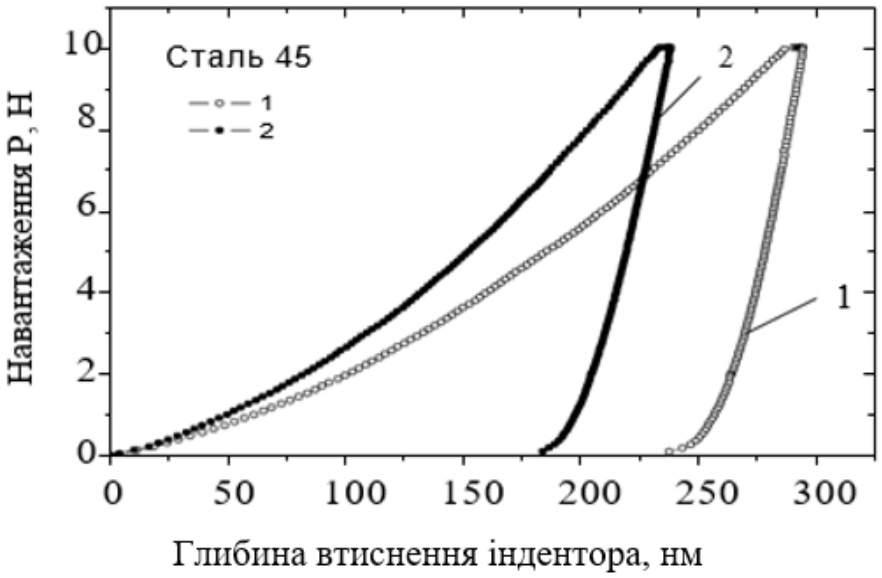

1 – steel 45 without surface treatment;

2 – steel 45 after carbonitriding

Fig 3.10 – Indentation diagram of steel 45

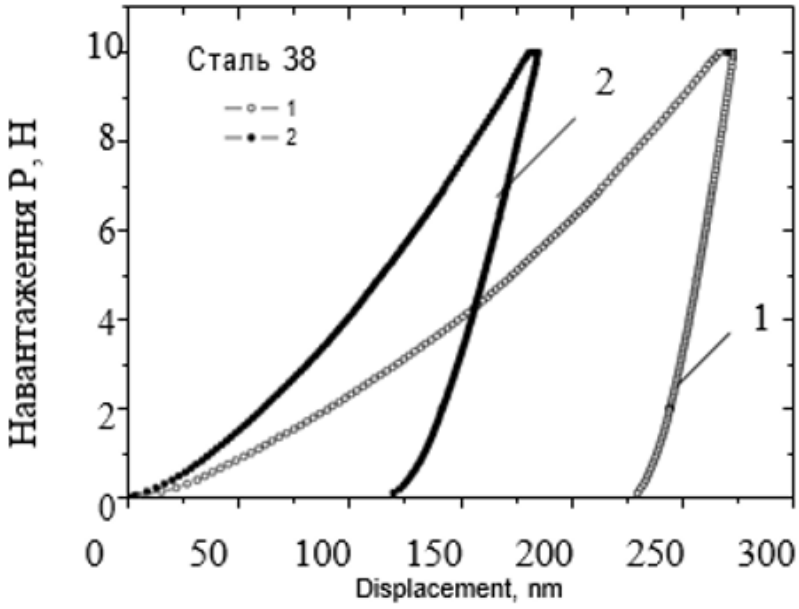

Глибина втиснення індентора, нм

○ 1 – steel 38X2MФЯA without surface treatment;

• 2 – steel 38X2MFYUA after applying Ti -N plasma coating

Fig 3.11 – Diagram of indentation of steel 38X2MFYUA

Table 3.10

Results of nanoindentation for steel 38X2MUA

Type of steel processing 38X2MUA	Depth of indentation ind . (nm)	loading , mH	Modulus of elasticity E, GPa	Value of hardness H, GPa	Hardness level according to ISO 14577
Polished without coating	286.6	10.0	211	4.9	Microhardness
	286.5	10.0	213	4.9	
	282.1	10.0	215	5.0	
	273.3	10.0	216	5.4	
	300.6	10.0	204	4.5	
	285.8	10.0	212	4.9	
stand leave	9.9	0.0	5	0.3	
with coating Ti -N	191.1	10.0	229	11.3	Nano hardness
	181.7	10.0	246	12.4	
	193.3	10.0	230	11.7	
	188.8	10.0	226	11.0	
	185.1	10.0	220	12.3	
Average	188.0	10.0	230	11.7	
stand deviation	4.6	0.0	10	0.6	
with coating Ti -N	500.4	50.0	228	10.3	Microhardness
	484.9	50.0	247	10.9	
	501.7	50.0	236	10.2	
Average	495.7	50.0	237	10.5	
stand deviation	9.3	0.0	9	0.4	

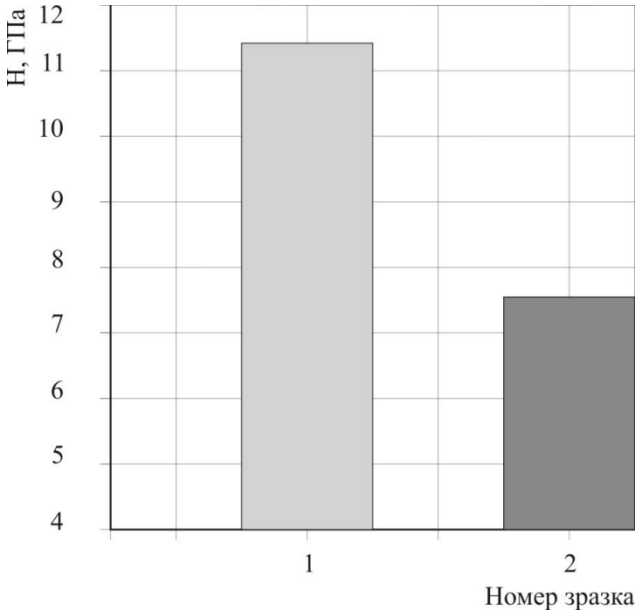

1 – nanohardness of the plasma coating applied to steel 38X2MUA;

2 – nanohardness carbonitride coating applied to steel 45

Fig 3.12 – Histograms of nanohardness under a load of 10 mN

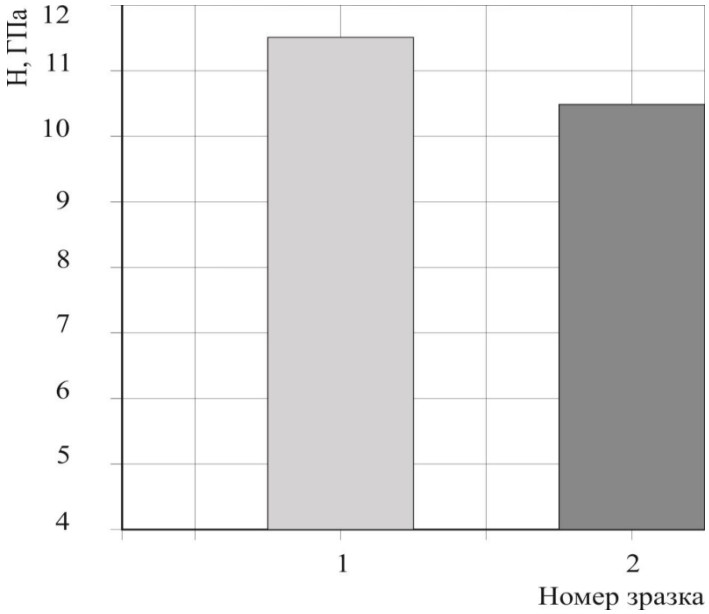

1 – load 10 mN ; 2 – load 50 mN

Fig 3.13 – Histograms of the nanohardness of the plasma coating applied to steel 38X2MUA

It should also be noted that the higher modulus of elasticity of the plasma coating applied to steel 38X2MUA compared to the carbonitride coating applied to steel 45 (Fig. 3.14).

This indicates that the moment of plastic deformation occurs in steel 38X2MUA at higher stresses.

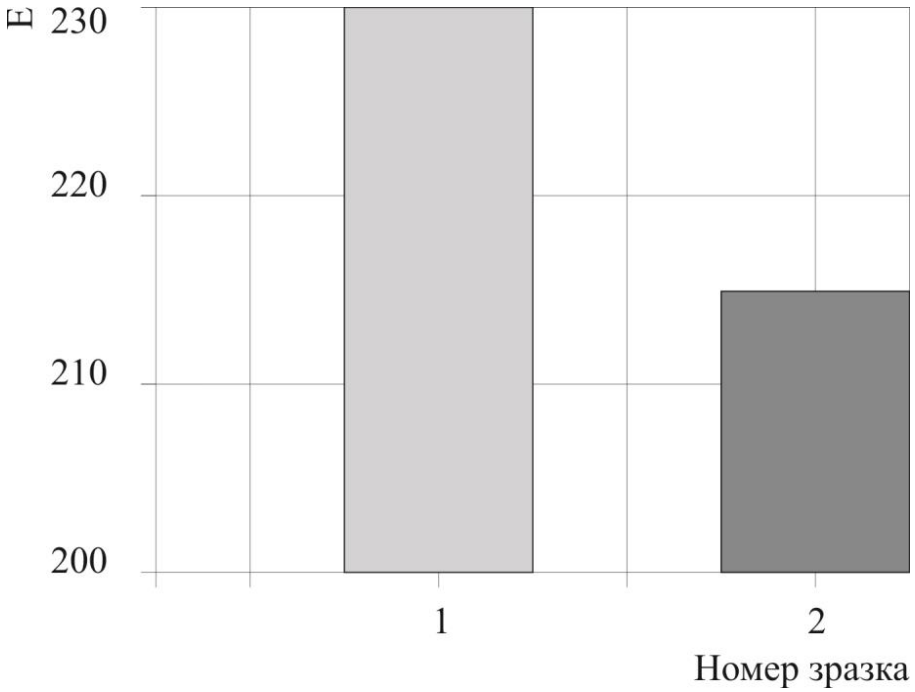

1 – steel 38X2MUA with plasma coating;

2 – steel 45 with carbonitride coating

Fig 3.14 – Histograms of the modulus of elasticity E

The strengthening effect due to the application of the coating is also indicative. So, for example, plasma coating applied to steel 38X2MUA contributes to an increase in hardness by 2.5 times, and carbonitride coating on steel 45 provides an increase in hardness by only 1.5 times (see Fig. 3.15 and Fig. 3.16 for comparison).

Thus, in order to increase the wear resistance and mechanical properties of the working surfaces of the counterbodies of precision friction

units, it is possible to recommend the use of 38X2MUA steel, which is coated with a plasma coating.

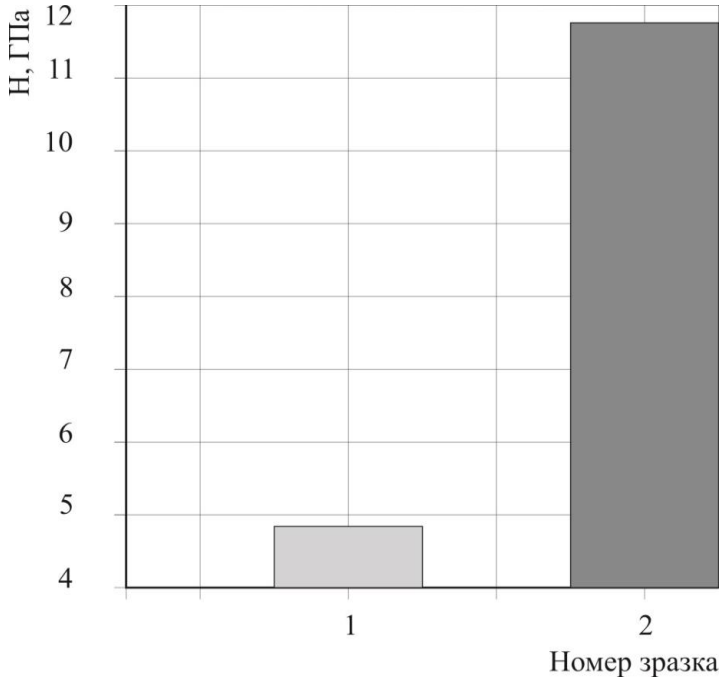

1 – without coating; 2 - with plasma coating

Fig 3.15 – Nanohardness histograms of steel 38X2MUA

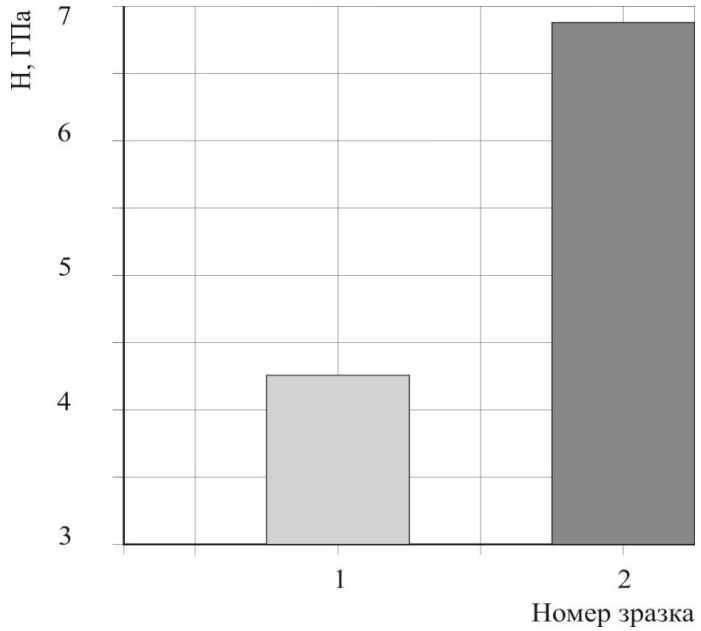

1 – without coating; 2 - with carbonitride coating

Fig 3.16 – Nanohardness histograms of steel 45

In order to improve the working characteristics of the parts of the volumetric hydraulic drive, made of 38X2MUA steel, an ion-plasma Ti -N coating with a thickness of 6 μm was chosen.

Wear tests have shown that applying a Ti -N coating to 38KhMYUA steel reduces wear by 3 times.

It was established that the nanohardness of 38X2MYUA steel with plasma coating is 2 times higher than the nanohardness of 45 steel with carbonitride coating.

Using the methods of X-ray and micro-X-ray research, it was established that the coating applied according to the selected modes consists of titanium, nitrogen, and carbon. Compressive stresses (up to 1800 MPa) are formed in it, which helps to increase the working characteristics.

SECTION 4.
MODELING OF THE STRUCTURE AND PROPERTIES OF THE STUDIED MATERIALS WITH APPLICATION OF THE THEORY OF MULTIFRACTALS

4.1. On the incompleteness of formal axiomatics in the tasks of identifying quality characteristics

The relevance of the implementation of this chapter is due to the fact that establishing an unambiguous correspondence between the elements of the metal structure and its properties is often a problematic task, since the elements of the structure often at different scale levels (macrostructure, microstructure, fine structure) have a complex geometric shape configuration. Based on the analysis of the quantitative and qualitative assessment of the real structures of many iron-carbon alloys, there are some discrepancies that are significant for practical use between the results of direct experiments to identify the structure of the metal and the methods of their prediction. So, for example, discrepancies between the results of the prediction of impact toughness (Fig. 4.1 *a*) and hardness (Fig. 4.1 *b-g*) of rolled cast iron rolls of SPKH execution, based on the determination of the area of structural components (perlite, carbides , lamellar graphite) and the ball (semi-quantitative) evaluation of graphite, indicating the difficulties that arise when predicting the quality characteristics of rolls from using previously known methods .

This fact testifies to the incompleteness of the formal axiomatics that arises when describing the elements of the metal structure using the

traditional figures of Euclid's geometry, which initiates the need to use other promising approaches to structure assessment.

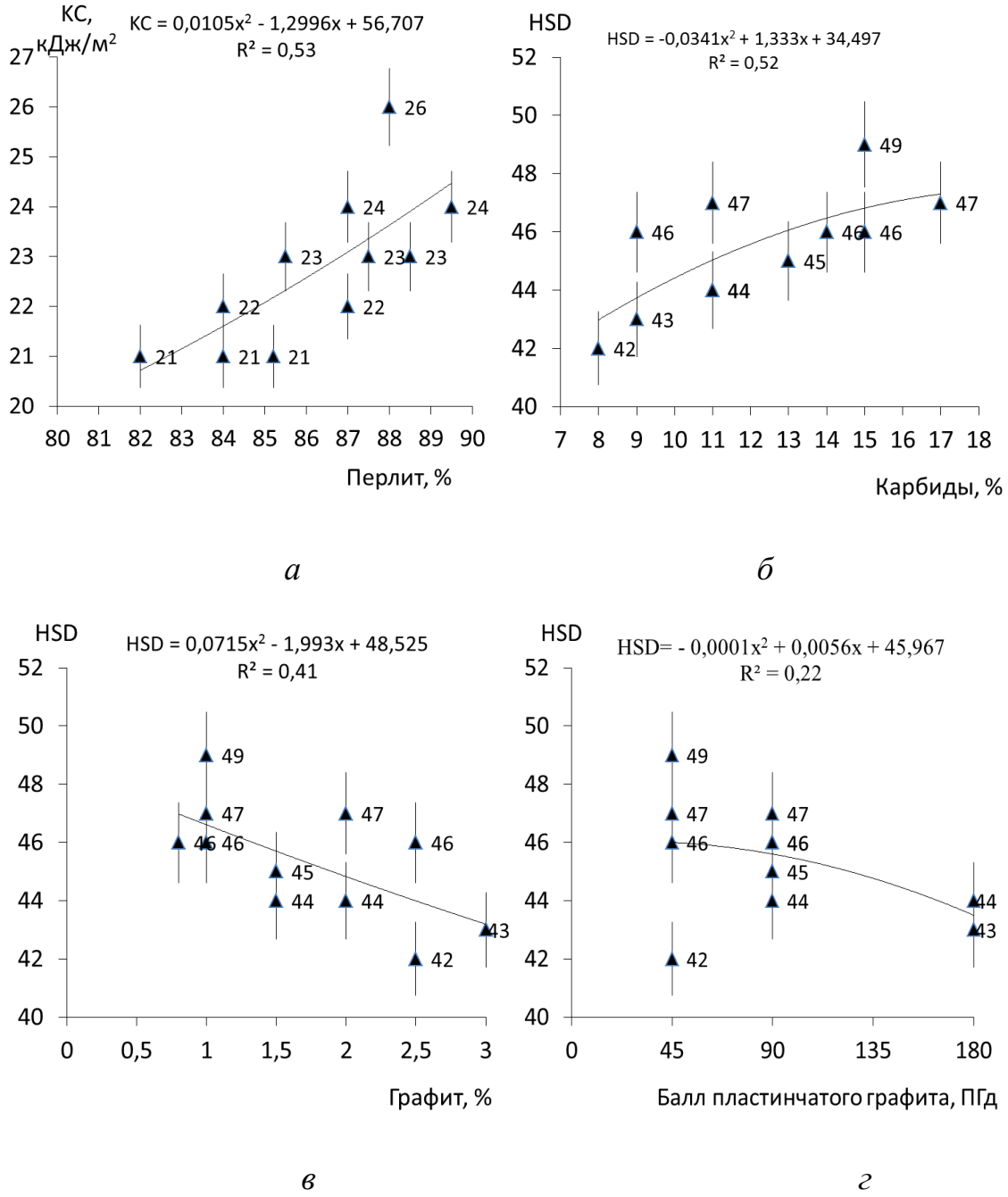

Fig. 4.1. Dependence of impact viscosity (*a*) and hardness (*b-d*) on the parameters of the structure of rolled cast iron with lamellar graphite

Gödel's incompleteness theorem proved that in theories constructed on the basis of formal axiomatics, the values of the original terms and their interpretations are incomplete, which is due to linguistic incompleteness of statements [101].

In this, extending the conclusions from this theorem to the interpretation of the statement that determines, for example, one or another numerical value of the quality of some metal, we accept that this statement is incomplete. This incompleteness is caused by some uncertainty, caused, first of all, by the relativity of measurements, which cannot be dispensed with when determining one or another regularity, and the inevitable incompleteness of statements made in the language used to interpret these statements. To partially eliminate the incompleteness of the formal axiomatics of the statements of S. Beer recommended the use of the principle of external complementation, based on the application of a higher-level language used to formulate statements [121]. Newly chosen solutions, expressed in a higher-level language, are designed to eliminate the shortcomings of the originally used language. The use of the newly chosen language acts as a practical method aimed at partially overcoming the complexity that is a consequence of Gödel's theorem . WITH. Beer recommended that in order to go beyond the initially chosen language, but at the same time not to break away from the real situation, one should be attached to such a property of the system that is inextricably linked to its actual existence.

For example, obviously, for most materials, this property is one or another characteristic of their quality. In order to show this, let's stop our choice on the currently existing processes of identification of the structure of the material, which, as experience and numerous theoretical studies show , reflects the characteristics of its quality [93-117]. At the same time,

the approximation of structural elements with a complex geometric shape configuration is usually carried out by whole Euclid figures [62], which introduces a certain error in finding the characteristics of the material quality. This fact initiates the need for a possible replacement of the geometric characteristics of the structural elements (length, area, volume) with a more differentiated assessment, which, it is assumed, should partially compensate for the incompleteness of the existing formal axiomatics.

The development of methods for assessing the structure of materials, taking into account scientific and technical progress, has brought to a new level the possibility of conducting their quantitative assessment. To study the structure and properties of metals and alloys, traditional methods of X-ray structural analysis, optical and electron microscopy, thermal analysis, micro-X-ray spectral sounding, nuclear magnetic resonance, Auger are used –spectroscopy, etc. The relationship between the parameters of the structure of metals and their physical complex has been studied by many authors [75-110]. This approach allows you to take into account the influence of elements of the metal structure on its properties for the purpose of clarification. However, the difficulty in obtaining such results is that many elements of the metal structure, due to their complex configuration, are difficult to describe quantitatively, which leads to the loss of important information about the tandem structure and properties –. Such characteristics include the currently existing assessment of the elements of the metal microstructure with the help of existing normative documents, which mainly use point (semi-quantitative) assessment. For a metal, the presence of an element of subjectivity in the assessment of its structure parameters is observed, for example, in the quantitative assessment of lamellar, vermicular and spherical graphite, ledeburite

eutectic, acicular ferrite, needles of martensite, Widmanstett ferrite, upper and lower bainite. which is explained by the complex configuration of their geometric shape. To evaluate such structures, it is necessary to introduce a new quantitative indicator of the structure.

The listed difficulties of assessing the structure of a metal initiate the search for fundamentally new methods of assessing its structure in order to determine the spectrum of its physical and mechanical properties, which would ensure the necessary accuracy of research results at the minimum possible costs.

In order to partially eliminate the incompleteness of the formal axiomatics of statements produced during the identification of the metal structure, according to the principle of external addition S. Bira , we use a higher-level language to formulate statements, which should eliminate the shortcomings of the language that is initially used.

To partially compensate for the incompleteness of the formal axiomatics of the metal structure, we will apply a higher-level language. In our opinion, such a language is the language of fractal geometry introduced by B. Mandelbrot [120]. Fractals existing in the world are called physical, and they have a finite interval of scales. Their physical definition is as follows: *Fractals* –these are geometric objects (lines, surfaces, bodies) that have a strongly cut structure and have the property of self-similarity on a limited scale.

Definition 1.1. A fractal is a functional mapping or a set obtained by an infinite recursive process and has the following properties: 1). Self-similarity or scale invariance (n outline scaling), that is, fractals on small scales look on average the same as on large ones; 2). Fractal dimensionality –fractional value and strictly greater than its topological dimension

(Hausdorff dimension); 3). Fractals are characterized by non-differentiability .

Another, simple, definition of fractals : Fractals are objects that have a fractional dimension and have the property of self-similarity [1][62]. I am B. Zeldovych and D.D. Sokolov give fractal the following definitions: " Fractal - thick line, fractal - thick surface, fractal –foamed space-time, fractal –level line, fractal –a dense set of points" [62]. A.D. Morozov extends the concept of fractals to a geometric structure with statistical self-similarity [62].

Fractals existing in the world are called physical, and they have a finite interval of scales. Their physical definition is as follows:

Definition 1.2. " Fractals –these are geometric objects (lines, surfaces, bodies) that have a strongly cut structure and have the property of self-similarity on a limited scale."

It should be noted that the presented definitions of fractals only complement each other, helping to understand their nature more deeply.

Fractal objects reflect the metric of space, in contrast to the entire Euclidean geometry, which studies not only the metric but also the shape of objects. The metric specifies a way to construct such a set that approximates the structure under consideration. Topology, in turn, studies only the shape of objects [68, 69].

In a number of scientific works of recent years, it was shown that one of the promising ways to adequately solve the problem of structure assessment is the use of the language of fractal geometry [60-80]. The multifaceted application of fractal geometry in materials science served as

[1]If according to the geometric shape of each parts object you can reproduce the whole object , then a part and the whole object are called self- similar Such operation invariant regarding the scale [120].

an impetus for the creation and development of fractal materials science. One of the first works on fractal materials science can be considered the works of B.M. Smirnova, E. Federa , V.S. Ivanova and others (see, for example, [60-80]). Among the scientific works of domestic scientists, the works of S.V. deserve high praise. Svechnikova, V.P. Shestopalova [62], A.F. Turbina and N.V. Hardworking [62]. In the work of S.V. Svechnikov "Materials with a cluster structure, –new properties, new possibilities" close attention is paid to the nanocrystalline structure of cluster materials, which is quantitatively described thanks to the fractal dimension. It emphasizes that in nature, as it turned out, fractal forms are extremely widespread. With clusters, they are brought together by the conditions of growth according to the same mechanism of diffusion segregation, –which is spreading, the distributed structure and fractional dimension, characteristic, generally speaking, of disordered systems. In materials science, to describe the elements of the microstructure, the Euclidean dimension is traditionally used d, characterized by four values: $d = 0$ for point defects (vacancies, interstitial atoms); $d = 1$ for linear defects (dislocations); $d = 2$ for planar defects (twins, grain boundaries , etc.); $d = 3$ for three-dimensional formations by the volume of the sample.

The concept of fractal is practically related to both the characteristics of the metal structure and the physical characteristics of products made from it: with a rough surface; volume; density, etc. This choice is based on the fact that a huge number of real physical systems have (in the corresponding ranges of scales) a fractal nature, characterized by the fractional dimension D_0 (the Hausdorff-Bezykovich dimension) [62]:

$$D_0 = \mathrm{tg}\alpha = \frac{\ln N(\delta)}{\ln \delta}, \qquad (4.1)$$

where $N(\delta)$ –the number of cells that covered the object under study, δ –linear cell size.

fractal dimension is invariant to the scale of the object under study (Fig. 4.2). When choosing scales smaller than critical [2]or larger critical, the fractal dimension depends on extrapolation or interpolation [62].

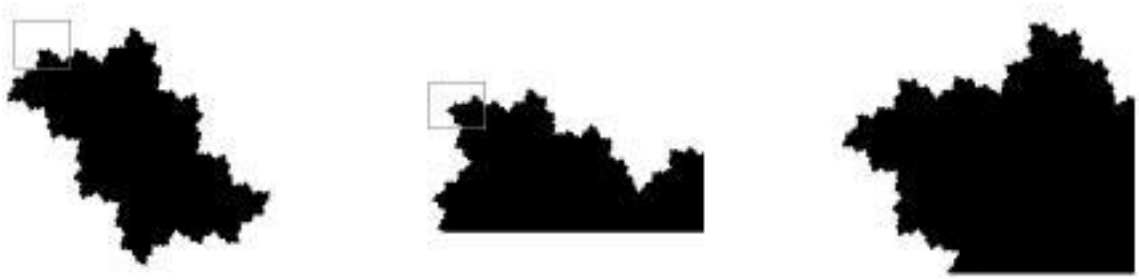

Fig. 4.2. Scale invariance
fractal dimension of the object [62]

Fractal objects reflect the metric of space, in contrast to the entire Euclidean geometry, which studies not only the metric but also the shape of objects. The metric specifies a way to construct such a set that approximates the structure under consideration. Topology, in turn, studies only the shape of objects [62].

Let's assume that the object of identification is the grinding structure of some material. Let's call the distance between two points a and b the surface of this cut the length of the shortest arc that lies with all its points on its surface and connects these two points. The metric given in this way is the internal metric of the surface, and the surface itself is transformed into a metric space. It follows from this that the internal metric of the structure of the grinding surface is a regularity "embedded" in this

[2]The critical scale is the scale which larger than the original scale and commensurate with the dimensions object .

structure. Note that the concept of metric is inextricably linked with the concept of dimension. For example, the length of a fractal curve L can be calculated as $L(\varepsilon) \approx \varepsilon^{1-d}$, where ε –the length of the link of the broken line that replaces the curve L, a d –the fractal dimension of this curve. It follows that the internal metric of the structure of the surface of the cut is a function of its fractal dimension, so it reflects the qualitative characteristics of the material [62].

Fractal geometry made it possible to give a quantitative characterization of the Cantor set, Peano curves, Weierstrass functions and their numerous varieties, which were considered nonsense. Equal to unity for a line (infinite, semi-infinite , or finite segment), the Hausdorff-Bezykovich dimension increases as the tortuosity increases, while the topological dimension obstinately ignores all changes that occur to the line unless they are accompanied by breaking or gluing of some points. In this case, increasing its value, the dimension of Hausdorff - Bezykovich does not change it by a jump, but takes fractional values (Fig. 4.3).

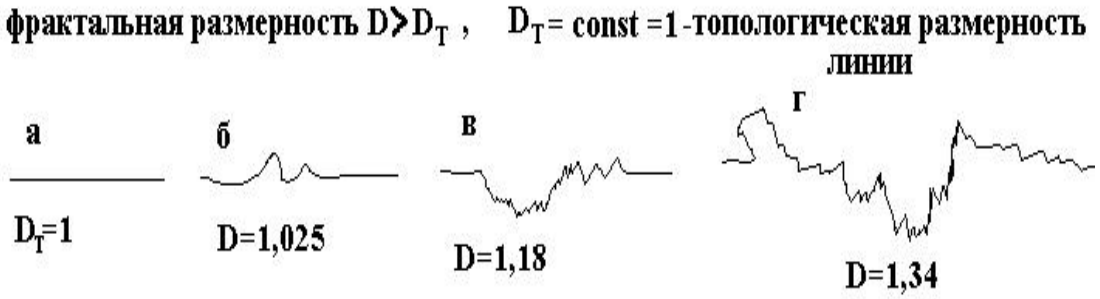

Fig. 4.3. *a* –topological and fractal dimensions are equal to one for a straight line; *b* –the fractal dimension is 1.025 for a slightly sinuous line; *c* –for a more tortuous one, it is equal to 1.18; *d* –for very winding - 1.34 [62]

Taking into account the lack of satisfactory mathematical descriptions of the processes that occur, for example, in the alloying of metals (that is, those that would be used in practical calculations and would be sufficiently reliable), it can be assumed that such a complex system as a metal, or rather its components, does not have a whole , and the fractional dimension, i.e. this system refers to fractals .

Euclidean dimensions can be characteristics of symmetric microstructures, which are often formed even in materials obtained under quasi-equilibrium conditions, since the formation of a real structure is due to phenomena far from equilibrium. Unlike integer Euclidean geometry, fractal geometry is characterized by a spectrum of fractal dimensions for each element of the metal structure in one-dimensional space (line), two-dimensional space (plane) , etc. Fractal dimensionality is sensitive to changes in structural components, which can be taken into account by integer Euclidean geometry. So, for example, the interface between a solid body and the surrounding space can be fractal . It can be:

–surface fractal - in this case, the surface area is characterized by an indicator of fractal dimension D, and the volume of the solid body and the volume of pores change as the volume of the sample in the entire range of analyzed scales, i.e. are characterized by an integer numerical Euclidean dimension R^3;

–mass fractal - in this case, the surface area and volume of a solid body are characterized by the indicator D, and the volume of pores changes as the total volume;

–fractal pores - in this case, the surface area and the volume of the pores change equally (with the indicator D), and the volume of the solid body changes as the total volume (see Fig. 4.4).

Although the algorithms for constructing some fractals have been known for a long time, it was only with the development of computer technologies that it became possible to see them through a complex implementation. Fractals shown in fig. 4.5 was obtained only thanks to computer simulation. Some of those shown in fig. 5.5 fractal objects can be compared with real structures of materials. So, for example, a fractal obtained with the help of "rotation - compression" (Fig. 4.5 *e*) can resemble dendritic structures of metals. By choosing different ways of transforming Euclidean figures, it is possible to obtain such structures with the help of modeling that will be analogs of real structures of materials or their individual elements. This will allow a deeper understanding of the real structure of the material structure.

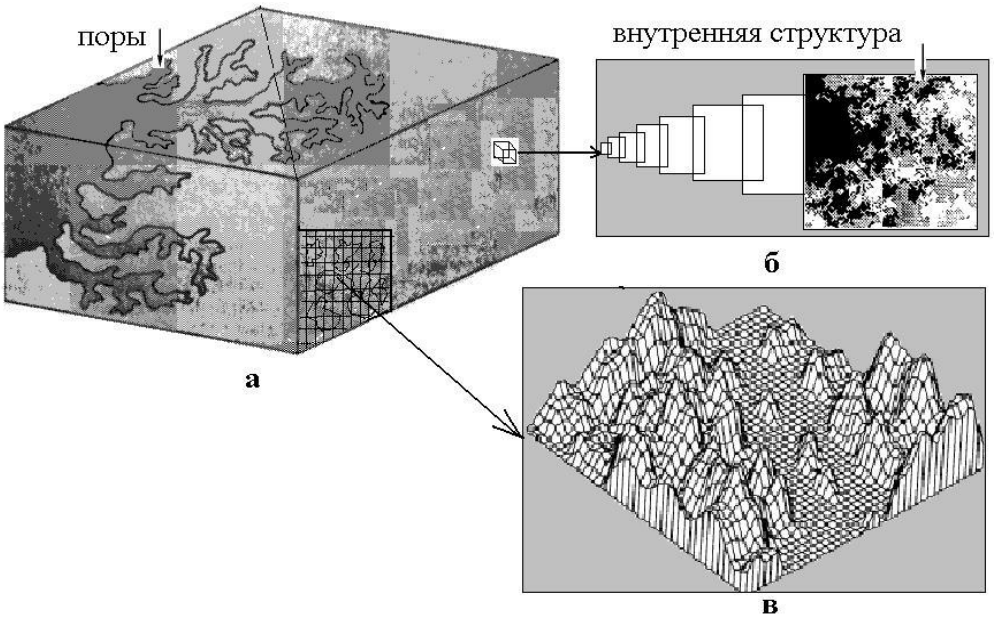

Fig. 4.4. Fractal pores (*a*), mass fractal (*b*), surface fractal (*c*)

Thus, only for $D \to 3$the three classes considered above, the fractals coincide. It is possible to qualitatively determine whether this or that

surface of the material is fractal by examining it under an optical microscope, and if necessary, under an electronic one, at different magnifications. Fractal surfaces have no length scale, and at different magnifications they should have practically the same fractal dimension and look the same. Therefore, the application of the fractal dimension of the quantitative assessment of the metal structure is an important tool for the study of quantitative indicators of the metal structure. Many publications emphasize that the fractal (small) dimension serves as a strict quantitative characteristic of the parameters of the structure of metals with a complex configuration, for example: grains , grain boundaries , brittle and viscous fracture surfaces, clusters of dislocations, etc. [62]. The fractal dimension reflects the compactness of filling the space with the studied material. Since the structure of any metal determines its properties, and the fractal dimension quantifies the structure, then, based on this, it must somehow reflect some of the properties of the metal. In favor of the use of fractal dimensions to identify the qualitative characteristics of metals, in particular, mechanical properties, says their universality. Among them are methods of vertical sections and Fourier analysis of profiles, scaling (self-similarity) of power spectrum, correlation function, small-angle scattering, optical diffraction, variograms , as well as methods of adsorption probes, skin effect, methods of thermodynamics, nuclear magnetic resonance 62] . Fractality in nature is manifested at all scale levels: starting from the structure of atoms and ending with clusters of galaxies. Obviously, due to the fact that it is impossible to objectively describe the complex structure of a real material with only one value of the fractal dimension, the concept of multifractal was introduced . The use of the multifractal formalism opens up wide possibilities in this regard. This is characteristic, first of all, for metals whose structure consists of several phases (for example, ferrite -

pearlite, mixed ferrite-bainite , ferrite - bainite -martensitic structures , etc.), which are characterized by a spectrum of statistical dimensions . Using the concept of multifractals opens up the possibility of finding correlations between property indicators and parameters of external influence, on the one hand, and the structure of the metal, –on the other. The use of statistical dimensions of structural elements in order to assess the quality characteristics of metal contributes to their formalization as a function of fractal dimension. In turn, this makes it possible to determine and predict the physical and mechanical properties of the metal without performing special mechanical tests . It should be noted that the use of fractal dimension to assess the structure of a metal in order to determine its qualitative characteristics does not in any way replace other methods aimed at solving this problem, but complements them, as it provides the researcher with additional information about the relationship between structure and properties.

If Euclidean geometry is an integer dimension, for example, zero dimension at a point (internodal atom), unit dimension at a line (dislocation), at plane 2 (grain boundary), at volume 3 (dispersive particle), then the fractal dimension gives each component structure own quantitative assessment. It turns out that practically all materials in nature are fractal at different scale levels [62]. The upper scale level is limited by the dimensions of the entire object, the lower one is limited by its atomic structure.

Fractal famous classical objects such as Koch snowflake, Sierpinski triangle and carpet , fractal Minkowski are obtained by the appropriate step-by-step transformation of Euclidean figures: line, triangle, square, cube, etc. There are still many modifications of the transformation of Euclidean figures into fractal ones (Fig. 4.5) [622].

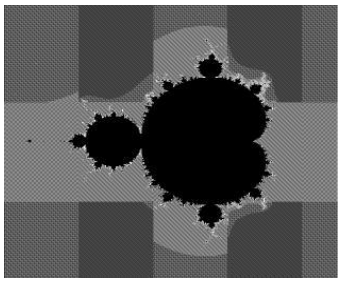

a – Fractal Mandelbrot

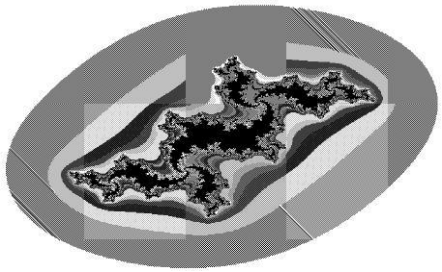

b – Fractal Julia

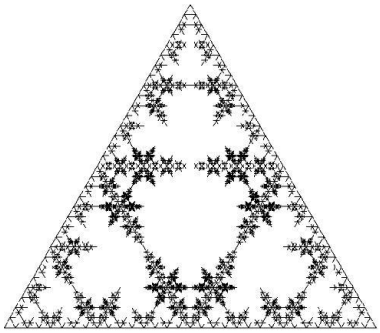

c – "Ice" *triangle* – "Tree" of Pythagoras

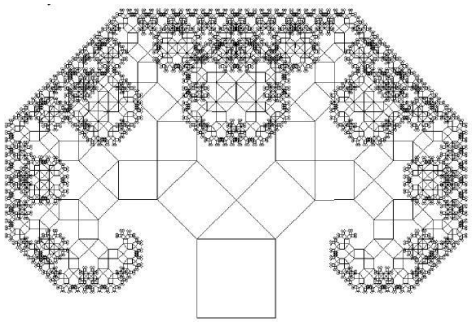

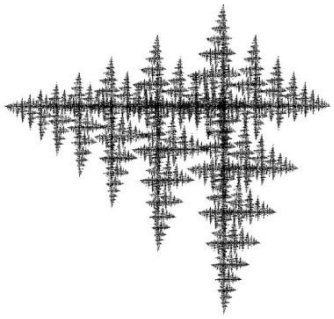

d – Fractal , obtained with the help of "rotation - compression"

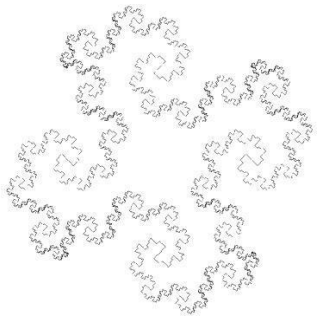

e – Minkovsky's "Island".

Fig. 4.5. Fractal objects obtained by step-by-step transformation of Euclidean figures

The complex configuration of microstructural components does not allow giving a full adequate assessment of these parameters and the entire microstructure in general. Basically, this calculation is carried out due to the study of statistical parameters of the microstructural components of the

metal and the study of each phase separately, and the study of multiphase systems is quite difficult.

In addition, taking into account various types of transformations and phase transitions, in metals and composites there are no clearly established boundaries between structural components, due to which they themselves and their boundaries acquire a complex shape, and do not have, in the classical sense, a finite measure (length, area etc.) . Fractal structures of metals are shown in fig. 4.6.

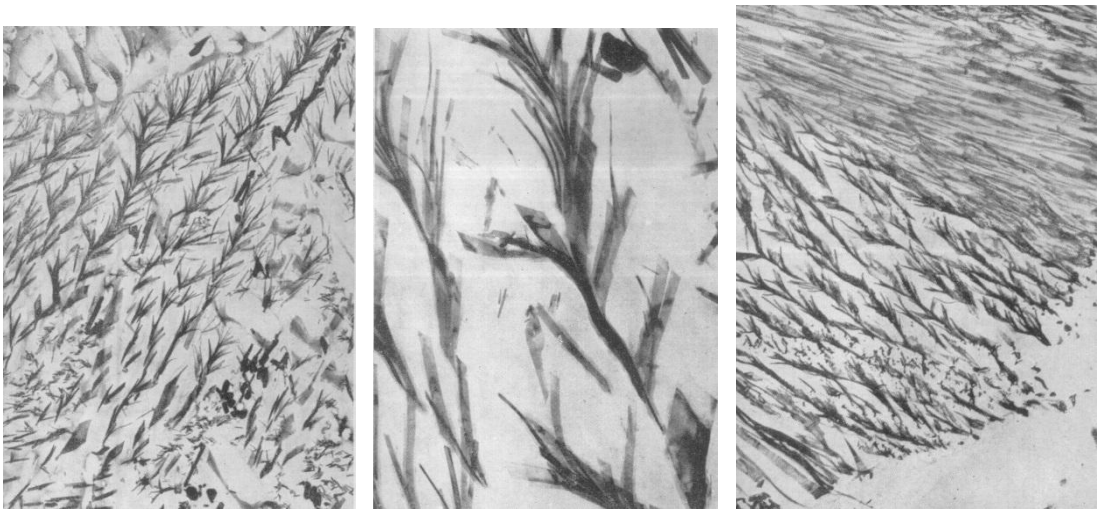

a *b* *c*

Fig. 4.6. Metal structure: *a* – extraction replica of the dendritic structure of lamellar carbides chrome-molybdenum steel, ×10,000;

b – area of the dendritic structure of the picture , ×40000;

c – extraction replica of pearlite carbide Me_7C_3 (×5000) [62]

Therefore, it is advisable to use the apparatus of fractal geometry for the quantitative assessment of the microstructure, since, as shown in publications [75-80], the fractal dimension of the structure can be an indicator of its qualitative characteristics. However, on this path there are certain difficulties associated with establishing a connection between the fractal structure of

materials and their properties. The latter is dictated by the absence of a rule of transition from the size of the fractal dimension of the structure to the numerical value of one or another qualitative characteristic of the metal. Fed Ens studied the fractal structure of clusters of iron, gold, and zinc [62].

The list of the main areas of use of fractal geometry in materials science can currently include:

Modeling the structure of real objects.

Description of the processes of formation of the real structure of materials (nucleation and growth of clusters, dendrites).

Parameterization of structures or individual elements, in particular, have a complex configuration:

–for the microstructural level , jagged –grain boundaries , martensitic and bainite structures, acicular ferrite, etc.;

–for the macrostructural level –of pores, cracks, dendrites in the structure of ingots, etc.

We will show how the quality characteristics of cast iron differ with the use of both the method of metallographic analysis and the method based on the application of fractal theory to approximate its structure [62]. For a specific example and the reliability of the experiment, we examine the structure of two identical cast-iron rolls No. 26 and No. 28 of SSHKHNM-55 performance, cast in the same technological conditions with an identical chemical composition (Table 4.1) and without heat treatment.

Table 4.1

Chemical composition of rolled cast iron of the SSHKHNM-55 performance

C	Si	Mn	P	S	Cr	No	Mo	Cu	V	Mg
2.95	1.22	0.56	0.034	0.012	0.63	3.55	0.43	0.10	0.008	0.058

The size of the barrels of the rolls was 380630 ×mm. At the same time, for both rolls, grinds were made from the bottom of the barrel, the photos of the microstructure are visually different (Fig. 4.7). The difference in the images of the slices is probably due to some uncertainty caused, first of all, by the relativity of the measurements used, and the incompleteness of the statements interpreting the results of the experiments, their traditional formal axiomatics. Regardless of the degree of visual convergence of images of the structure of the cuts, from their statistical "similarity", they can practically, to the same extent, reflect the characteristics of the quality of cast iron, which, at the moment, satisfies the practical application of the results of such an analysis.

Roll No. 26 *Roll No. 28*

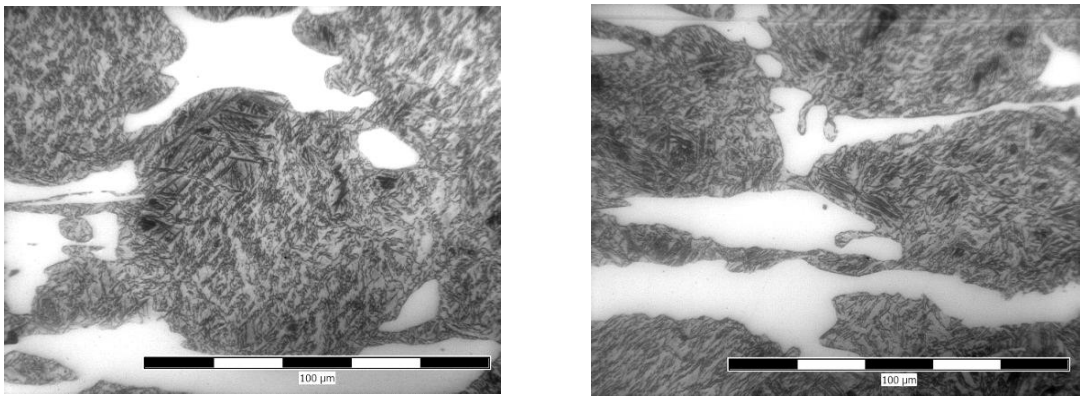

and *b*

Fig. 4.7. The structure of the bottom of the barrel of the SSHHNM-55 barrel, consisting of bainite, martensite, cementite and spherical graphite

From the currently existing methods of identifying the structure and properties of cast iron, the method of metallographic analysis was chosen, as it is knowledge-intensive and productive.

At the same time, numerical values of quality indicators obtained by analyzing the structure of cast iron rolls in three areas were compared: the bottom of the barrel, the upper club and the lower club. The structure of these areas is the same in composition, but different in the geometric shape of its elements (Fig. 4.7).

The results of the conducted metallographic analysis of the bottom of the barrels are identical for rolls #26 and #28, i.e.

$$Ts25 \rightarrow Tsp6000 \rightarrow ShGf4 \rightarrow ShGd25 \rightarrow ShGr1 \rightarrow ShG2,$$

where C is cementite, SHG is spherical graphite.

The evaluation of the structure of cast iron, determined based on the analysis of the fractal dimension of the elements of its structure, is given in table 4.2, lines 1-4. According to the results of full-scale experiments, the characteristics of the quality of the rolls (hardness) were determined, lines 5 and 6 of the table. 4.2.

The hardness was calculated statistically taking into account the fractal dimension of the structure:

$$HSD = 11571 \cdot D_{ц}^{3} - 65754 \cdot D_{ц}^{2} + 124279 \cdot D_{ц} - 78058, \qquad (4.2)$$

$$HSD = 1719.5 \cdot D_{R}^{3} - 9594.7 \cdot D_{R}^{2} + 17792 \cdot D_{R} - 10906, \qquad (4.3)$$

where HSD is Shore hardness , D_{c} and D_{D} - the fractal dimension of cementite and graphite, respectively.

The hardness of cast iron calculated by these equations is slightly different from the hardness obtained by field tests (a difference of up to 4%), which indicates the feasibility of using the language of fractal geometry to assess the quality of the metal.

Table 4.2

The structure and hardness of the rolls at a distance of 15 mm from the surface

o	Characteristic	Roll No. 26			Roll No. 28		
		botto m barrels	upper club	lower clubs	botto m barrels	upper clubs	lower clubs
1	2	3	4	5	6	7	8
1	Fractal dimension cementite	1,935	1,971	1,939	1,938	1,969	1,947
2	Fractal dimension of borders cement _ _ turn on	1,384	1,416	1,399	1,390	1,418	1,409
3	Fractal dimension of graphite	1,707	1,880	1,870	1, 724	1,920	1,888
4	Fractal dimension of graphite inclusion boundaries	1,080	1,226	1,222	1,385	1,257	1,261
5	Shore hardness , determined by field tests	60	55	58	61	55	58

							End of table 4.2
6	Shore hardness , taking into account the fractal dimension structures (according to equations (5.1 and 5.2))	58	54	56	61	53	57

The obtained results show that the characteristics of the quality of cast iron, calculated taking into account the fractal ones dimensions of its structure, it is economically expedient to produce, while minimizing the number of full-scale tests.

4.2. Formalization of the methodology

In order to establish the relationship between the elements of the cast iron structure: pearlite, graphite, carbides and selected mechanical properties: breaking and bending strength limit; impact viscosity; hardness, the authors used the method of multifractal formalism [60-80]. The proposed method is the most suitable for the quantitative assessment of most real structures, the approximation of which by whole numbers of Euclid's figures introduces a certain error due to the integrity of their approximation, and therefore is not always acceptable in practical tasks. According to the proposed method, based on the multifractal formalism, the structural elements of most cast irons and steels (ferrite, pearlite, bainite, martensite, carbides , graphite inclusions, etc.) with non-homogeneous areas can be estimated using the spectrum of statistical Regny sizes [69]. Some of the dimensions already have their own physical (material- based) interpretation.

For example, works [62-72] show the practical application of the theory of fractals , in particular the multifractal formalism, in the description of the physics of the process of forming the structure of various materials [306-309], as well as the connection of their physical and mechanical properties with dimensional estimates of phases, for example for of low-carbon, low-alloy St3ps steel after various heat treatment regimes [62]. With the use of multifractal analysis, many material science problems have been solved: the modes of obtaining and properties of oxide coatings on aluminum alloy have been optimized [62], the changes in the grain structure of an aluminum alloy under the impact of a high-speed particle have been recorded , the bainite - martensite models have been implemented to assess the dissipative properties of various metal materials ; the mechanical properties of the metal of the equipment of chemical productions during the examination of industrial safety were identified [62]. G.V. Vstovsky [62] notes that the use of the concept of multifractals makes it possible to give an adequate quantitative assessment not only of the configuration of the studied structure as a whole, but also of the inhomogeneity of the distribution of geometric, physical, chemical and other characteristics on it, according to the nature of the structure being studied, which cannot be achieved by conventional methods.

Let us consider the multifractal nature of the thin metal structure using the example of 14X2HMR steel [62].

The structure of the metal grain is heterogeneous. The reason for the inhomogeneity of the grain structure lies, for example, in the possible fluctuation of the chemical composition in different areas of the grain (micro-flocculation), which can be the result of crystallization, heat treatment, deformation , etc. This affects the change in the structure of the metal grain, that is, different areas of the grain have structural

features. For example, microsegregation on a prepared section is noticeably different from other areas of the grain in color, and accordingly in chemical composition and properties. From a fractal point of view geometry, there is a discrepancy between the probabilities of filling the space with the geometric dimensions of the corresponding areas (for example, for metals, this is observed at different large-scale structural levels). At the same time, the fractal dimension of different parts of the grain, which have a similar geometric configuration, may turn out to be the same, but at the same time, the chemical composition and properties will differ significantly. It turns out that along with the geometric characteristics determined by the value of the fractal dimension D , such fractals have some statistical properties.

Let's consider this on an example. Let us study the heterogeneous structure of 14X2HMR steels [62]. Let's highlight the triangular area ABC on the photo [3](Fig. 4.8). When considering this area, it may turn out that the density of filling it with elements of the structure of different sections of the ABC triangle is different.

Let's start sequentially cutting out equilateral triangles from the region ABC. In this case, we apply the method of random iterations, as in [62]. Let's give preference to one of the vertices of the triangle (cementite area). That is, let's assume that 90% of black inclusions from the entire selected area got into this vertex. The other two peaks, B and A, are still equal, but their share accounts for only 5% of the dark inclusions.

[3] It is constructed by analogy with Koch 's triad curve.

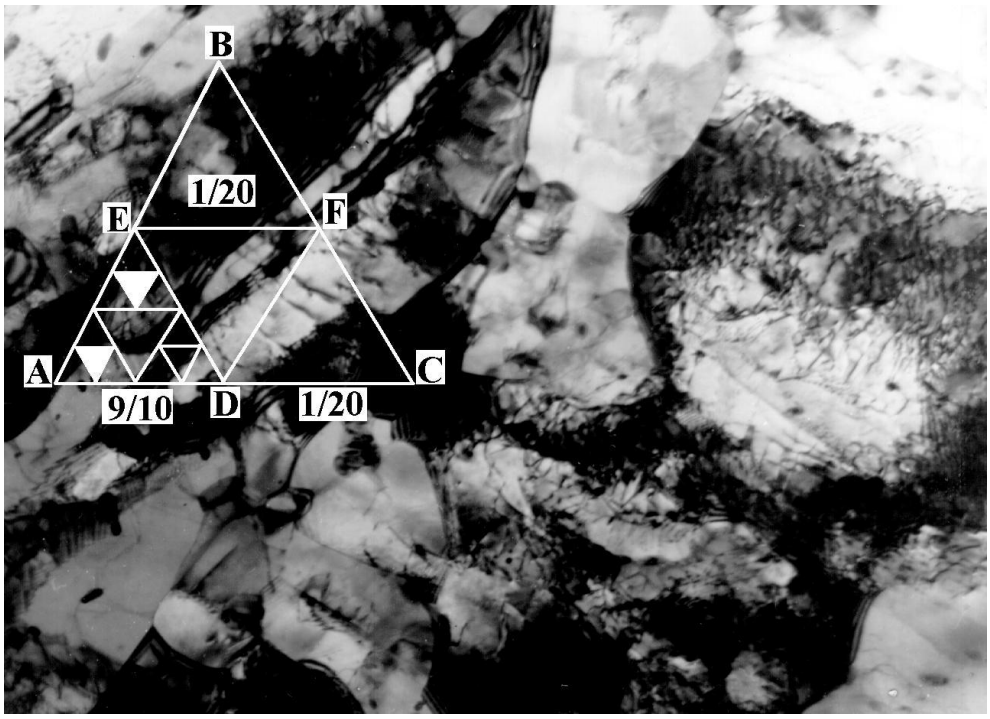

Fig. 4.8. An example of a fractal with a heterogeneous structure (multifractal). The structure of 14X2HMR steel after hardening and tempering for one hour at 700 ^{0} C/c. In the equilateral triangle is the bainite region, ×30,000

When covering the triangular area ABC with smaller and smaller triangles, it can be seen that the dark points inside the ABC triangle are now extremely unevenly distributed. Most of them are located in vertex C or its vicinity, at the same time in vertices B and A (and their vicinity) there are fewer dark points. Nevertheless, this set of points (when the number of iterations tends to infinity) is a fractal , since its main property is preserved– self-similarity . Indeed, the DFC triangle, although 90% of the dark points are concentrated in it, is similar to the large ABC triangle in its statistical (number of points, inclusions or grains per unit area) and geometric (structural configuration) properties. However, despite the uneven distribution of points along the fractal , its fractal dimension

remained the same, $D = ln3 / ln2$. The reason is that along with the geometric characteristics determined by the size of the fractal dimension, such fractals have some statistical properties. The considered structure is a multifractal .

According to the multifractal approach, each element of the structure can be characterized by the following spectrum of generalized statistical dimensions Renyi [69]:

$$D(q) = \frac{1}{q-1} \cdot \lim_{\delta \to \infty} \frac{\ln \sum_{i=1}^{N} p_i^q}{\ln \delta}, \qquad (4.4)$$

Where δ –cell, which is a single element of a square grid, which covers the object under investigation to calculate its dimension, p_i –represents the probability of a point located on the object under study hitting the i -th cell of a square grid with size $\delta, \sum_{i=1}^{N} p_i^q$ –a generalized statistical sum, characterized by an indicator of the degree –q , which describes changes in the spectrum of statistical dimensions of the object in the range ($-\infty;+\infty$).

As shown in [103], the dimensions of the spectrum $D_0, D_1, D_2, D_\infty, D_{-\infty}$ have the following physical meaning: D_0 –homogeneous fractal at ($q = 0$ Hausdorff-Bezykovich dimension); D_1 –information dimension at $q = 1$ (information entropy), which characterizes the rate of growth of the amount of information and shows how the information necessary to determine the location of a point located on the object of study grows, when the size of the cell is desired δ to zero;

D_2 –correlation dimension at $q = 2$, which characterizes the probability of two points located on the observation object being in the same cell of the grid; D_∞ –the dimension that characterizes the most rarefied space in the object of observation (light areas of the structure); $D_{-\infty}$ –dimension that characterizes the most concentrated space (black areas of the structure).

In fractal analysis, it is always assumed that the object being studied, regardless of the scale of its representation, is characterized by self-similarity , which consists in the fact that at any scale its structure has the same geometric features. Of course, for a real natural fractal , which certainly is the structure of many metals, there is a certain length scale l such that with an increase slightly smaller or larger than this scale, the property of self-similarity disappears. Therefore, the property of self-similarity of natural fractals is considered at certain scale intervals.

$$l_{min} \le l \le l_{max} \qquad (4.5)$$

At each scale level, new features of the structure of the material are revealed, characterizing one or another of its qualities. So, for example, in steels at the microstructural level, the peculiarities of the grain structure are revealed, the parameters of which significantly affect the strength properties of the metal [13].

Thus, to choose the scale of representation, for example, structural elements of rolled iron or steel, to determine its fractal dimension, it is necessary to determine the interval (4.5) in which its self-similarity is observed , and on this interval to choose the only scale at which the calculation of the fractal dimension will give the most accurate result.

scaling l_{min} step from Δl to is given empirically l_{max}. Then, in the interval (4.6), the fractal estimates are calculated dimensions in scale points

$$l_{min} + (l_{min} + \Delta l) + (l_{min} + 2\Delta l) + ,...,+ (l_{min} + n\Delta l), \qquad (4.6)$$

where $n = \frac{l_{max} - l_{min}}{\Delta l}$

The optimal scale of the structure presentation is taken to be the one at which, at least in two adjacent points from the series (4.6), the fractal dimensions differ minimally from each other. The latter is explained by the fact that the self-similarity property of the structure is best observed.

Below is an example of choosing the scale of the presentation of the structure of SPKH rolls (Fig. 5.9 *a*) and rolls of SSHKHN (Fig. 4.9 *b*) on the increase interval from ×100 to ×1000 with a given step $\Delta l = 100$.

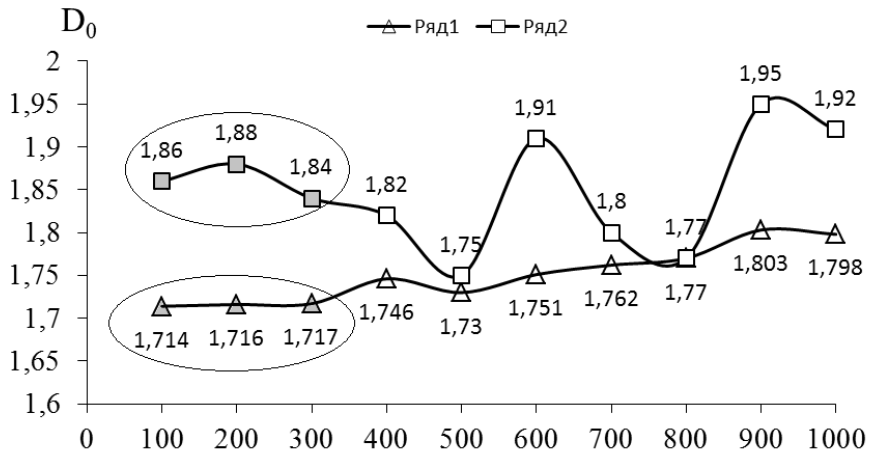

a

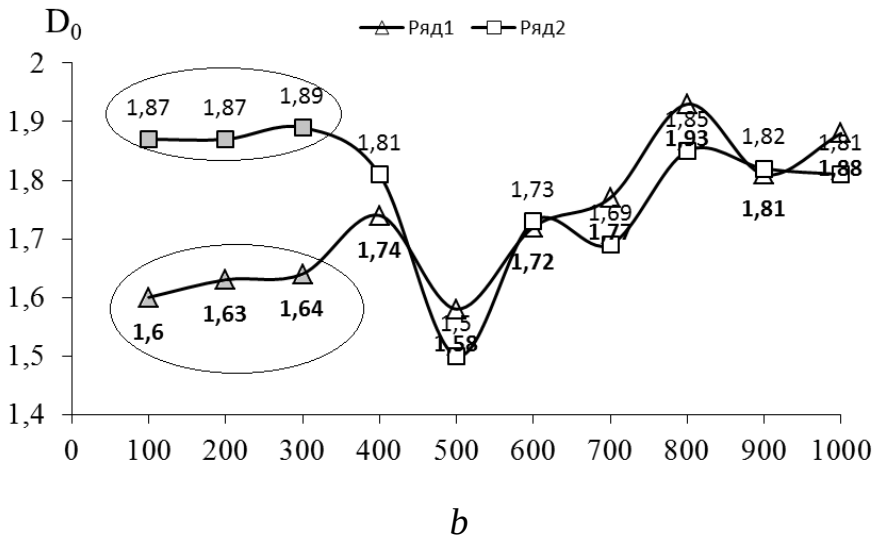

b

Fig. 4.9. Choosing the optimal scale of the representation of the structure cast iron (*a* - SPHN, *b* - SSHHN) depending on the fractal dimension of its elements (dimensions of graphite - row 1 and carbides - row 2)

From fig. 4.9 it follows that self-similarity , as the main qualitative characteristic confirming the fractal nature of the object under study, is preserved in the selected areas in the specified scale interval. Based on the results of the calculation of the fractal dimensions of the structural elements of cast-iron rolls of the SPKH performance based on 235 photographs, the scale 200 was chosen as the optimal scale for representing the structure of cast iron, ×since the fractal dimensions differed minimally from each other in two adjacent scales (×100, ×300) : 1.714,...1.717 lamellar graphite (row 1); 1.860, ... 1.840 - for carbides (row 2).

In fig. 4.9b *shows* the results of choosing the optimal scale for representing the structure of spherical graphite rolls of the SSHHN. The scale 200 was also chosen as the optimal scale for representing the structure of cast iron. ×In the range of magnification from ×100 to ×300, the fractal dimension of graphite varied from 1.600 to 1.640, and that of carbides - from 1.870 to

1.890, which indicates the preservation of the self-similarity of the structural elements given their fractal nature.

The self-similarity of the pearlite structure in the specified range of scales from ×100 to ×1000 were investigated separately for ferrite and cementite plates. The results of such calculations are shown in fig. 4.10. As a result of the calculations carried out according to a similar scheme, the scale 500 was chosen as the optimal scale for presenting the pearlite structure ×. Its choice is due to the fact that the optimal scales of representation of the structural components of pearlite: ferrite and cementite are close to and equal to ×500 and ×600, respectively (Fig. 4.10 *a*) and ×400 and ×500, respectively (Fig. 4.10 *b*) . With further increase in the structure of pearlite, the fractal dimension of its components: ferrite and cementite begins to change more sharply, which is due to an increase in their linear dimensions in photographs and, first of all, the thickness of the plates. When the magnification of the microscope is less than ×400, the calculations of the fractal dimension of the pearlite components are difficult due to the insufficient resolution of the microscope magnification, which affects the accuracy of the obtained results.

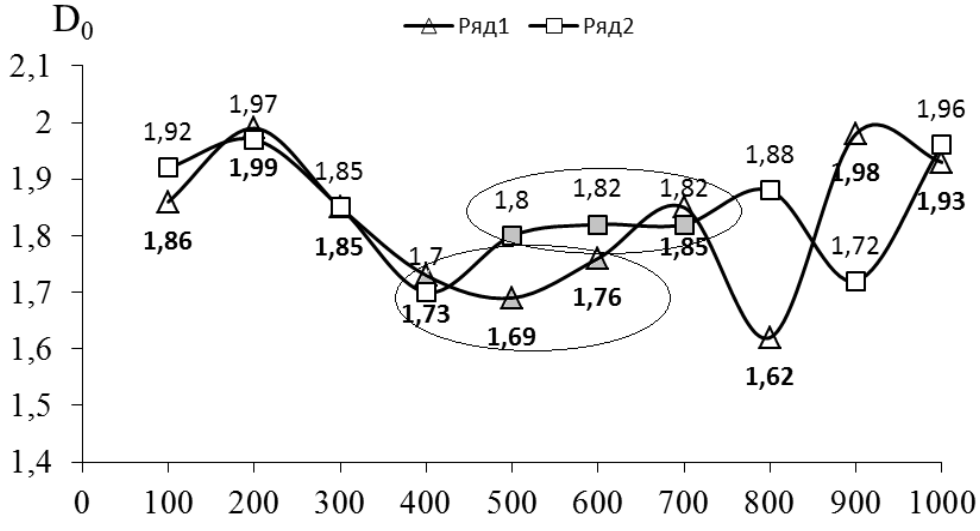

a

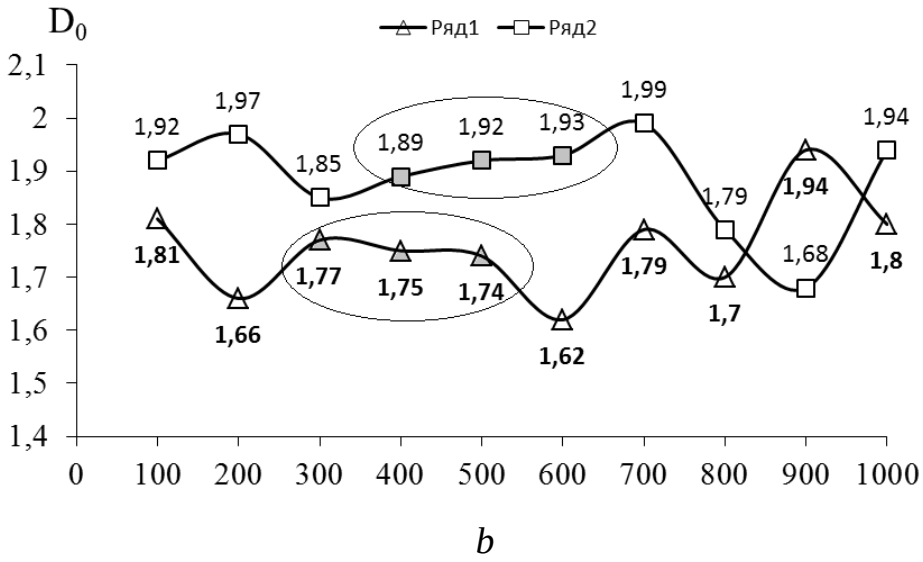

Fig. 4.10. Selection of the optimal scale of representation of the pearlite structure of pig iron (*a* - SPKHN, *b* - SSHKHN) depending on the fractal dimension of its elements (the dimension of ferrite is represented by order 1; the dimension of cementite - order 2)

Similar calculations regarding the establishment of the optimal scale of representation of the metal structure are presented in [62]. It shows that the optimum scale for presenting the ferrite -pearlite structure of low-carbon, low-alloy steel St3ps in the range of magnification from ×100 to ×1000 is the scale of ×550 .

The implementation of this stage of research made it possible to determine experimentally the optimal scale of representation of the structure of rolled iron at a magnification of ×200 –for multifractal analysis of its elements: lamellar and spherical graphite inclusions, carbides , as well as the optimal scale of representation of the structure of ×500 for multifractal analysis of the structure of lamellar pearlite consisting of ferrite and cementite.

The algorithm for calculating the spectrum of the dimensions of the structural elements using the " Multifractal " program, implemented on a computer in the Delphi software environment , was chosen as follows: all images of the microstructure of cast iron hot-rolled rolls measuring 10 ×15 cm at magnifications of ×200 and ×500 were converted into electronic form by scanning photographs for high-quality display surface relief.

In fig. 4.11 shows a photograph of a fragment of a metal microsection , covered with a square grid in the program mode on a personal computer for calculating the generalized spectrum of statistical dimensions of the elements of the structure of the working zone of the metal barrel of the cast iron roll of SPKHN-45 according to the above formula (4.4).

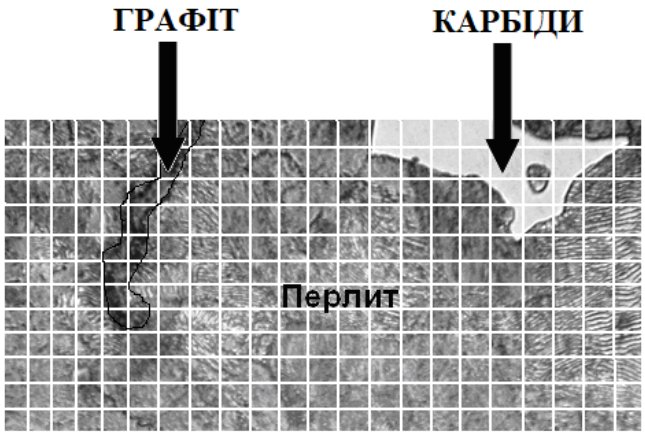

Fig. 4.11. To calculate the spectrum of dimensions of the structural elements of cast iron (SPKHN-45)

For each sample of cast iron, three photographs of the microstructure were obtained at magnifications of ×200 and ×500 in five arbitrarily selected fields on the section.

At the next stage, five main dimensions were calculated $D_0, D_1, D_2, D_\infty, D_{-\infty}$ multifractal spectrum for each element of the

structure of each photograph (Fig. 4.12). As limit values $D_{-\infty}$, D_{∞} values of the spectrum function in the range from 200 to 200 were chosen experimentally.

When describing the complex configuration of the elements of the structure and shape of the studied metal, the quantitative assessment of their dimensions was carried out in the established scale range (×100, ×300) - for lamellar and spherical graphite, as well as for carbides in the form of ledeburite eutectic and in the range of increase (×400, ×600) - for the structural components of pearlite: ferrite and cementite, where the indicators of two adjacent dimensions change minimally in the investigated scale range (×100, ×1000) .

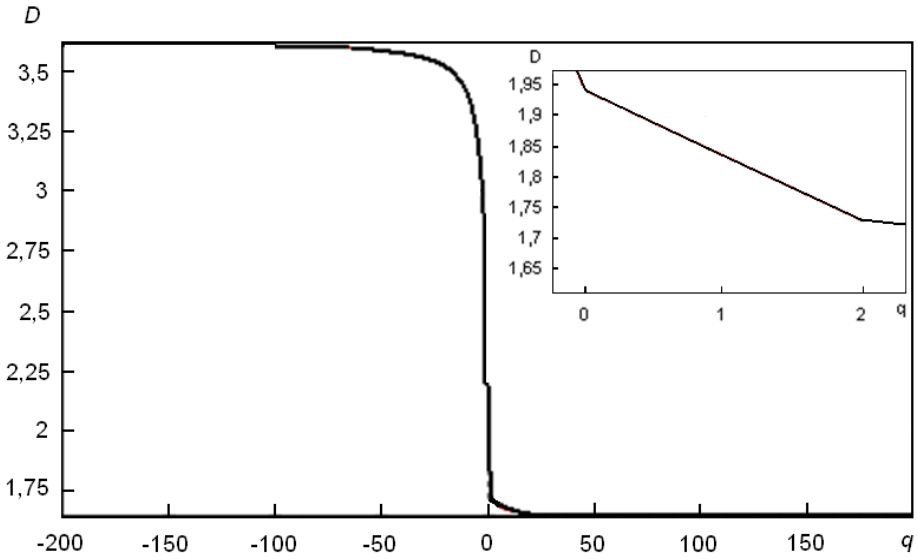

Fig. 4.12. The spectrum of dimensions calculated for lamellar graphite of SPKHN-45 rolls: $D_0 = 1{,}94$; $D_1 = 1{,}84$; $D_2 = 1{,}73$; $D_{200} = 1{,}65$; $D_{-200} = 3{,}62$. In the upper right corner of the figure, an enlarged section of the dimension spectrum in the interval $0 < q < 2$

It was established that the fractal dimension of the studied elements of the structure varied within the error of experience of 5...7%, which

indicates the universality of this assessment, and, accordingly, the reliability and economic gain, from the point of view of equipping factory laboratories with expensive metallographic microscopes with a higher resolution.

4.3. Software implementation of the algorithm

The " Multifractal " program works with scanned images in 256 shades of gray. After starting the program, the file is opened: File ⇒Open (Fig. 4.13 *a*):

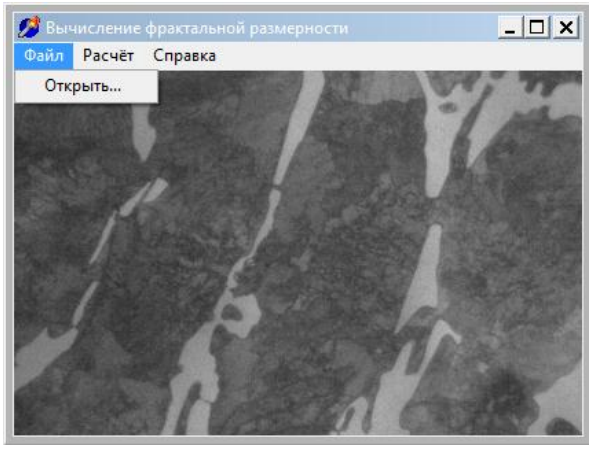

a

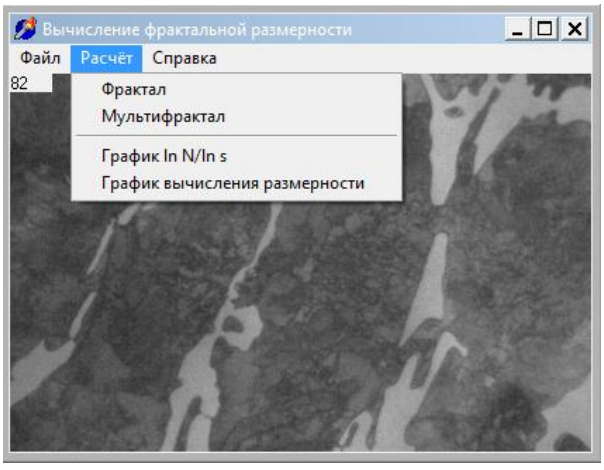

b

Fig. 4.13. *a* - Program menu: File ⇒Open image metal structures;

b - Multifractal Calculation menu⇒

After loading the image, it is necessary to select the object in the image (structural component), for which the calculation of the dimension spectrum will be carried out in a modified way and the characteristics listed above. To do this, select the Calculations command in the Work menu (Fig. 4.13 *b*). At the same time, a panel will appear on the screen for entering or correcting data depending on the color of the elements of the structure of one phase, the size of the cells covering the photograph of the structure with a given step, and the limits of the calculated range of changes in the spectrum of statistical dimensions multifractal (Fig. 4.14).

Fig. 4.14. Data input panel

In fig. 4.14 graph of grayscale statistics is their distribution from 0 (black color) to 255 (white color) depending on the number of image pixels occupied by them. After this operation, the maxima of the white and black –color gradation of the most frequently occurring points close to the black and white border are determined. Next, the image is converted to two-color (black and white), and the gray gradations that lie below the limit equal to half the sum of the white and black maxima are converted to black and white, respectively. The program automatically selects a threshold equal to

half the sum of the white and black maxima, depending on the selected image. The accuracy of the results increases due to the automatic selection of the interface between black and white. This is explained by the fact that the color of the image of the microstructure directly depends on the selection of the composition of the herb and the time of exposure of the grind in the etching process; exposures of photographs of the structure in the process of their manifestation. At the same time, most often the light inclusions of the structure can be counted among the dark ones and vice versa, which introduces a significant error when determining their size estimates. If it is necessary to calculate the dimensions of a separate object of the image, the user determines the chromaticity limits for it with the help of the cursor. The initial value of the cell length and its final value, given in pixels, are set by the researcher in the following steps (Fig. 4.14). After this operation, the image can be filtered if necessary. The use of a filter allows you to achieve the removal of polygraphic printing noise.

During the analysis of digital photographs of the microstructure, such fragments were found that had polishing defects in the form of "garbage" (spots and scratches), blurred and non-contrast boundaries between light and dark areas of the structure elements. In order to improve the quality of photographs of the microstructure, they were processed on the basis of wavelet analysis [62].

Wavelet image processing algorithms are based on relatively strict criteria – a limited set of decomposition levels [4], a limited set of optimal wavelet bases , etc. This made it possible to formalize the wavelet processing procedure and minimize the error arising from incorrectly set processing parameters. Processing was performed locally using a discrete

[4]Actually usually are considered *t=1* (wave-wavelet) and *t = 2* (mhat-wavelet). Higher derivatives are applied rarely [62].

wavelet Haar of the second order with the smoothness of the function 5 [62], which made it possible to detect the contrasting boundaries between them and eliminate polishing defects during the analysis of the color boundaries of the structural elements.

In fig. 4.15 shows an example of a selected fragment of the structure of rolled iron before wavelet processing with partially blurred and darkened boundaries between the elements of the structure and after processing with contrasting boundaries.

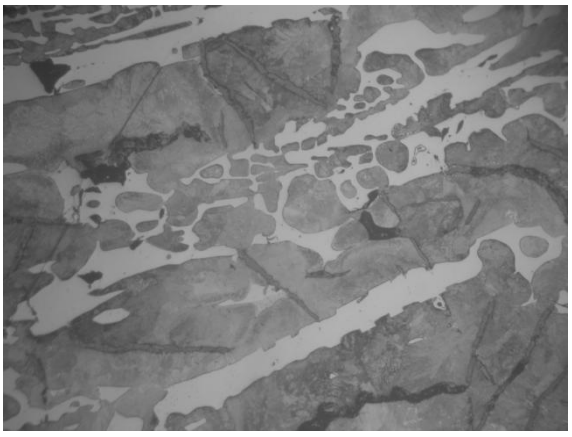

a

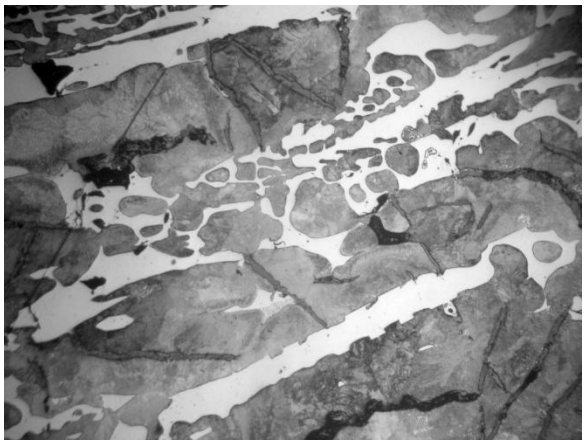

b

Fig. 4.15. Enlarged fragment of the structure of rolled iron
with plate form of graphite before (*a*) and after (*b*) wavelet processing

When you press the "Start" button on the data input panel, the spectrum of statistical image sizes is calculated. On the graph fig. 4.16 shows the results of calculating the dimension spectrum of carbides for cast iron rolls of SPKHN-45 performance. The indicators of dimensional estimates D(q) of the elements of the structure of the spectrum being calculated are plotted along the ordinate axis, and the interval of their changes along the abscissa axis. In the case of changing the q indicator, no more than –200 to 200 was set.

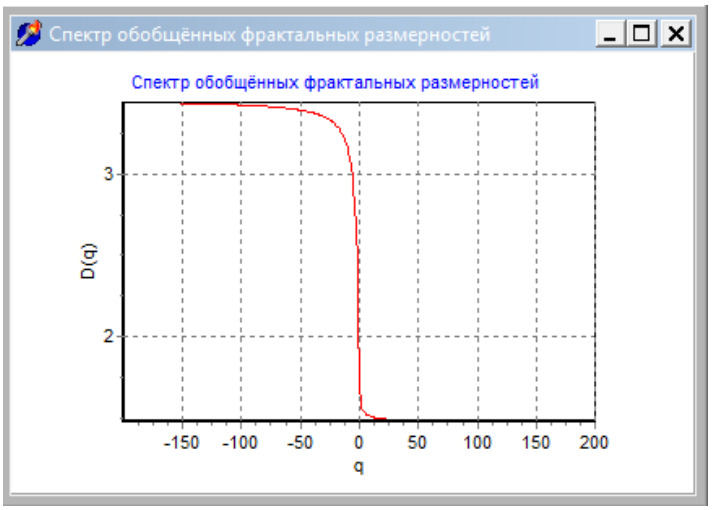

Fig. 4.16. The results of the calculation of the spectrum of dimensions carbide component

At the same time, the calculation part of the " Multifractal " program is considered finished. More detailed information can be found in the ⇒Help Help menu.

4.4. The sensitivity of the quality characteristics of the target product to changes in the input parameters

Recently, in many articles devoted to issues of materials science, examples of objects are given for the description of which the language of fractal geometry is used. However, the use of such an approach must be

strictly justified, as it must be based on the confidence that the fractal dimension characteristic of the material under study can characterize its qualitative properties. Until now, this problem was proposed to be solved using the F criterion. Takensa . The fulfillment of the conditions satisfying this criterion is reduced to the measurement of any one characteristic of the studied system at different moments of time with an interval of Δt. These measurements yield some limited sequence $\{a_i\}$, $0 \le i < \infty$. If this sequence manages to construct a smooth deterministic model of the form $\frac{d\vec{x}}{dt} = \vec{f}(\vec{x})$, we are dealing with a complex deterministic process and it is pointless to use the language of fractal geometry. But, firstly, we cannot always obtain such a sequence experimentally, and secondly, since we are always dealing with a sample of finite length, the question naturally arises as to what should be the number N, so that the correlation coefficient can be reliably determined? As you can see, the problem is not as simple as it seems at first glance. In our opinion, at the beginning of the study, the sensitivity of the fractal dimension of the material to those characteristics, which they are aimed at identifying, should be shown . The latter is explained by the fact that the fractal dimension inherent in the studied material can change in a very narrow range, and in this connection it can be insensitive (little sensitive) to changes in those characteristics of the material whose identification is performed.

The approach based on the application of the multifractal theory for the quantitative assessment of the structure allows, by comparing the spectrum of statistical dimensions of its elements, to determine sensitive indicators of quality characteristics, in particular, mechanical properties, describing the mutual unequivocal correspondence between the data of the dimensions of the structure and these properties. This, in turn, will lead to

the reduction of the incompleteness of formal axiomatics that occurs when describing the elements of the metal structure using traditional figures of Euclidean geometry by identifying structurally sensitive dimensional estimates of quality criteria.

To solve this problem, it is proposed to introduce a criterion– K, which reflects the sensitivity of a certain dimension of the elements of the structure of the multifractal spectrum of statistical dimensions to changes in the studied characteristics of the material [115]. Let X_1 her X_2 –two numbers characterizing some quality of the material from the set of its values, and Y_1 let Y_2 –corresponding numerical values of dimensional estimates obtained on the basis of studying a certain field $i = 1,...,n$ of this material. Let's determine how the difference between indicators X_1 and affects X_2 the difference between Y_1 and Y_2. Since X and Y –number, then the measure can be taken $|X_1 - X_2|$ accordingly $|Y_1 - Y_2|$. So, for example, for materials science tasks, it is convenient to study the sensitivity of the fractal or any other dimension of the elements of the material structure to changes in their qualitative characteristics, calculating the sensitivity coefficient K_i (4.7) according to the proposed V.I. Bolshakov and Yu.I. Dubrov method [115]:

$$K_i = |Y_i - Y_{i+1}| / |X_i - X_{i+1}|. \qquad (4.7)$$

To distinguish a useful signal against the background of obstacles, naturally obtained point values of sensitivity of fractal or statistical dimension were compared with the error– ψ techniques:

$$\forall K_i >> \psi , \quad i = 1,..., n . \qquad (4.8)$$

In this, if the condition (4.8) is violated, that is, when

$$\exists \left[\left(K_j \approx \psi \right) \cup \left(K_j \le \psi \right) \right] \in K_i , \qquad (4.9)$$

then it is assumed that from each $j \in i$ - areas, the dimension Y_j is not correlated with the studied characteristics of the material and the application of the method of multifractal analysis of the structure of the material, for example, the forecast of its qualitative characteristics, is incorrect. The sensitivity will be maximum at those points of the grinding structure where the maximum change in metal properties is observed. In work [103], it was shown that the sensitivity of the dimension spectrum of the elements of the ferrite -pearlite structure of low-carbon steel is quite high, and this fact can be used in the identification, for example, of its mechanical properties, in particular, with regard to hardness indicators indirectly. To minimize costs, it is suggested to divide the experiments into two stages.

1. The first preliminary stage should include determining the sensitivity of quality criteria to dimensional estimates of the elements of the structure of the material under study, $D_0, D_1, D_2, D_{200}, D_{-200}$ from the calculated generalized spectrum of statistical dimensions by conducting direct experiments or statistical data obtained at the enterprise or from literary sources [5].

[5] In the subject region that studied , accumulated huge number published experimental data that include photographs grinds , on the base analysis which , with enough high reliability , you can determine the dimension value and carry out the previous one

2. The second stage of the experiment, aimed at predicting the quality criteria of the rolls of SPKHN and SSKHN, is carried out when and only when the sensitivity of the dimensional characteristics is confirmed at the first stage by fulfilling the condition (4.7) or excluding from the analysis of the areas characterized by the condition (4.9).

In fig. Fig. 4.17 –4.22 shows the results of calculating the sensitivity coefficients K and of the mechanical properties of rolled cast iron with lamellar graphite to dimensional estimates $D_0, D_1, D_2, D_{200}, D_{-200}$ of graphite, carbides and pearlite (ferrite+cementite), calculated according to formula (4.7).

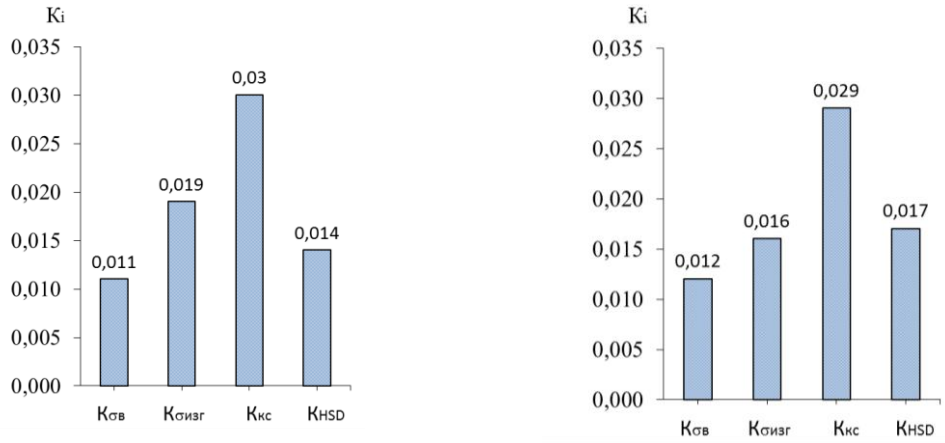

a *b*

Fig. 4.17. Sensitivity of mechanical properties to the fractal (*a*) and informational (*b*) dimensions of the graphite of the working area of the barrels of the rolls of the SPKH

The sensitivity coefficients of the fractal (0.011...0.030), information (0.012...0.029) and correlation (0.011...0.048) dimensions of lamellar graphite (Fig. 4.17 and Fig. 4.18) exceed K_{D+200} (0.008...0.014) by 2-3

assessment its sensitivity to changes quality characteristics of the material that is being studied .

times and $K_{D\ -200}$ (0.001...0.012) from the multifractal spectrum of generalized statistical dimensions Renyi . Therefore, for the further use of dimensional estimates of graphite when predicting the mechanical properties of cast iron, its most sensitive dimensions were determined D_0, D_1, D_2, and the limiting dimensions D_{200}, D_{-200} due to their insignificant sensitivity indicators, they were not taken into account in further quality calculations.

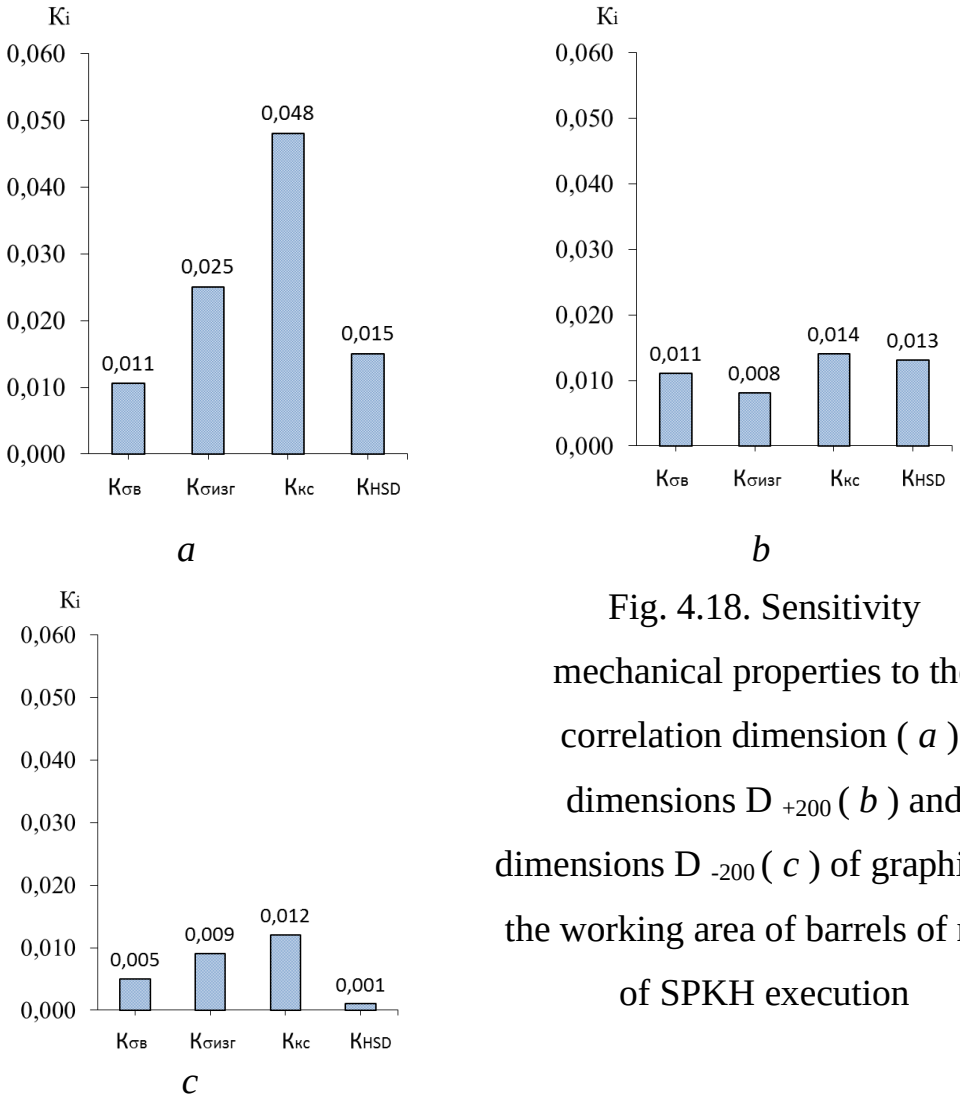

Fig. 4.18. Sensitivity mechanical properties to the correlation dimension (*a*), dimensions D_{+200} (*b*) and dimensions D_{-200} (*c*) of graphite of the working area of barrels of rolls of SPKH execution

As a result of the experiment, it was established that the best sensitivity of the analyzed mechanical properties to the dimensional characteristics of carbides is observed for the fractal , information and

correlation dimensions (Fig. 4.19, Fig. 4.20). Therefore, these dimensional estimates of carbides D_0, D_1, D_2 it is advisable to use in the future to predict the mechanical properties of the working zone of cast iron with a lamellar form of graphite.

Low indicators of sensitivity of properties to dimensional estimates D_{200}, D_{-200} elements of the structure, which characterizes the dimensions of the lightest and darkest areas of the studied object on the section , respectively, in the scale range (100 ×, ×1000) , as the results of the experiment showed, are unsuitable for predicting the following mechanical characteristics of cast iron : σ_B , σ_{izg} , KC and NSD . Coefficients of sensitivity of mechanical properties to statistical dimensionality D_{200} of carbides , calculated according to formula (4.4), do not exceed 0.02 (Fig. 4.20 *b*), but to the dimension D_{-200} –do not exceed 0.016, which is not enough when using these dimensional estimates for practical purposes for forecasting the quality criteria of grade-rolled iron rolls of SPKHN and SSKHN execution.

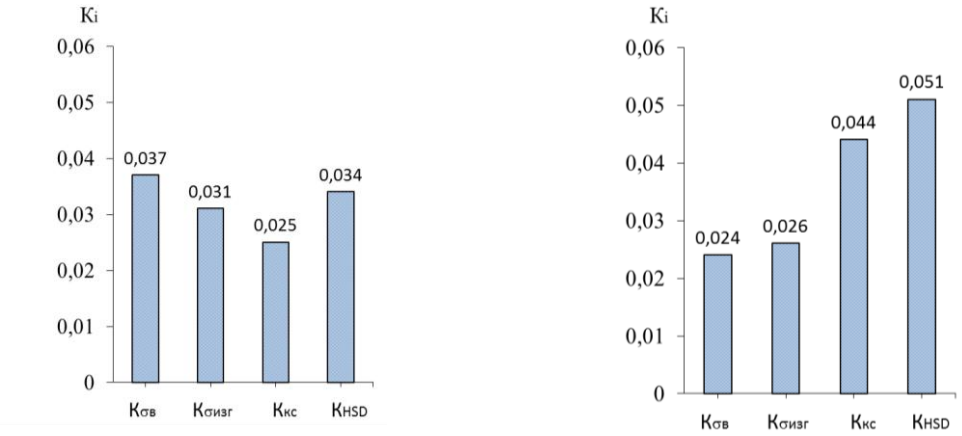

a *b*

Fig. 4.19. Sensitivity of mechanical properties to fractal (*a*) and informational (*b*) dimensions carbides of the working area of the barrels of the rolls of the execution of SPHN

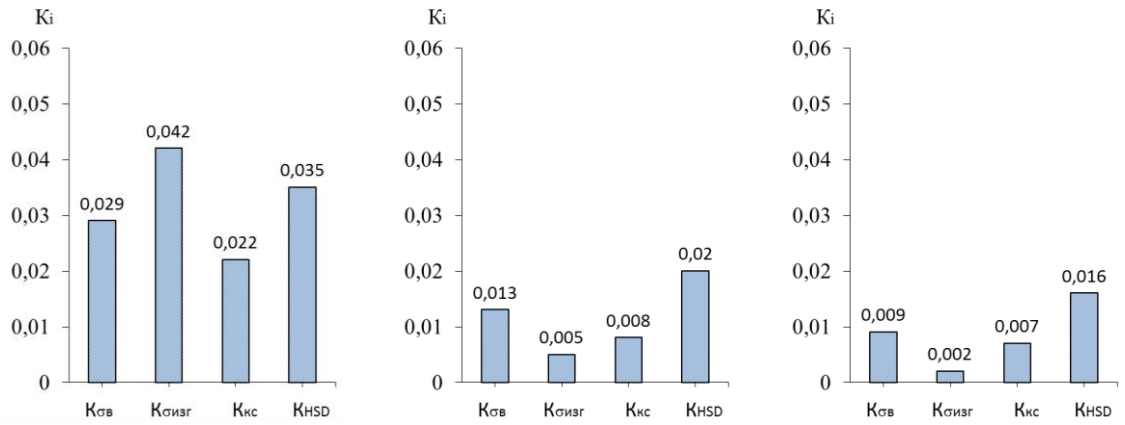

a *b* *c*

Fig. 4.20. Sensitivity of mechanical properties to the correlation dimension (*a*), dimension D_{+200} (*b*) and dimension D_{-200} (*c*) of carbides of the working area of the barrels of the rolls of the execution of SPHN

When analyzing the results of the calculation of the indicators of the sensitivity of the characteristics of the quality of cast iron to the dimensional characteristics of the structural components of pearlite (ferrite and cementite), shown in the graphs of fig. 4.21 and fig. 4.22, relatively low coefficients of sensitivity of properties to all statistical dimensions from the considered spectrum are observed. The average coefficient of sensitivity of mechanical properties to the fractal dimension D_0 of pearlite (ferrite+cementite) is 0.006±0.003; 0.008±0.004 –to the information dimension D_1; 0.005±0.003 –to the correlation dimension D_2; 0.005±0.003 –to dimensionality D_{+200} and 0.007±0.004 –to the dimension D_{-200} is low , which indicates the ineffectiveness of the practical use of these estimates for the forecast of the quality criteria of the working area of cast iron rolls for the execution of the SPKH.

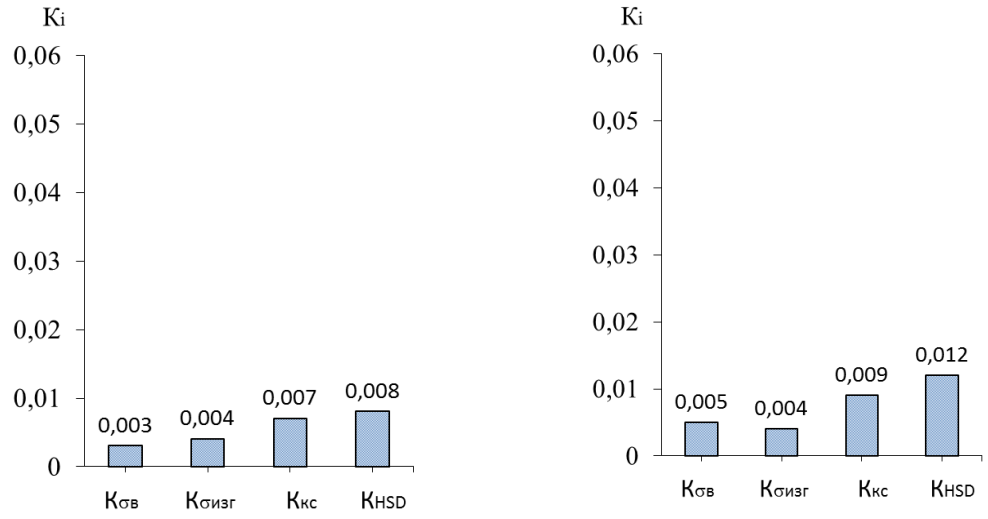

Fig. 4.21. Sensitivity of mechanical properties to fractal (*a*) and informational (*b*) dimensions of pearlite (ferrite+cementite) of the working zone of the barrels of the rolls of the execution of SPHN

On the basis of the conducted experiment on the detection of the sensitivity of the mechanical properties of the working zone of the barrels of cast iron rolling mills for the performance of SPKH to the statistical generalized dimensions of the structural elements from the studied multifractal spectrum $D_0, D_1, D_2, D_{200}, D_{-200}$ the following conclusions were made:

1. To predict the mechanical properties of rolled cast iron with lamellar graphite, it is advisable to use dimensional estimates D_0, D_1, D_2 graphite and carbides with an increase of ×200.
2. A low sensitivity was established between the mechanical properties and dimensional estimates of the structure of pearlite (ferrite and cementite), which does not allow them to be used for practical purposes to predict the quality of rolls. Obviously, this fact is related to some geometric features of the elements of the pearlite structure (size,

dispersion, degree of tortuousness of the borders of its individual elements). In order to establish a higher sensitivity between these characteristics, it is necessary to search for such a large-scale level of presentation of the structure of cast iron, which will allow to reveal these features of the pearlite matrix. However, this is a separate applied task, which was not considered in this work.

3. Dimensional evaluations of pearlite, graphite and carbides D_{200}, D_{-200}, due to their low sensitivity to mechanical properties, it is incorrect to use for their prediction in the investigated large-scale range of structure presentation (×100, ×1000) .

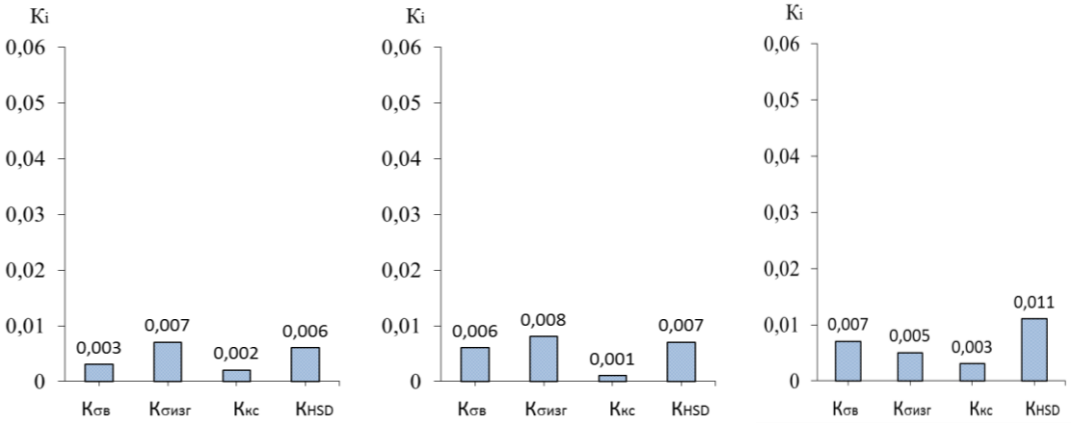

a *b* *c*

Fig. 4.22. The sensitivity of mechanical properties to the correlation dimension (*a*), dimension D_{+200} (*b*) and D_{-200} (*c*) of pearlite (ferrite+cementite) of the working area of the barrels of the rolls for the execution of SPKH

The sensitivity of the mechanical properties to the fractal , information and correlation dimensions of spherical graphite and carbides at a fixed magnification of the structure of ×200 is also observed for the rolls made by SSHKHN (Fig. 4.23, –Fig. 4.26). Indicators of the sensitivity of the mechanical properties of rolled iron to the dimensionality of

structural element estimates D_0, D_1, D_2 are 3-5 times higher than the indicators of sensitivity to the extreme dimensions from the spectrum D_{200}, D_{-200}. As can be seen from fig. 4.23 *and* among the analyzed, the greatest sensitivity of the mechanical properties of the working zone of the barrels of the rolls of the SSHHN execution to the fractal dimension of graphite is observed for the hardness of 0.61, and the smallest –for the breaking strength limit of 0.007. This probably indicates the effect of graphite shape on these quality criteria.

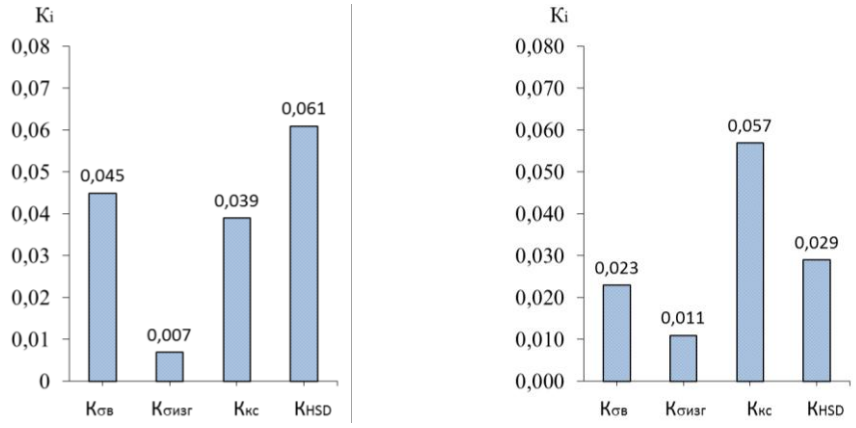

a *b*

Fig. 4.23. Sensitivity of mechanical properties to the fractal (*a*) and informational (*b*) dimensions of the graphite of the working area barrels of rolls of the SSHHN execution

The maximum sensitivity index of impact viscosity to the information dimension of spherical graphite was determined (Fig. 4.23b*)* , the calculated value of which is 0.057. Relatively low values of the sensitivity coefficients of the mechanical properties under consideration were found to statistical dimensions from the Rainier spectrum D_{200}, D_{-200} (Fig. 4.24 *b, c*), which are within 0.003...0.021 and 0.006...0.017, respectively.

For carbides (Fig. 4.24 *b, c*), spherical graphite (Fig. 4.25 *a, b*) and structural components of pearlite (Fig. 4.26 *b, c*) in all considered cases, the sensitivity of mechanical properties to dimensional characteristics is low D_{200}, D_{-200} testify to the low efficiency of their further use in the equations of the forecast of the quality of rolled iron in comparison with other dimensions D_0, D_1, D_2, calculated from the Regny spectrum . These dimensional estimates of the structural elements of grade-rolled cast iron rolls of the SSHKHN may possibly be correlated with other characteristics of the quality of cast iron, which is the subject of separate studies and is not considered within the scope of this work.

Indicators of sensitivity to the correlation dimensionality of graphite in the working zone of the barrels of the rolls of the SSHHN execution (Fig. 4.24 *a*) exceed by two or more times the sensitivity indicators of the dimensional characteristics D_{+200} and D_{-200} , which makes it possible to further search for a correlation between the quality indicators of rolled iron.

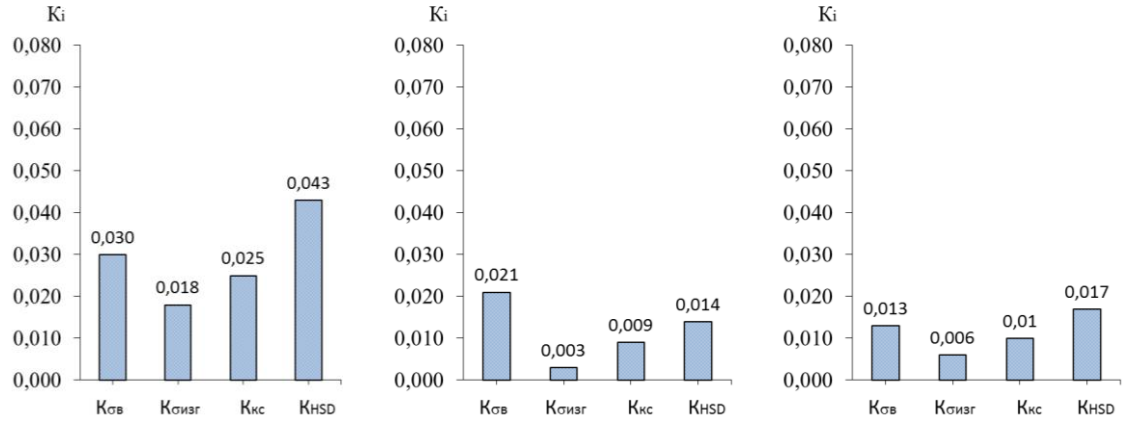

a *b* *c*

Fig. 4.24. The sensitivity of the mechanical properties to the correlation dimension (*a*), dimension D_{+200} (*b*) and dimension D_{-200} (*c*) of the graphite of the working zone of the barrels of the rolls of the SSHHN

For cast iron with a spherical shape of graphite, the best indicators of sensitivity are found in the limits of bending strength of 0.08 and impact toughness of 0.067 (Fig. 4.25 *a*) to the fractal dimension of carbides ; the limits of bending strength 0.062 and hardness 0.041 to their information dimension (Fig. 4.25 *b*), impact toughness 0.071 to the correlation dimension (Fig. 4.25 *c*), which indicates a possible correlation between these characteristics.

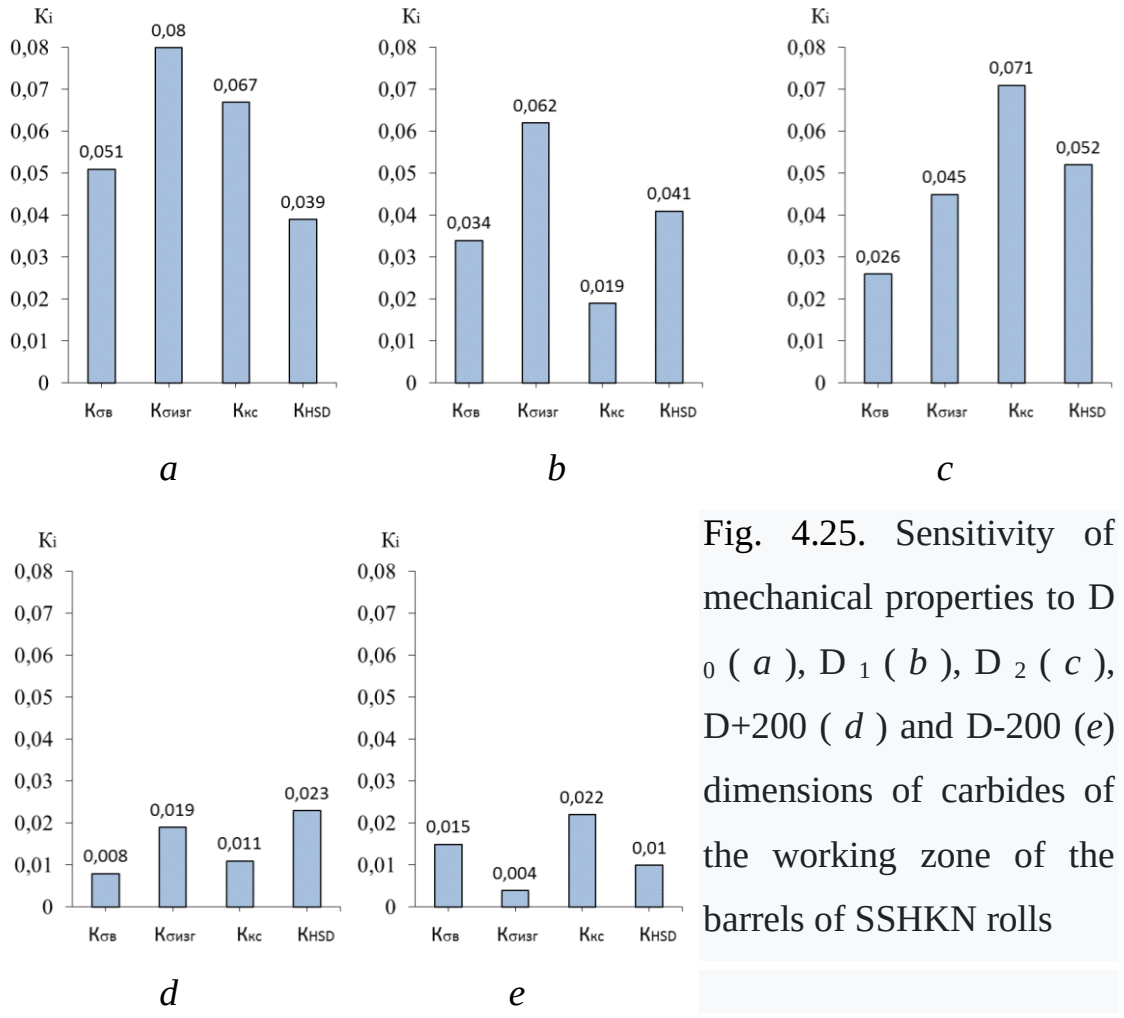

Fig. 4.25. Sensitivity of mechanical properties to D $_0$ (*a*), D $_1$ (*b*), D $_2$ (*c*), D+200 (*d*) and D-200 (*e*) dimensions of carbides of the working zone of the barrels of SSHKN rolls

Indicators of the sensitivity of σ $_{in}$, σ $_{izg}$, KC and NSD to the dimensional estimates of the structural components of pearlite are relatively

low compared to the dimensional estimates of graphite and carbides , which indicates a low correlation between these characteristics (Fig. 4.26).

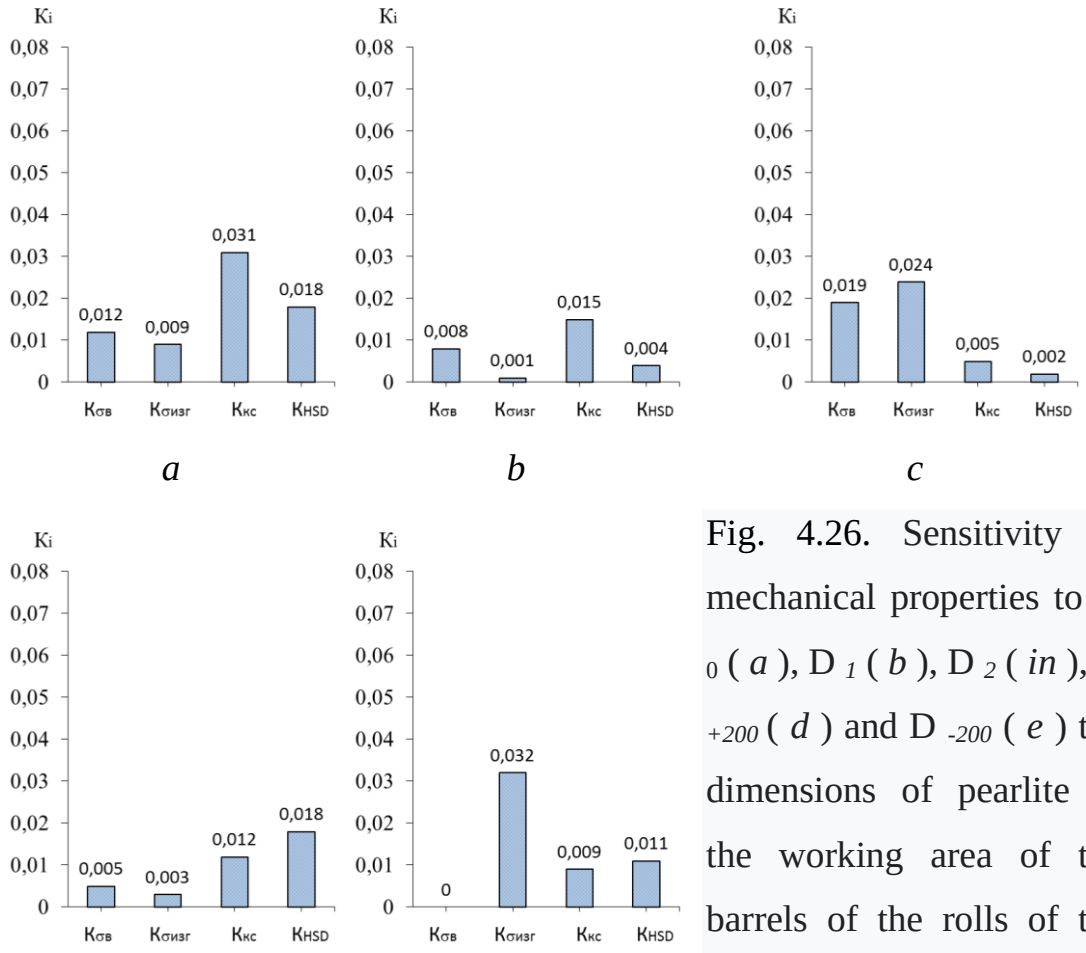

Fig. 4.26. Sensitivity of mechanical properties to D $_0$ (*a*), D $_1$ (*b*), D $_2$ (*in*), D $_{+200}$ (*d*) and D $_{-200}$ (*e*) the dimensions of pearlite in the working area of the barrels of the rolls of the SSHKHN

4.5. Establishing a mutually exclusive correspondence between quality characteristics and input parameters

When comparing the dimensional estimates of the structural elements of the roll material (graphite and carbides) with its mechanical properties, equations and coefficients reflecting their adequacy were obtained (Fig. 4.27 - Fig. 4.30). Graphs describing the influence of

statistical dimensions of the structural components of rolled iron on its mechanical properties are obtained based on the establishment of sensitivity (4.7) between these characteristics. Below are those dependencies where the statistical characteristics and mechanical properties most sensitive to each other were revealed by comparing the obtained results.

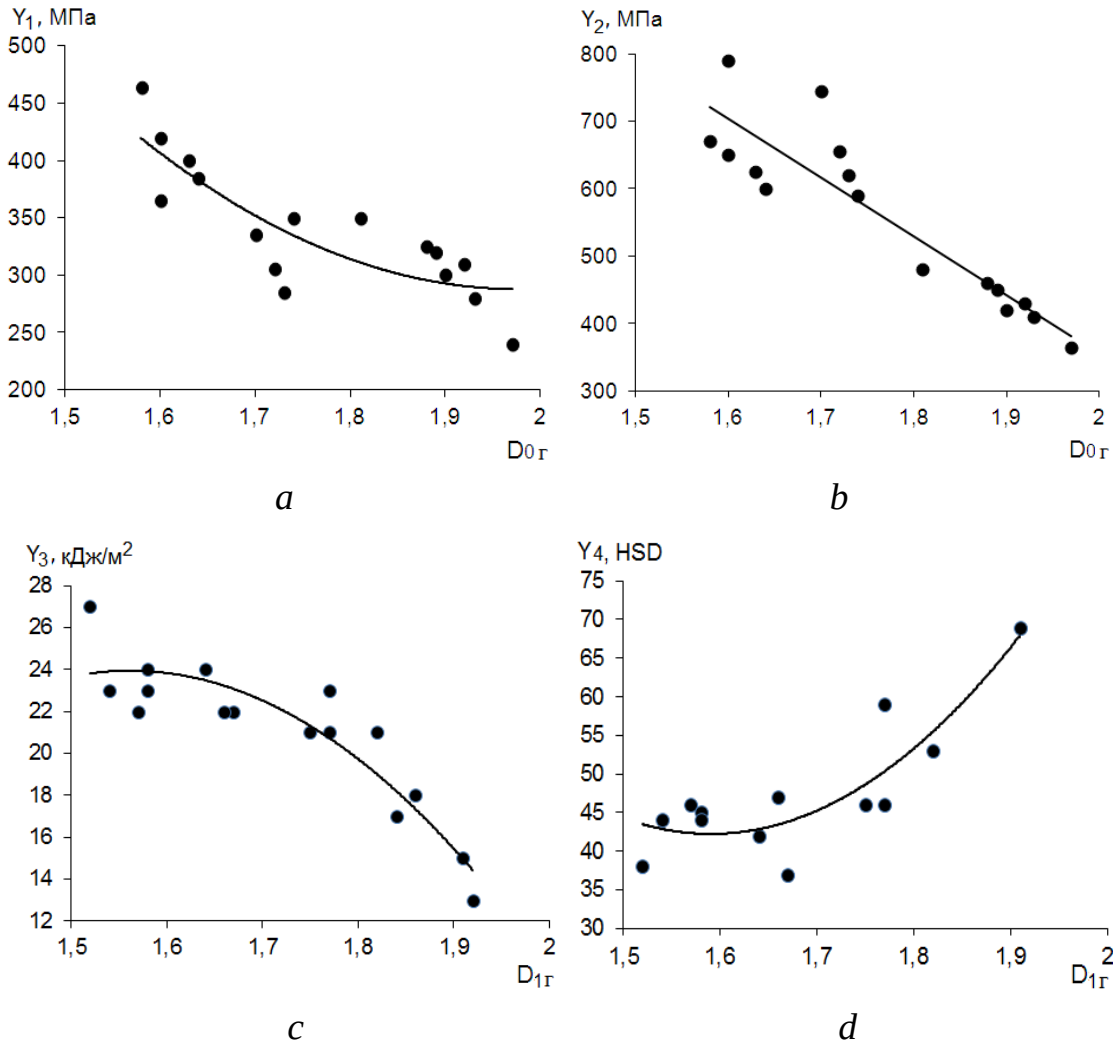

Fig. 4.27. Dependence of the breaking strength limit $-Y_{1}$ and bending strength limit $-Y_{2}$ on the fractal dimension of lamellar graphite (*a*, *b*), impact viscosity $-Y_{3}$ and hardness $-Y_{4}$ from the information dimension of lamellar graphite (*c*, *d*) of SPKHN rolls

$$Y_1 = 834.03 \cdot D_{0г}^2 - 3299.1 \cdot D_{0g} + 3550, \quad R^2 = 0.70 \quad (4.10)$$

$$Y_2 = -874.36 \cdot D_{0g} + 2103.2, \quad R^2 = 0.83 \quad (4.11)$$

$$Y_3 = -74.075 \cdot D_{1г}^2 + 231.39 \cdot D_{1g} - 156,76, \quad R^2 = 0.84 \quad (4.12)$$

$$Y_4 = 252.22 \cdot D_{1г}^2 - 802.42 \cdot D_{1g} + 680.43. \quad R^2 = 0.75 \quad (4.13)$$

The established dependencies make it possible to assess the degree of influence of the cast iron structure on its mechanical properties. The boundaries of lamellar graphite inclusions serve as microstress concentrators , and an increase in its content weakens the metal matrix of cast iron, which indicates an influence on the mechanical properties of cast iron both by the content, size, and distribution of graphite, and by the shape of the inclusions. According to K.L. Vashchenko and L. Sofroni [62], with this form of graphite, only 30...50% of the strength of the metal base of cast iron is effectively used, and there is practically no possibility of using its plastic properties. The analysis of the spectrum of statistical generalized dimensions of rolled cast iron showed that the fractal dimension of the studied phase depends to a greater extent on the shape and geometric dimensions of its elements, and the information and correlation dimensions depend mainly on their content and distribution.

There is a tendency to decrease the strength characteristics of grade-rolled iron rolls with an increase in the fractal dimension of lamellar graphite (Fig. 4.27 *a*, *b* of equations (4.10, 4.11), which describe the given dependencies). This is to a certain extent due to an increase in its content in cast iron from 0.5 to 2.5% and an increase in the length of inclusions– from PGd45 to PGd180, as well as increasing the nickel content from 0.99 to 1.17% by mass. The application of traditional methods of point assessment of the geometric characteristics of lamellar graphite in accordance with

existing standards made it possible to record a change in its shape within the relatively narrow limits of –PGf1, PGf2 for the studied graded rolled rolls; sizes –PGD45-PGD180; distribution of –PGr1, PGr2 and the occupied area –of PG2 and PG4, which does not make it possible to evaluate the quality characteristics with the accuracy necessary for practical purposes based on these data. A decrease in impact viscosity indicators was recorded with an increase in the information dimension of lamellar graphite (Fig. 4.27) and a simultaneous increase in hardness (Fig. 4.27 *d*), the dependencies of which are described by a second degree polynomial (4.12, 4.13). Low hardness indicators of HSD 36...46 (Fig. 4.27 *g*) are observed in the range of graphite information dimension 1.52...1.68 and, in addition, are partly due to the uneven distribution of graphite inclusions, which is described by the PGr2 score, as well as low ledeburite content at the level of 8...14%. The obtained results show that the distribution of graphite inclusions has a greater influence on the indicators of impact viscosity and hardness than their shape.

Carbides (cementite and ledeburite) crystallize mainly in the surface layers of the rolls during intensive removal of heat from the liquid cast iron that is poured into the mold, and have a high Shore hardness of 80...100 units. However, their high content in the working layer of the rolls simultaneously increases their fragility. The influence of the complex geometric configuration of carbides on the physical and chemical properties of the rolled material has not been fully investigated, but the results obtained in Fig. 4.28 *a* - *d* results show that such a relationship exists. An increase in the breaking strength limit (Fig. 4.28 *a* , (4.14)) was recorded when the fractal dimension of ledeburite increased to 1.99, and for bending (Fig. 4.28 *b* , (4.15)) - when its informational dimension increased to 1.98, when the indicators of the area occupied by it are

20...35%. When the correlation dimension of ledeburite is reduced from 1.86 to 1.58, a doubling of the hardness of the working zone of the metal barrels of grade-rolled rolls with HSD 37 to 70 (Fig. 4.28 *d* , *(* 4.17)) and a simultaneous decrease in the impact viscosity indicators from 2 m ^{2} (Fig. 4.28, (4.16)), which is partly caused by an increase in the content of ledeburite from 8 to 35% and carbon from 2.84 to 3.32%.

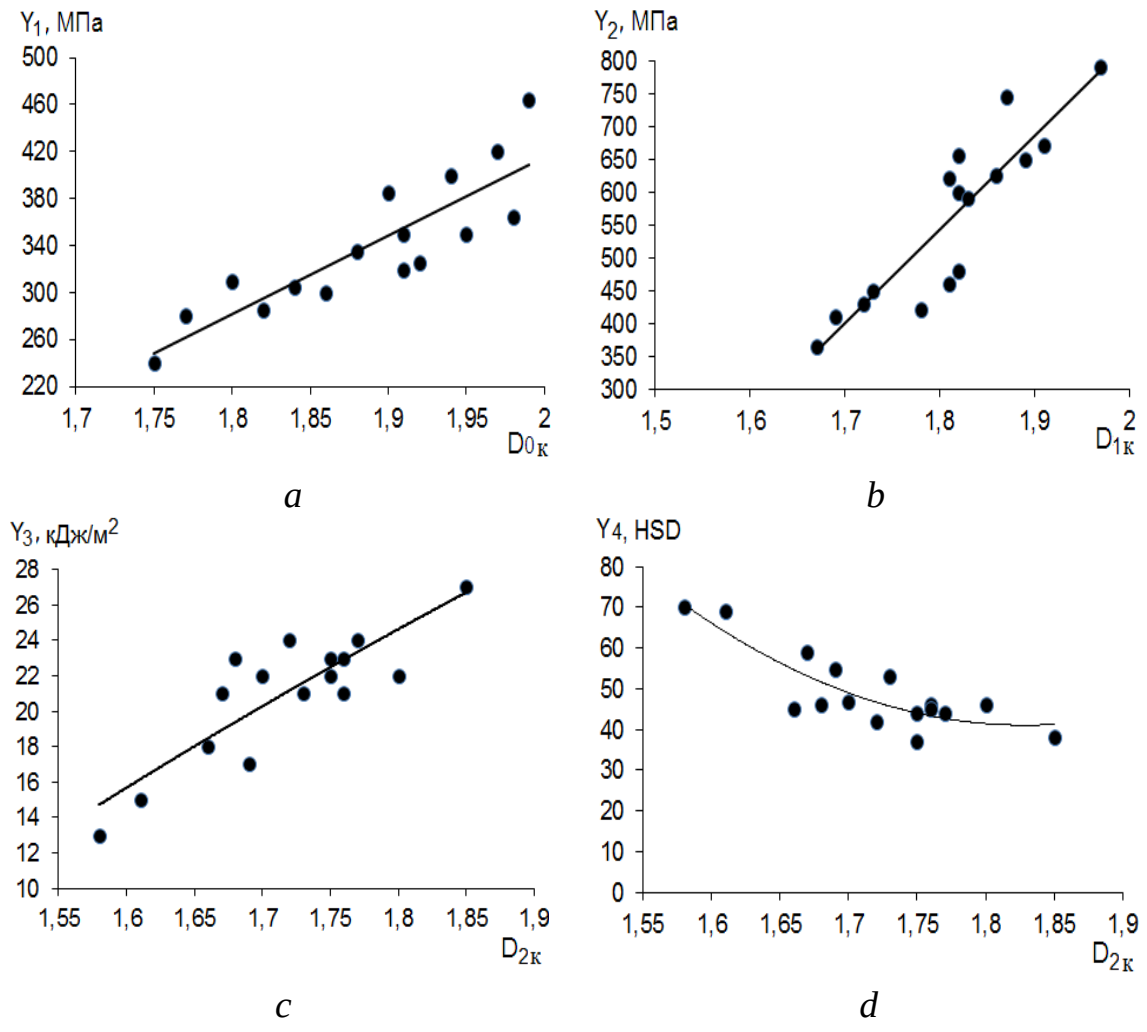

Fig. 4.28. Dependence of Y $_{1}$ on the fractal dimension of carbides (*a*), Y $_{2}$ on the informational dimension of carbides (*b*), Y $_{3}$ and Y $_{4}$ from the correlation dimension of the carbides (*c*, *d*) of SPHN rolls

Y $_{1}$ = 667.89 ·D $_{0\ to}$ –918.72, R ^{2} = 0.75 (4.14)

$$Y_2 = 1432.20 \cdot D_{1\,to} - 2035.90, \qquad R^2 = 0.80 \quad (4.15)$$

$$Y_3 = 75.89 \cdot \ln(D_{2\,k}) - 19.989, \qquad R^2 = 0.73 \quad (4.16)$$

$$Y_4 = 478.35 \cdot D_{2\,к}^2 - 1749.8 \cdot D_{2\,to} + 1641.2. \qquad R^2 = 0.72 \quad (4.17)$$

Dependencies for cast iron with spherical graphite have also been established . For the rolls of SSHKHN with the structure of spherical graphite, based on the analysis of the graphs shown in fig. 4.29 *a-c*, the increase in indicators of the quality characteristics of rolled iron occurs according to the state law.

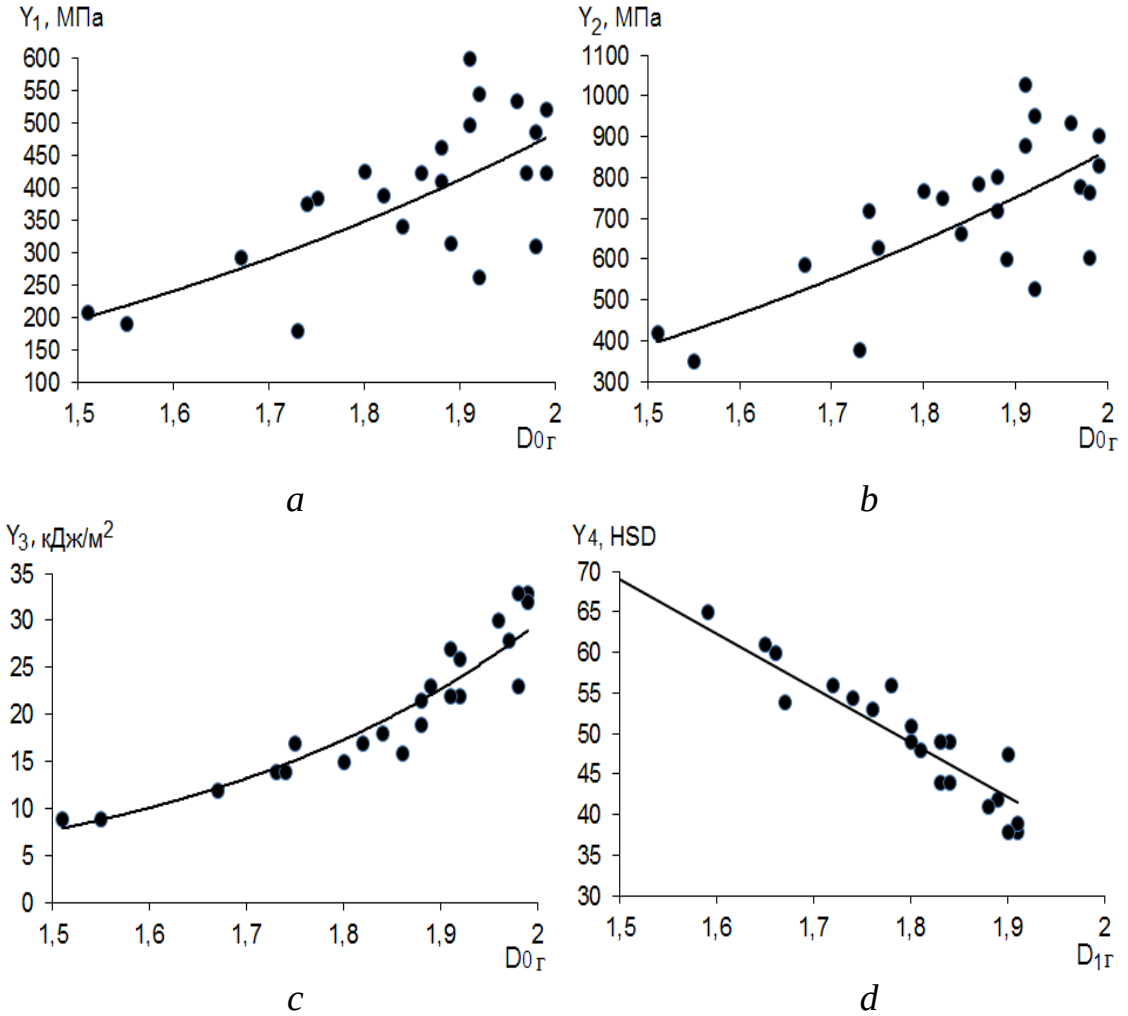

Fig. 4.29. Dependence of Y_1, Y_2, Y_3 on the fractal dimension of spherical graphite (*a, b, c*) and Y_4 from the information dimension of spherical graphite (*d*) of rolls of SSHKHN

Indicators σare increasing from 230 to 460 MPa; σ_{izg} –from 350 to 790 MPa; CS –from 9 to 33 kJ /m ^{2} in the case of an increase in the fractal dimension of graphite from 1.51 (the form of spherical graphite) to the topological dimension of the plane 2 (the form of compact graphite). When reducing the information dimension of graphite from 1.92 to 1.58, the HSD hardness indicators of rolled iron rolls increase from 40 to 60 units according to the linear law (Fig. 4.29 , (4.20)).

The experimental data given above testify to the effect of the shape of spherical graphite, expressed through the value of the fractal dimension, on the studied mechanical properties of grade-rolled rolls in SSHHN iconing, and the distribution of graphite inclusions on their hardness.

$$Y_1 = 55.185 \cdot D_{0г}^{3,1302}, \qquad R^2 = 0.51 \qquad (4.18)$$

$$Y_2 = 126{,}000 \cdot D_{0г}^{2,7811}, \qquad R^2 = 0.54 \qquad (4.19)$$

$$Y_3 = 0.1323 \cdot \exp(2.7074 \cdot D_{0g}), \qquad R^2 = 0.91 \qquad (4.20)$$

$$Y_4 = -67.239 \cdot D_{1g} + 170. \qquad R^2 = 0.90 \qquad (4.21)$$

There is a trend of increasing strength indicators (Fig. 4.30 *a, b*, equations (4.22) and (4.23)) and shock viscosity with a decrease in correlation (Fig. 4.30 *a*, equation (4.22)), information (Fig. 4.30 *b*, (4.23)) and fractal dimensions (Fig. 4.30 , (4.24)) of ledeburite and an increase in hardness indicators as its fractal dimension increases (Fig. 4.30 *d*, (4.25)). This testifies to the influence of the geometric characteristics of graphite inclusions of spherical graphite: shape configuration, quantity, and distribution on the quality indicators of cast iron rolls made by SSHKHN.

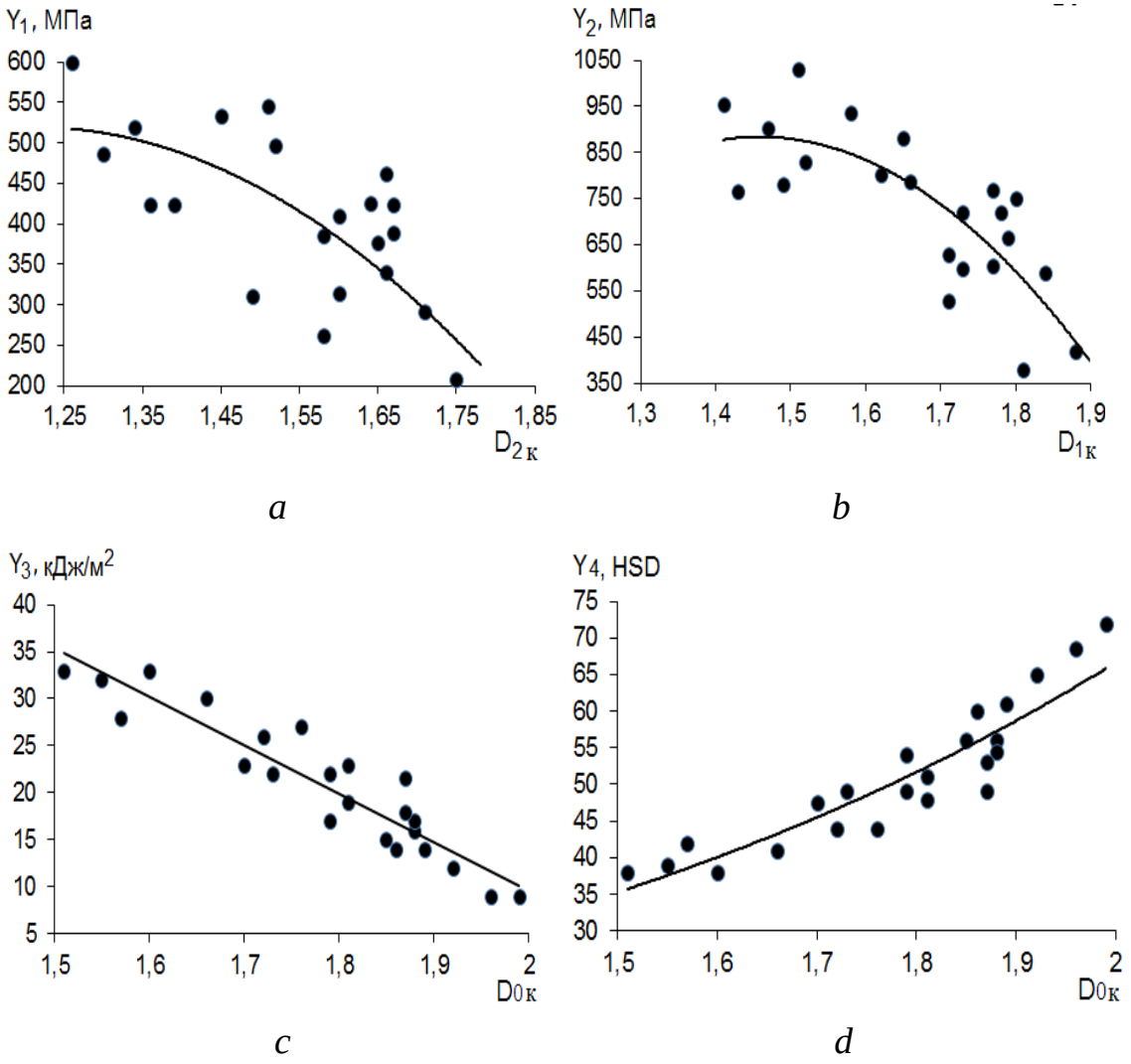

Fig. 4.30. Dependence of Y_1 on the correlation dimension of carbides (*a*), Y_2 from the information dimension of carbides (*b*), Y_3 (*c*) and Y_4 (*d)* from the fractal dimension of the carbides of SSKHN rolls

$$Y_1 = -907.09 \cdot D_{2к}^2 + 2198.30 \cdot D_{2\,to} - 812.48, \qquad R^2 = 0.85 \qquad (4.22)$$

$$Y_2 = -2497.70 + 7286.50 \cdot D \cdot D_{1к\,1}^2 K - 4430.20, \qquad R^2 = 0.69 \qquad (4.23)$$

$$Y_3 = -51.52 \cdot D_{0\,to} + 112.66, \qquad R^2 = 0.87 \qquad (4.24)$$

$$Y_4 = 5.2061 \cdot \exp(1.2751 \cdot D_{0\,k}). \qquad R^2 = 0.86 \qquad (4.25)$$

The analysis of the obtained results showed the promising application of the theory of multifractals for the quantitative assessment of the structural elements of cast iron rolls with a complex geometric shape configuration. Deviation of dimensional indicators not exceeding ± 0.06 –for SPKHN rolls and ± 0.05 –for SSHKHN rolls was revealed. This approach allows you to use statistical estimates of the dimensions of graphite and carbides , in particular ledeburite, to forecast and adjust the quality indicators of rolled metal according to the obtained equations (4.10-4.25) along with traditional methods of quantitative metallography, which are used to evaluate their geometric characteristics: shape, distribution, dimensions (length, diameter) and content.

Thus, it is advisable to use dimensional estimates of the metal structure to predict mechanical properties after establishing their sensivity.

SECTION 5.
USING THE LANGUAGE OF FRACTAL GEOMETRY TO EVALUATE THE MECHANICAL PROPERTIES OF THE SURFACE OF DUAL PURPOSE PARTS

5.1. Fractal modeling of the mechanical properties of the metal surface after ion- plasma chromium plating

Recently, to solve the problem of improving the mechanical properties of materials [118], new methods of surface strengthening [91, 92] are used, in particular, laser surface treatment [119, 120], surface surfacing [121, 122], detonation sputtering [87], surface nanomodification [76] and other progressive techniques. It should be noted that not all of the listed methods are able to provide the required level of physical and mechanical properties [89, 123].

Publications of recent years, for example [118] , show that the application of ion-plasma coating is one of the promising approaches to ensuring increased wear resistance of the working surfaces of machines and parts that are operated under conditions of abrasive wear. Ion- plasma processing changes the structure of the working surfaces of machines and parts, which in turn determines their properties. In most cases, such a structure is inhomogeneous, which complicates its quantitative assessment using traditional methods of metallography. The difficulty of identifying such structures is determined by the choice of measurement metrics [124]. Recently, the theory of fractals introduced by B. Mandelbrot [125], which is based on a non-integer (fractal) dimension, has been used to evaluate structures of varying degrees of complexity. As shown in many

publications, for example [126, 127], fractal dimensionality acts as an indicator of structural changes and properties of the material.

Based on the above, the purpose of this work is to apply the fractal formalism to evaluate the heterogeneous structure of the metal surface after ion- plasma treatment, with the subsequent establishment of a relationship between the spectrum of the structure's dimensions and the mechanical properties of the metal. To solve the set goal, the following tasks are implemented in the work:

1. Investigate the effect of ion- plasma treatment on the nature of damage to applied coatings during wear.
2. Apply multifractal analysis of heterogeneous structure to evaluate the mechanical properties of the metal surface after ion-plasma treatment.

strengthened by ion- plasma chrome plating have good wear resistance [128].

In the work, strengthening treatment (ion- plasma chrome plating) was performed according to the improved technology, which excludes overheating of parts during the process of coating and crushing it during the test.

High-quality coatings made of pure metals are obtained at substrate temperatures of at least 80–100 °C. The initial technological materials for vacuum ion- plasma sputtering are cathodes of sputtered metals, in this case chromium (VH-1). Vacuum ion- plasma sputtering was carried out on a vacuum-arc unit (Fig. 5.1).

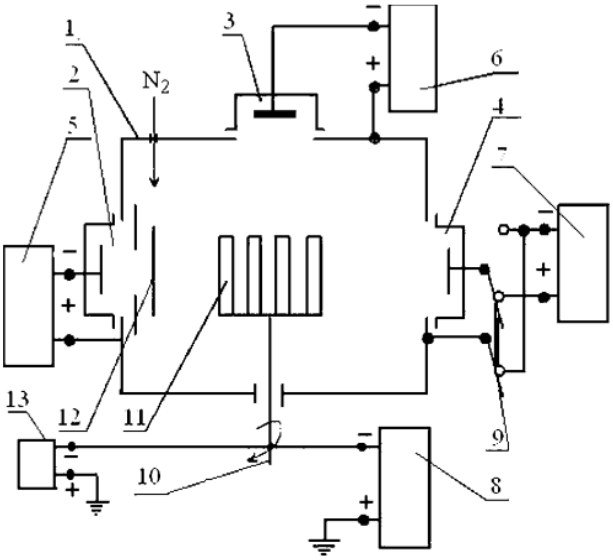

Fig. 5.1. Schematic diagram of a modernized vacuum-arc installation:

1 – vacuum chamber housing; 2, 3, 4 - vacuum-arc evaporators; 5, 6, 7 – power sources of evaporators; 8 - substrate power source; 9 – switch; 10 - rotary device; 11 - processed products; 12 – screen; 13 - generator of high-voltage pulses [129]

The study of the surface of parts strengthened by ion- plasma chromium plating was carried out using multifractal analysis [130], which is caused by the heterogeneity of the structure.

Multifractal analysis is based on the assessment of statistical characteristics of the elements of the metal structure, which are calculated according to the spectrum of dimensions Renyi D (q) (5.1) [131]. The dimensions of $D(q)$ are a set of statistical dimensions [132] of homogeneous subsets (elements of the structure) of the original set (structure), which give the largest contribution to the statistical sum $\sum_{i=1}^{N} p_i^q$ at given values of the exponent q. This statistical sum determines the distribution of probabilities over all points of the studied surface:

$$D(q) = \frac{1}{q-1} \lim_{\varepsilon \to \infty} \frac{\ln \sum_{i=1}^{N} p_i^q}{\ln \varepsilon}, \qquad (5.1)$$

where p_i - the probability of finding the investigated point (pixel for a computer) belonging to the object under consideration in the *ith* cell of a square grid of size ε. The exponent q can take any values in the range from $-\infty$ to $+\infty$. In the work, the exponent q varied in the range from $q_{min} = -600$ to $q_{max} = 600$.

Marking through $D_0, D_1, D_2, D_\infty, D_{-\infty}$ the dimensions of the Regny spectrum , characterized respectively: D_0 - homogeneous fractal (Hausdorff dimension) at $q = 0$; D_1 - the information dimension at $q = 1$ (information entropy) characterizes the rate of increase in the amount of information and shows how the information necessary to determine the location of a point located on the object of research grows when the size of the cells δthat cover the object increases , to zero; D_2 - the correlation dimension, which at $q = 2$ characterizes the probability of finding two points located on the object of observation in the same cell of the grid; $D_{+\infty}$ - dimension characterizing the most rarefied space in the object of observation (at $q = +\infty$); $D_{-\infty}$ - the dimension that characterizes the most concentrated space (at $q = +\infty$), which is observed in this object.

Fractal dimension (Hausdorff dimension) was calculated according to the formula of the dimension spectrum (5.1).

To determine the degree of heterogeneity of the structure, the singularity spectrum was calculated $f(\alpha)$ (5.2). This spectrum is described by the filling of square cells ε with equal probabilities when $p_i(\varepsilon) \approx \varepsilon^{\alpha}$.

$$\begin{cases} \alpha = \dfrac{d\tau(q)}{dq}, \\ f(\alpha) = q\alpha - \tau(q) \end{cases} \qquad (5.2)$$

The spectrum *f (α) was calculated by means of* Legendre transformations of the function *τ(q)* for each studied photograph of the surface microstructure of machine parts.

To solve the task, the following stages were implemented:

1. Analysis of the damaged working surfaces of the tested machine parts according to the nature and location of the zones in order to implement the technological process of their strengthening with the use of ion- plasma chrome plating.

2. Registration of changes in the structure and properties of the strengthened surface areas of the studied parts in the process of operation using the fractal formalism.

In the course of the implementation of the first stage, the nature of the damage of the parts after wear, strengthened by ion- plasma chrome plating according to the improved technology, was investigated (Fig. 5.2 and Fig. 5.3).

Cracks are observed on the tested parts of the investigated variant (Fig. 5.2 and Fig. 5.3).

On the body and sleeve, cracks are observed in the "A" and "B" zones. Their depth on the body reaches 0,55 мм, on the sleeve - 0,4 мм. There are no cracks in zone "C". On the striker, cracks are fixed in the "N" zone with a depth of up to 0.3 mm and in the "M" zone - up to 0.6 mm. At the peak, cracks are observed only in the "M" zone, with a depth of up to 0.6 mm.

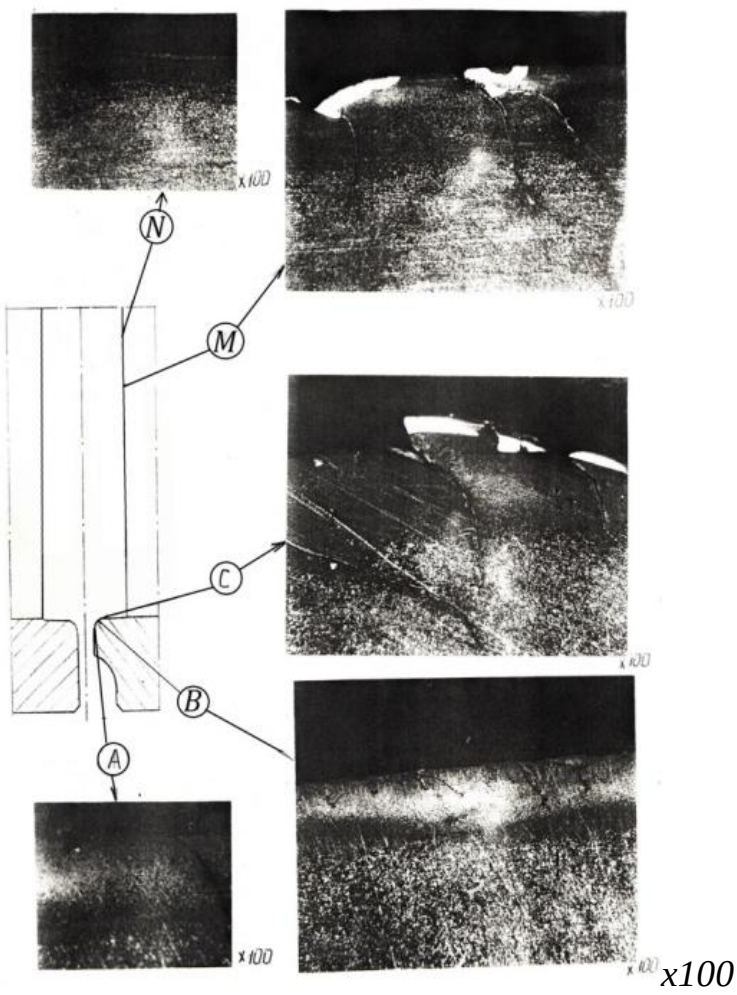

Fig. 5.2. Structural changes in the material of the case and striker, strengthened by ion- plasma chrome plating (according to improved technology)

The type of cracks in fractures is similar to what was previously observed in other strengthening options (defined contour, oxidation and surface smoothness).

On the body and bushing, the remains of the coating are observed in the "A" and "C" zones.

The thickness of the coating on the sleeve in zones "A" and "C" is 10 microns , on the body (channel) in zone "C" up to 10 microns . At the battle

and peaks, the coverage was preserved only in the "N" and "E" zones. The thickness of the layer on the strike is 10 μm , at the peak - up to 5 μm.

Structural changes are observed in the metal of the studied parts in the damage zones. On the bushing, structural transformations to a depth of 0.25–0.30 mm are noted in zones "A" and "B", on the top - to a depth of 0.15–0.20 μm in zones "A", "B" and "C" » respectively.

The hardness of the HB material in the zones of structural transformations varied within 510–645 units.

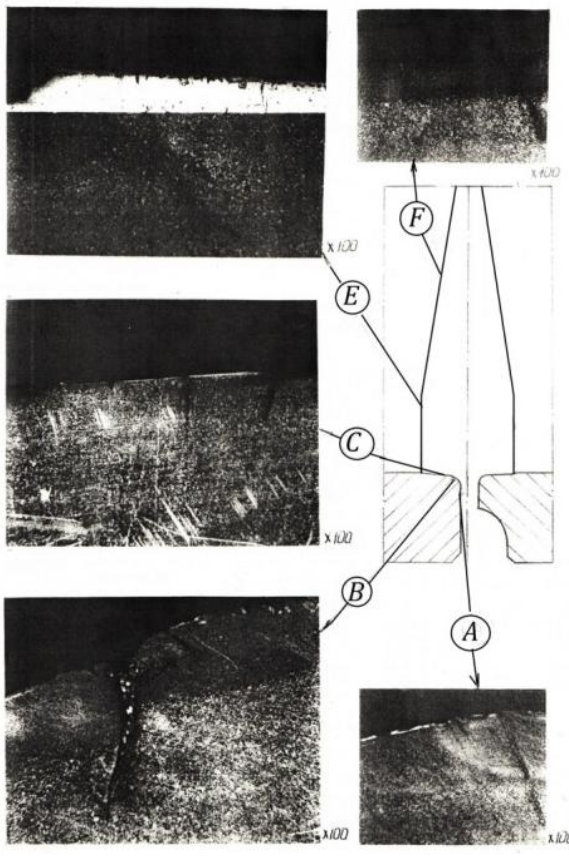

Fig. 5.3. Structural changes in the material of the spikes and bushings strengthened by ion- plasma chrome plating (according to improved technology)

In the peak material, structural changes to a depth of 0.25–0.30 mm are observed in the "N" and "M" zones. The depth of structural changes in

these zones is 0.15–0.20 mm. The hardness of the material in the zones of structural changes is HV 510–585.

The hardness of the material of the investigated parts is:
sleeve - NRS 40-42; peak - NRS 40-42;
case - NRC 40-42; fight - NRS 40-42.

sorbitol- type parts with a finely dispersed structure.

fractal approach was used to implement the second stage of research.

Based on the results of the analysis of the spectrum of statistical dimensions $D(q)$ and the spectrum of singularities $f(\alpha)$, the following statistical characteristics of the structure were calculated [60]:

– *homogeneity* , which describes the local defectiveness of the analyzed structure, the porosity or roughness of its individual elements. In this case, it corresponds to the value of D (at $q = 600$), the increase in the values of which indicates an increase in the homogeneity of the structure. If the structure is completely homogeneous, the spectrum $f(\alpha)$ degenerates into a point. The heterogeneity of the structure means an uneven distribution of points in the areas into which the structure is divided, that is, its geometrically identical elements are filled with points with different probabilities;

– *orderliness structures or hidden periodicity* $\Delta = D_{1} - D_{600}$ and *regularity* $K = D_{-600} - D600$. The dimension D_{1} is called the information dimension and is calculated from the spectrum of dimensions when the indicator q is equal 1. These characteristics describe the degree of symmetry violation of the structure or the degree of imbalance of the system. The higher the numerical values of indicators Δ and K , the more

periodic components (repeated structural elements of one structural component) in the structure, and the more it is ordered.

In fig. 5.4 and fig. 5.5 shows the calculations of the spectra of the functions *D(q)* and *f(α)* for the structures of the striker surface shown in Fig. 5.2 and peaks (see Fig. 5.3). The characteristics of homogeneity, orderliness and regularity are calculated based on the analysis of the spectrum *D(q)* (Fig. 5.4). The spectrum *f(α)* (Fig. 5.5) determines the degree of dimensional homogeneity of the structure.

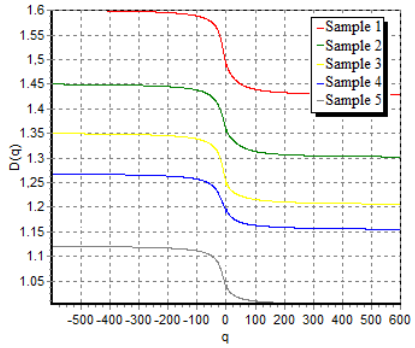

a

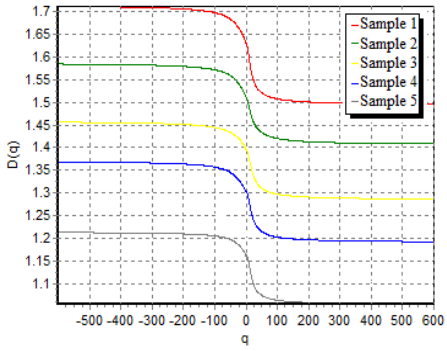

b

Rice. 5.4. Spectrum of statistical dimensions Renyi *D(q)* for spades (*a*) and spades (*b*)

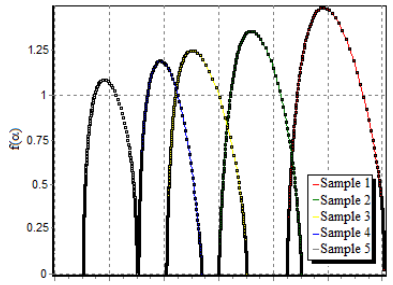

a

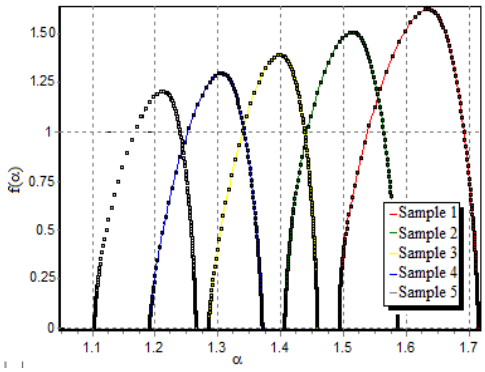

b

Rice. 5.5. Spectrum of singularities *f(α)* for spades (*a*) and spades (*b*)

Dimensionality *D-* $_{600}$ describes the most concentrated space (dark areas of the structure) with a predominance of cementite. This is due to the

fact that sorbite is a eutectoid mixture of cementite and ferrite. The cementite plates in the sorbite structure under consideration have a dark color, and the ferrite plates have a light color. Therefore, the dimension D_{600} corresponds to the light areas of the structure (ferrite plates).

The results of the experiment on determining the mechanical properties of machine parts (strength limit σ_{in}, yield strength $\sigma_{0.2}$, relative elongation δ and narrowing ψ), and the spectrum of multifractal characteristics of its sorbite structure according to formulas (6.1) and (6.2) are given in table. 5.1.

Table 5.1.

The value of the characteristics of homogeneity, orderliness and regularity of the sorbite structure (axial direction of sample cutting)

Detail	Sample number	Mechanical properties				Multifractal characteristics			
		σ_{in}, MPa	$\sigma_{0.2}$, MPa	δ, %	ψ, %	D_{600}	Δ	K	D_0
peen	1	1390	1310	9.0	25	1.49	0.06	0.15	1.50
	2	1410	1320	8.0	23	1.35	0.05	0.15	1.36
	3	1400	1330	8.5	24	1.25	0.04	0.14	1.27
	4	1420	1345	7.5	23	1.20	0.05	0.12	1.21
	5	1430	1360	7.0	22	1.04	0.03	0.11	1.05
of spades	1	1450	1360	8.0	15	1.50	0.08	0.21	1.64
	2	1440	1380	8.5	11	1.41	0.09	0.17	1.54
	3	1460	1370	7.0	8	1.29	0.12	0.18	1.42
	4	1470	1380	6.4	5	1.20	0.09	0.17	1.30
	5	1480	1390	6.0	3	1.05	0.06	0.16	1.17

In fig. 5.6 shows histograms of the influence of multifractal characteristics of the microstructure of the striker and peaks on the mechanical properties of the metal. The histograms are built on the basis of the analysis of the correlation coefficients between the multifractal characteristics and the mechanical properties of the metal.

The analysis of multifractal statistical characteristics of homogeneity, orderliness, and regularity of the elements of the structure showed that a high sensitivity to them is observed for the yield point (Fig. 5.6 *a*). It was experimentally established that the sensitivity coefficients of the multifractal characteristics of the structure K_i vary from 0.67 to 0.97.

Statistical characteristics of the microstructure of the peak are most sensitive to relative narrowing (Fig. 5.6 b*)* . The coefficients of sensitivity ψ*to* the dimension of the lightest parts of the structure (ferrite plates) are 0.98, and for δthe indicator K_i is 0.85. Forδ and ψ relatively high indicators for their fractal dimension were also recorded - 0.97, respectively. Such results are explained by the fact that ferrite has high plastic properties compared to the cementite under consideration. That is why plastic properties are so sensitiveδ and ψ to multifractal statistical characteristics of ferrite is natural. In this case, for the peak (Fig. 5.6 *b*), the sensitivity between the regularity index $K = D_{-600} - D_{600}$ and the yield strength is 0.92, since cementite determines the strength properties more than ferrite.

The results of the multifractal analysis show that the statistical characteristics of the structure can be an indicator of changes in mechanical properties.

Based on the analysis of the results of the sensitivity indicators of the mechanical properties to the multifractal statistical characteristics of the

structure (Fig. 5.6), fractal models for the strike (6.3) and peaks (6.4) were obtained.

$$\sigma_{0.2} = 1488,16 + 115,50 \cdot D_{600} + 32.57 \cdot \Delta - $$
$$- 460.62 \cdot K - 188.62 \cdot D_0, \qquad R^2 = 0.88. \qquad (5.3)$$
$$\psi = - 29.17 - 33.03 \cdot D_{600} - 24.82 \cdot \Delta + 28.17 \cdot K +$$
$$+ 54.72 \cdot D_0, \qquad R^2 = 0.89. \qquad (5.4)$$

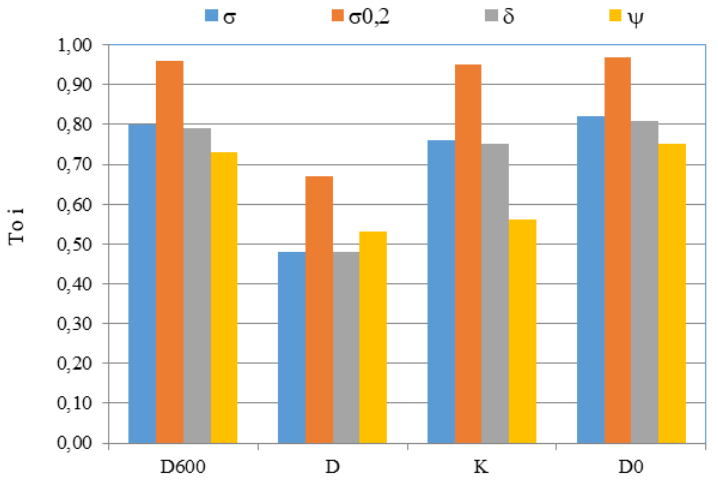

a

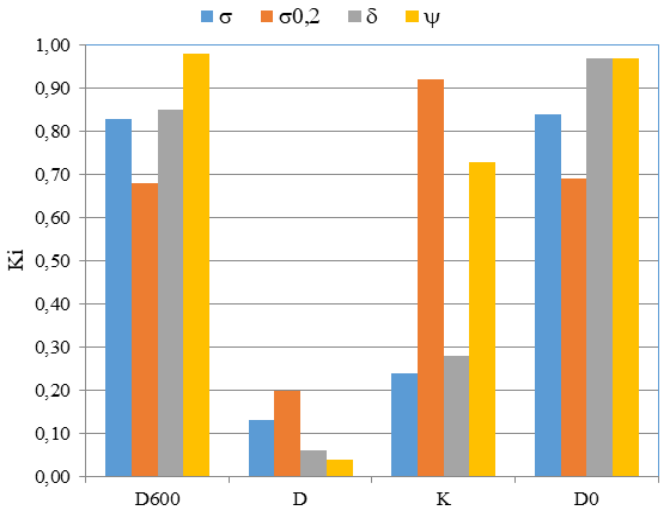

b

Fig. 5.6. The influence of indicators of homogeneity D_{600}, orderliness Δ, regularity K and fractal dimension D_0 on the properties of strength and plasticity (*a*) and peaks (*b*)

The adequacy of the model (5.3) according to the Durbin-Watson statistic was 2.62, and for the model (5.4) it was 3.12.

Fractal models (5.3) and (6.4) describe the complex influence of homogeneity, orderliness, regularity and fractal dimension on the mechanical properties of $\sigma_{0.2}$ and ψ.

It should be noted that additional connections between the structure and physical and mechanical properties of the metal during operation after ion -plasma treatment have been established. This approach makes it possible to use these fractal models as a non-destructive method of assessing mechanical properties.

The following conclusions can be drawn on this topic:

1. The effect of ion- plasma treatment on the nature of damage to the coatings of parts was investigated. Damage to parts is characterized by wear of the coating, metal slander, the formation of burrs and cracks . In the most heavily loaded parts of the parts (in the zones "B" and "C" on the body of the striker and sleeve and "M" and "F" on the striker and pick), the reinforcing coating has almost completely worn out. The improved technology of ion- plasma chrome plating ensures the operation of hardened parts without chipping and chipping of the coating. A feature of the test results of this strengthening option is less wear of the lower parts (sleeve, peak) compared to the upper ones.

2. Multifractal analysis of the heterogeneous sorbite structure was used to evaluate the mechanical properties of parts after ion- plasma treatment. The adequacy of the obtained models (5.4) and (5.5) is confirmed by Durbin-Watson statistics . The sensitivity of the multifractal characteristics of cementite to strength properties σin (0.80) and $\sigma_{0.2}$ (0.96),

as well as ferrite to plastic properties δ and ψ (0.97), was established , which is confirmed by the histograms in Fig. 5.6.

6.2. Application of modern methods of fractal formalism to study the effect of plasma coatings on the wear resistance assessment of volumetric hydraulic drive parts

The structure and properties of many materials are influenced by the methods of their production, their processing regimes, phase and chemical composition, etc. [91 , 92, 118 , 119].

Applying a titanium nitride coating to the parts of the volumetric hydraulic drive affected the tribotechnical characteristics: the wear resistance increased, the friction coefficient decreased. But the efficiency of these important parts depends on durability, which in this case involves reducing or reducing to zero the danger of surface hardening and on such an important indicator as corrosion resistance [97, 120-122]. Based on the analysis of the works devoted to the use of plasma coatings [76, 89, 123], the coating of the Ti – Cr –N system with preliminary ion bombardment of the surface with chromium was chosen. Cr was chosen as the material for ion bombardment . Ion bombardment increases the density of the centers of the formation nucleus, reduces the number of vacancies and pores, introduces thermal energy directly into the surface zone, stimulating diffusion processes. For each temperature and type of coating, there are optimal modes of ion bombardment that lead to the most perfect structure. Ion bombardment leads to a decrease in grain size , which contributes to the formation of nanocrystalline films. By adjusting the energy and flow density of the bombarding ions, the grain sizes can be controlled . It is known that the best combination of strength and plastic properties occurs with grain sizes less than 10 nm [125].

The purpose of the work is to investigate the feasibility of using the fractal approach to assess the effect of plasma coatings to increase the wear resistance of parts of a volumetric hydraulic drive. The chosen fractal analysis has successfully proven itself for modeling the structure and properties of many materials [101, 105, 107, 108] .

To apply the Ti – Cr –N coating on the surface of the 38X2MUA steel, the installation chamber was converted (Fig. 5.7).

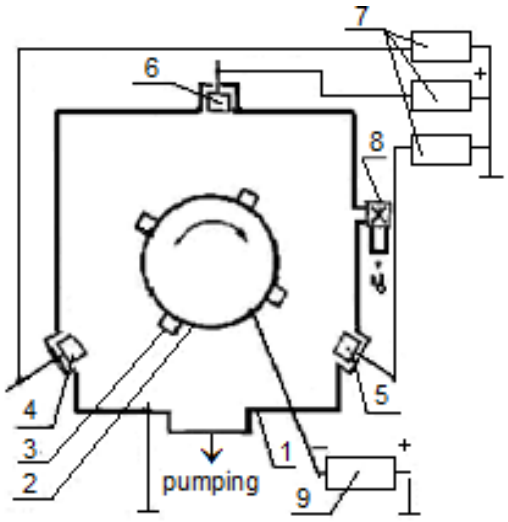

1 – vacuum chamber; 2 – cylindrical custom; 3 – details; 4, 5, 6 – cathodes; 7 – welding rectifiers; 8 – push button; 9 – a source of negative voltage

Fig. 5.7. Scheme of a vacuum chamber for deposition of coatings from double nitride systems

In the center of the vacuum chamber, a cylindrical shell 2 is mounted with parts to which a coating 3 is applied. On the side flanges of the vacuum chamber, there are plasma sources 3 based on vacuum arcs, which contain metal cathodes 4, 5, 6. One of the plasma sources (cathode 4) was evaporated Ti , and the remaining two – Cr . The radius of the pipe adjusts the distance from the parts to the evaporators. This distance may vary depending on the size of the installation chamber. In the process of rotation, the sputtered surface of the parts passes alternately under the

working cathodes 4, 5, 6. The deposited coating depends on the distance from the part to the evaporator, the speed of rotation of the nozzle, the number of evaporators, the material of the cathodes). Determining these parameters in each specific case is important, since when three cathodes work simultaneously, there are areas where the direct flow of the substance does not condense, where condensation of the substance vaporized by only one evaporator occurs, and areas where the flows from two evaporators overlap. The angular size of these areas depends on the ratio between the radius of the base (r) and the radius of the chamber of the "Bulat" installation (R).

For our operating conditions, the ratio r/R = 0.6 was chosen. The speed of rotation of the die with sprayed parts was 10 rpm during the operation of three evaporators. The device received a positive decision on application No. 2010 03834 dated 04.2.2010. Evaporators made of chromium (VKH1-17) and titanium (VT1-0) were used.

The strength of the connection between the coating and the substrate was evaluated according to the method based on joint plastic deformation of the coating and the substrate during the introduction of the indenter of the Rockwell hardness tester . Tensile stresses arise at the coating-substrate boundary. If the adhesion strength of the coating to the substrate is good, there is no violation of integrity around the impression. The smaller the connection between the coating and the substrate, the larger the area of its chipping around the print. The strength of the connection of the coating with the base metal was judged by the size of the relative chipped area of the coating around the impression. The area was determined using an optical microscope with a magnification of 100 times. An eyepiece with a grid was used.

The strength of the compound K_α was estimated according to the formula (5.5):

$$K_\alpha = \frac{S_0}{S_k + S_0}, \quad (5.5)$$

where S_0 is the footprint area in the plane of the working surface;

S_k is the chipped area of the coating in the plane of the working surface.

The values varied from zero (poor connection) to one (with good adhesion to the substrate).

When conducting research, the metallographic method was used to measure the thickness of the coating, which consists in measuring the thickness of the coating using an optical microscope on cross sections. But this method is destructive and makes it possible to measure only in the plane of the cut.

Wear tests were carried out on the SMC-2 friction machine, which allows comparison of the tested materials according to wear-resistant properties according to the "roller-pad" scheme (Fig. 5.8).

The friction pair consists of a rotating roller with a diameter of 50 mm, against the cylindrical surface of which a fixed block is rubbed in a special mandrel. The pad is a part of the ring, the inner surface of which (the working surface) is made strictly according to the radius of the roller. The contact of the counterbody made of cast iron СЧ20 during operation is carried out on a surface with an area of about 2 cm^2 to ensure the stability of the block during tests. Lubrication was carried out with I20A industrial oil with the addition of 0.1% of abrasive particles with a dispersion of up to 5 μm . The rollers were made of steel 45 and 38Х2МЮА in various heat-treated states.

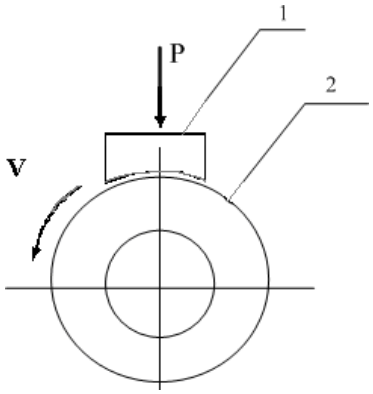

1 – still sample (pin feather); 2 – moving sample (roller)

Fig. 5.8 . Scheme trials, What are held on car friction SMC- 2

The surface structure of the Ti – Cr –N coating was studied using a SEM scanning electron microscope at an accelerating voltage of 30 kV in the magnification range from 20 to 10,000 times.

In fig. 5.9 shows the structure of the studied material. The Ti – Cr –N coating is characterized by the presence of Ti and Cr droplets , some of which are on the surface, and some are fixed in the volume of the coating (Fig. 5.9, *b*, *c*). The distribution of Ti and Cr droplets on the surface is heterogeneous in size, which is determined by the nature of the deposited metal and the deposition conditions.

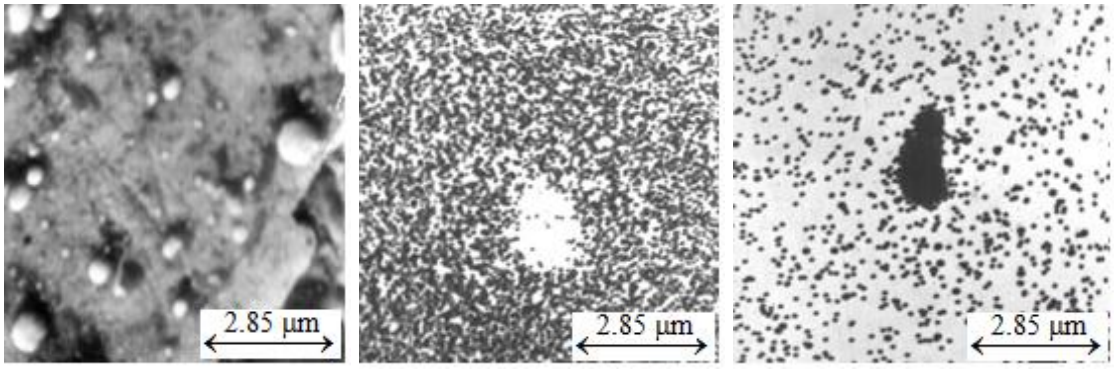

a *b* *c*

Fig. 5.9. *a* – general type of coating; *b* – the nature of the distribution of Cr in the coating in the characteristic rays of Cr ; *c is* the nature of the distribution of Ti in the coating in the characteristic rays of Ti Rice. 6.9. Ti – Cr –N coating

Ti - Cr -N coating process on the working surfaces of the parts of the volumetric hydraulic drive are given in table. 5.2.

Table 5.2

Ti - Cr -N coating process on the working surfaces of parts of a volumetric hydraulic drive

Emission cathode material	arc current, I_1, A	arc current, I_2, A	High-voltage u IN	Stru m I, A	Pressure R, tor	Time t, min
1st stage: cleaning, warmed up and activation ions chrome						
Chrome	80	–	90	2	$1 \cdot 10^{-4}$	7
2nd stage: spraying layer coating in atmosphere nitrogen or nitrogen-containing gas						
2 cathodes: 1st – chrome; 2nd - titanium	80	70	150	3	$5 \cdot 10^{-3}$	25

Fractal analysis was used to assess the influence of the structure of the Ti – Cr –N coating on its wear indicators.

The fractal dimension was calculated according to the Hausdorff method [132]. Photos of the structure were processed in 256-color format with shades of gray. To calculate the values of the fractal dimension D (4.1), the photograph of the structure was covered with N cells, the size l of which varied from 2 to 9 pixels.

An example of fractal 3D analysis for the structure in Fig. 5.9 and is given below (Fig. 5.10) .

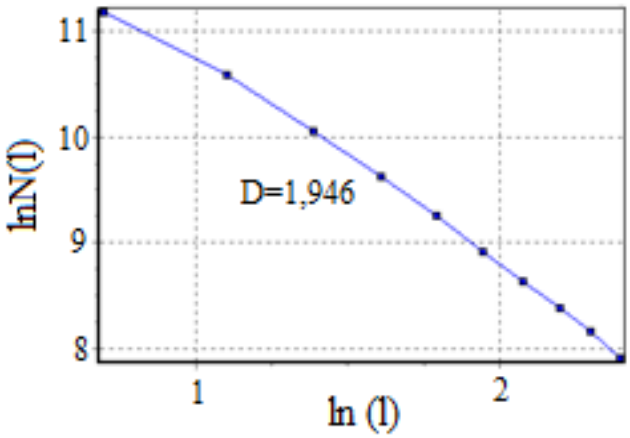

Fig. 5.10. Dependence of the cells covering the object on their size

It is known that not only the composition of the applied coating is of great importance, but also such parameters as the hardness of the substrate material, the roughness of the surface on which the coating is applied, and the thickness of the coating. Hardness is chosen as one of the indicators, as it can be easily checked at any point of the product without harming the integrity both before and after use. The practice of operating products made of this grade of steel with the application of plasma coatings on the working surfaces showed that the hardness of the product to which the coating is applied should be at least 0.48 Ra . Otherwise, peeling of the coating is observed due to poor adhesion with the substrate. The research material was steel 38X2MUA, heat treatment is an improvement that provides the best ratio of strength and plasticity properties.

After heat treatment of steel 38X2MUA, its hardness ranges from 40...45 HRC. The thickness of the applied coating varied from 3 to 6 microns, which corresponds to good adhesion, a smaller thickness does not significantly affect the properties of the product, and in the case of a thickness of more than 6 microns, peeling is observed due to poor adhesion with the substrate. According to the methods of mathematical planning of the experiment, we will take the thickness of the coating and the roughness

as a variable factor, and denote them X_1 and X_2. As a response function, we will accept wear and denote Y. Based on the above considerations, we assume that the limits of the existence (change) of factors are $X_{1min} = 3$; $X_{1max} = 6$; $X_{2min} = 0.10$; $X_{2max} = 0.48$. Factor fluctuation intervals, respectively, $\Delta X_1 = 6 - 3 = 3$; $\Delta X_2 = 0.48 - 0.1 = 0.38$.

First, a first-order factorial experiment was conducted , the purpose of which was to obtain a mathematical model of the dependence of Y on X_1 and X_2 in the form of a linear polynomial. For this purpose, a full factorial experiment of type 2^n was implemented (for each hardness value) . His results are presented in Tables 2–6. Let's take the fractal dimension of the Ti - Cr -N coating of the working surface of the parts of the volume hydraulic drive as the indicator D.

The results of research on determining the parameters of the experiments are given in Table 5.3 - Table 5.7.

Table 5.3

The value of the thickness of the coating, roughness and wear at a substrate hardness of 42 HRC

No. of the experiment	X_1	X_2	Y_1	D
1	3.00	0.10	6.50	1.85
2	3.00	0.48	7.30	1.82
3	6.00	0.10	3.30	1.90
4	6.00	0.48	4.50	1.91
5	4.50	0.29	5.20	1.87
6	4.50	0.10	4.80	1.88
7	4.50	0.48	5.40	1.88
8	3.00	0.29	6.80	1.86

Table 5.4

The value of the thickness of the coating, roughness and wear at a substrate hardness of 43 HRC

No research	X_1	X_2	Y_2	D
1	3.00	0.10	6.30	1.81
2	3.00	0.48	7.00	1.77
3	6.00	0.10	4.00	1.87
4	6.00	0.48	4.40	1.87
5	4.50	0.29	5.20	1.87
6	4.50	0.10	4.80	1.85
7	4.50	0.48	5.40	1.88
8	3.00	0.29	6.80	1.86
9	6.00	0.29	4.20	1.88

Table 5.5

The value of the thickness of the coating, roughness and wear at a substrate hardness of 44 HRC

No research	X_1	X_2	Y_3	D
1	3	0.10	5.60	1.83
2	3	0.48	6.20	1.76
3	6	0.10	3.60	1.91
4	6	0.48	4.00	1.89
5	4.5	0.29	5.00	1.84
6	4.5	0.10	4.40	1.88
7	4.5	0.48	5.20	1.85
8	3	0.29	6.00	1.80
9	6	0.29	3.80	1.90

Table 5.6

Value of coating thickness, roughness and wear at substrate hardness of 45 HRC

No research	X_1	X_2	Y_4	D
1	3	0.10	3.50	1.80
2	3	0.48	3.80	1.77
3	6	0.15	2.11	1.94
4	6	0.48	2.40	1.89
5	4.5	0.29	2.51	1.87
6	4.5	0.10	2.45	1.86
7	4.5	0.48	2.76	1.84
8	3	0.29	3.50	1.79
9	6	0.29	2.17	1.92

Table 5.7

The value of the thickness of the coating, roughness and wear at a substrate hardness of 46 HRC

No. of the experiment	X_1	X_2	Y_5	D
1	3	0.10	4.40	1.83
2	3	0.48	4.80	1.78
3	6	0.10	3.00	1.90
4	6	0.48	3.40	1.88
5	4.5	0.29	4.00	1.90
6	4.5	0.10	3.80	1.85
7	4.5	0.48	4.10	1.84
8	3	0.29	4.60	1.82
9	6	0.29	3.40	1.87

According to the results of processing the values of the experiments in tables 5.3 - 5.7, linear models of the forecast of wear indicators (5.6)-(5.10) were obtained.

At 42 HRC:

$$Y_1 = 10.71 - 0.98 \cdot x_1 + 2.27 \cdot x_2 - 0.88 \cdot D \qquad R^2 = 0.96 \qquad (5.6)$$

At 43 HRC:

$$Y_2 = 11.65 - 0.80 \cdot x_1 + 1.48 \cdot x_2 - 1.69 \cdot D \qquad R^2 = 0.95 \qquad (5.7)$$

At 44 HRC:

$$Y_3 = 13.04 - 0.60 \cdot x_1 + 1.25 \cdot x_2 - 3.14 \cdot D \qquad R^2 = 0.98 \qquad (5.8)$$

At 45 HRC:

$$Y_4 = 17.64 - 0.12 \cdot x_1 + 0.16 \cdot x_2 - 7.73 \cdot D \qquad R^2 = 0.89 \qquad (5.9)$$

At 46 HRC:

$$Y_5 = 5.95 - 0.44 \cdot x_1 + 0.95 \cdot x_2 - 0.16 \cdot D \qquad R^2 = 0.98 \qquad (5.10)$$

The relative error of the calculations of wear indicators ranged from 0.04 to 8.96.

By performing a direct calculation, we will find the smallest wear value in each case. In the table 5.8 shows data on the smallest values of wear Y.

Table 5.8

The lowest values of wear indicators are in the range of 42...46 HRC

Hardness, HRC	arguments			function
	X_1	X_2	D	Y

End of table 5.8

42	6	0.10	1.90	3.30
43	6	0.10	1.87	4.00
44	6	0.10	1.91	3.60
45	6	0.15	1.94	2.11
46	6	0.10	1.90	3.00

As can be seen from this table, the lowest wear value of 2.11 is predicted for a hardness value of 45, a coating thickness of 6 and a roughness value of 0.15.

The response surface (Fig. 5.11) and the model for estimating the smallest values of wear at the rear point $X_1 = 6$ (7) are given below:

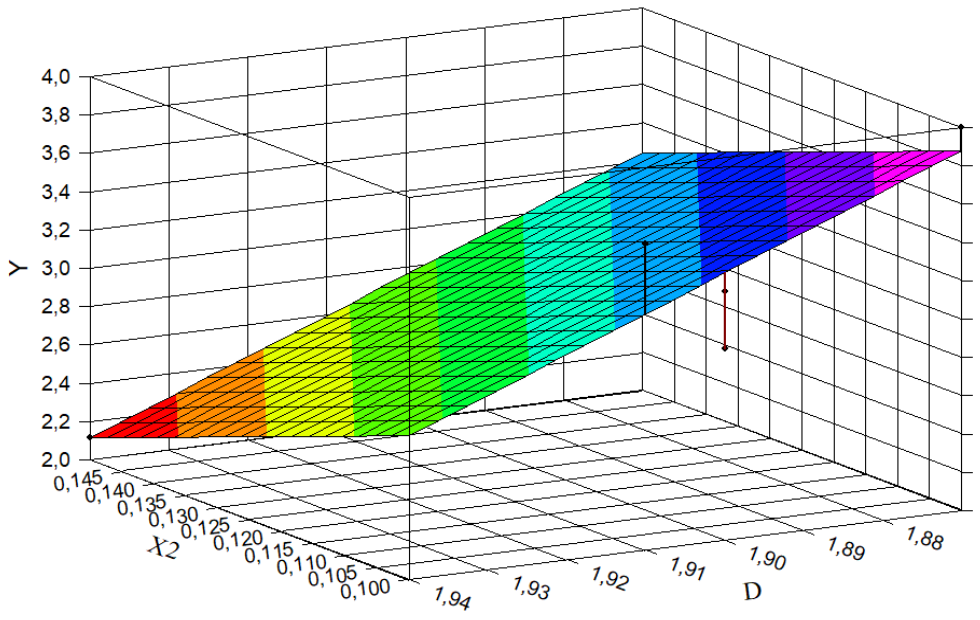

Fig. 5.11. Evaluation of the effect of roughness (X_2) and fractal dimension of the surface (D) on wear indicators (Y) at a fixed coating thickness of 6 microns

The pairwise correlation coefficient of the fractal model is 0.84 (5.11), and using only the roughness indicators of the base material, the correlation coefficient of this wear estimation model is 0.73 (5.12) at fixed values of the coating thickness of 6 μm .

$$Y = 35.28 - 12.80 \cdot X_2 - 16.11 \cdot D \qquad R^2 = 0.84 \qquad (5.11)$$

$$Y = 27.30 - 6.20 \cdot X_2 \qquad R^2 = 0.73 \qquad (5.12)$$

To confirm this hypothesis, an experiment was conducted to determine wear resistance at the level of 2.11 with a hardness of 45, a roughness of 0.16 and a coating thickness of 6.

At the same time, the following conclusions can be drawn:

1. Studies of the feasibility of using the fractal approach to evaluate the effect of plasma coatings to increase the wear resistance of parts of a volumetric hydraulic drive have been conducted.

2. Using the experiment planning method, it was established that the lowest wear value of the part made of 38X2MUA steel after heat treatment of improvement was obtained at the hardness of the main material 45 HRC, roughness 0.15 and coating thickness 6 μm .

3. Fractal analysis of the Ti – Cr –N coating was carried out , which is characterized by the presence of Ti and Cr droplets , some of which are on the surface and some are fixed in the volume of the coating. The fractal dimension was calculated using the Hausdorff cell method .

A fractal model with a correlation coefficient of 0.84 was obtained to evaluate the wear resistance of the parts of the volumetric hydraulic drive , and for the model using only the roughness indicators of the main material, the correlation coefficient is lower and is 0.73 at fixed values of the coating thickness of 6 μm , which indicates the feasibility application of fractals.

LIST OF USED SOURCES

1. Volchuk VM Application of new plasma coatings for restoration of the surface of material / Volchuk VM , Hlushkova DB // Functional Materials. - 2024. - 31(2). - pp. 205–209.
2. Hlushkova DB Development of optimal technological parameters for plasma coating deposition / Hlushkova DB, Volchuk VM, Demchenko SV, Polyansky PM / Problems of Atomic Science and Technology. – 2024. - 149(1) - Pp. 138–144.
3. Avrunin G. A. Fundamentals of volumetric hydraulic drive and hydro-pneumatic automation: study guide / G. A. Avrunin, I. G. Kyrychenko, I. I. Moroz / Ed. G. A. Avrunin. – Kharkiv: Khnadu, 2009. – 424 p.
4. Avrunin G. A. Modern volumetric hydraulic drives for mobile lifts with working platforms / G. A. Avrunin, I. G. Kyrychenko, O. O. Reznikov, I. I. Moroz / theses of reports of the 29th international scientific and practical conference MicroCAD -2021, May 18–20, 2021: at 5 p.m. Part I. / edited by Prof. E.I. Sokol - Kharkiv: NTU "KhPI". - 333 p. - P. 132.
5. Dvoruk V.I. Metallophysics of wear during sliding friction in the presence of an abrasive / V.I. Dvoruk, M.V. Kindrachuk / Proceedings of the National Aviation University. – 2005. – No. 2. – P. 65–67.
6. Stofel O. O. Improvement of the fractal analysis method for assessing the relationship between the structure and properties of structural steels : dissertation. on of science stupa candidate of technical sciences with special. 05.16.01 "Metalology and heat treatment of metals" / O. O. Shtofel / Kyiv. – 2021. – 163 p.
7. Ogorodnikov, V. A. Mechanics of processes of cold plastic deformation of axisymmetric workpieces with a blind hole: monograph / V. A. Ogorodnikov, I. Yu. Kyrytsia, V. Ye. Perlov. – Vinnytsia: VNTU, 2015. – 164 p.

8. A fractal approach to estimating the durability of critical parts /AV Uzhva, OV Orel, DB Hlushkova, VM Volchuk // Functional Materials. - 2024. - 31(3). - pp. 381–386.
9. Theory and practice of processing materials by pressure / Under the RSD. Boguslaeva V. O., Bobirya M. I., Titova V. A., Kachana O. Ya. - Zaporizhzhia, ed. AT "Motor Sich", 2016. - 522 p.
10. Zakalov O. V. Basics of friction and wear in machines: Study guide / O. V. Zakalov, I. O. Zakalov. – Ternopil: Publishing house of TNTU named after I. Pulyuya, 2011. – 322 p.
11. Avrunyn G. A. Modern achievements in transmissions and attached equipment of HTZ tractors / G. A. Avrunyn / Materials of the 2nd All-Ukrainian scientific and technical conference "Creation, operation and repair of road transport and construction equipment". – Poltava National Technical University named after Yury Kondratyuk, 2018. – P. 79–80.
12. M. A. Tkachuk Generalized parametric description of complex biomechanical systems / M. A. Tkachuk, V. O. Radchenko, Yu. V. Veretelnyk // Bulletin of the KhPI National Technical University. Series: Dynamics and strength of machines . - 2005. - No. 47. - 8 p.
13. Yakushchenko, I. V. Structural characteristics and physico-mechanical properties of multicomponent nitride coatings before and after ion implantation [Text]: dissertation ... candidate. physics and mathematics Science, special: 01.04.07 "Physics of the solid body" / I. V. Yakushchenko; of science director: O. D. Pogrebnyak, Yoshihiko Takeda. – Sumy: Sumy State University, 2018. – 142 p.
14. Bondar O. V. Structure and physical and mechanical properties of multi-component and multi-layered nanostructured coatings: diss. ... Dr. Phys.-Math. Sciences: 01.04.07 "Solid State Physics". – Sumy, 2021. – 429 p.

15. Matochniuk L. E. Reliability and durability of machines and structures // Encyclopedia of Modern Ukraine: encyclopedia [electronic version] / editors: I. M. Dzyuba, A. I. Zhukovsky, M. G. Zheleznyak, etc.; National Academy of Sciences of Ukraine, National Academy of Sciences. Kyiv: Institute of Encyclopedic Research of the National Academy of Sciences of Ukraine, 2020. - Vol. 22. URL: https://esu.com.ua/article-71545
16. D. B. Glushkova. Improvement of the technological process of increasing the durability of the working tool of hydraulic hammers by detonation spraying / D. B. Glushkova, V. A. Bagrov / KHNADU Bulletin: coll. of science pr. – Kharkiv: Khnadu, 2021. – Issue 94. – P. 39.
17. Kashytskyi V.P. Development of protective coatings with increased wear resistance based on epoxy composites modified with organosilicon varnish KO-921: dissertation. on of science stupa Ph.D. technical sciences with special 05.02.01 "Materials Science" / V. P. Kashytskyi / Lutsk. - 2006. - 151 p.
18. Glensdorf P. Thermodynamic theory of structure, stability and fluctuations / P. Glensdorf, I. Prigozhin / Trans. from English - 2003. - 280 p.
19. Popov S. M. Correlation dependences of the structure and properties of alloys when determining wear resistance / S. M. Popov // Materials science and metal processing. – 2003. – No. 2. – P. 42–48.
20. Cherevko O. I. Technological basics of mechanical engineering: training. manual: In 2 hours / O. I. Cherevko, V. M. Mykhaylov, I. V. Babkina, B. V. Lyashenko / Khark. state University of Food and Trade. - Kharkiv, 2005. - Part 1. "Theoretical foundations of mechanical engineering technology." - 83 p.

21. Kholyavko V.V. Physical foundations of strength and destruction [Text]: Synopsis of lectures on the discipline for students of the training direction 6.050403 "Engineering materials science" specialty 8(7).05040303 - "Composite and powder materials, coatings" full-time and part-time forms of education / Compiled by: V.V. Kholyavko. - K.: NTUU "KPI", 2015. - 100 p.
22. Popov S. M. Wear resistance of steels and alloys in conditions of adaptation to external energy-mechanical influences / S. M. Popov, V. S. Popov // Problems of tribology. – 2006. – No. 1. – P. 17–25.
23. V. I. Tikhonovych About mechanisms of wear of metals / V. I. Tikhonovych , V. P. Gavrilyuk // Metal science and metal processing. – 2003. – No. 1. – P. 27–31.
24. Timofeeva L.A., Komarova G.L. Materials science and technology of structural materials: Lecture notes. - Kharkiv: UkrDAZT, 2013. - Part 1. –68 p.
25. E. V. Kurits. Study of the effect of combined strengthening on the stress state of a cylindrical sample, which is a model of the part / E. V. Kurits, A. P. Lyubchenko, G. I. Pashkova / Metallophysics and the latest technologies . – 2000. – Vol. 22. – No. 1. – P. 72–76.
26. Konecna R. Influence of nitriding on the fatigue behavior and fracture micromechanisms of nodular cast iron / R. Konecna, G. Nicoletto, V. Majerova, P. Baicchi // Strength problems. – 2008. – No. 1. – P. 85–88.
27. Kalinovsky S. K. Basic classification of machine-building materials / S. K. Kalinovsky, V. Yu. Kostyria, A. G. Novgorodova // Metallurgy and mining industry . – 2001. – No. 1. – P. 50–57.
28. V. L. Bondarenko New tribotechnical materials - the way to durability of machines and mechanisms / V. L. Bondarenko, A. M. Baranov // Instrumental world . – 2006. – No. 2. – P. 12–15.

29. Yu. V. Ryzhkov Carbonization – an effective method of increasing the reliability of hydraulic drive parts / Yu. V. Ryzhkov, D. B. Glushkova, G. A. Avrunin // Bulletin of the Khnadu: coll. of science pr. – Kharkiv: Khnadu, 2007. – Issue 39. – pp. 126–128.
30. M. O. Vasiliev Peculiarities of the formation of the structural and phase state of the surface layers of D16 foot as a result of ultrasonic impact treatment with an iron hammer in different environments / M. O. Vasiliev, B. M. Mordyuk, S. I. Sydorenko, S. M. Voloshko, A P. Burmak // Metallofiz. Noveishie Tekhnol. - Institute of Metallophysics named after G. V. Kurdyumova, National Academy of Sciences of Ukraine, 2017. – Vol. 39. – No. 1. – P. 49–68.
31. Chufus V. M. Intensification of cooling of friction units of belt brake brakes of drilling winches to increase their efficiency : dissertation. on of science stupa Doctor of Philosophy PhD in Special. 131 "Applied mechanics" / V. M. Chufus // Ivano-Frankivsk. - 2020. - 235 p.
32. Shablya V. T. Mass transfer in metal systems based on Fe, Cu and Al during pulsed and intensive ion irradiation : dissertation. on of science stupa candidate of physical and mathematical sciences with special. 01.04.07 "Solid State Physics" / V.T. Shablya // Sumy. - 2008. - 140 p.
33. Avrunin G. A. To the selection of materials of working and distribution links of volumetric hydraulic machines for the needs of the construction and road industry / G. A. Avrunin, D. B. Glushkova, V. B. Samorodov, E. S. Pelypenko, Yu. V .Ryzhkov, D. M. Shevchenko, I. I. Moroz, A. I. Stepaniuk // Bulletin of the Khnadu: Coll. of science pr. – Kharkiv: Khnadu, 2020. – Issue 91. – pp. 172–186.
34. Hlushkova D. B. Strengthening and restoration of parts of the cylinder-piston group / Hlushkova D. B. – Kh.: 2021. – 200 p.

35. Oliynyk O. K. Increasing the durability of diesel engine parts by saturating the working layer with highly dispersed additives: autoref. thesis for obtaining sciences. candidate degree technical Sciences: specialist 02.05.01 "Materials Science" / O. K. Oliynyk. - Kharkiv, 2008. - 17 p.
36. D. B. Glushkova. Peculiarities of damage of welded joints of steam pipelines made of steel 12X1M1F and 15X1MF / D. B. Glushkova, G. A. Avrunin, Yu. V. Ryzhkov, O. I. Voronkov, A. I. Stepaniuk, A. A. Hnatyuk / Bulletin of the Khnadu: coll. of science pr. – Kharkiv, 2021. – Issue 94. – pp. 85–90.
37. Yu. V. Ryzhkov. Study of the effect of plasma coating on the stability of metal forms / Yu. V. Ryzhkov // Scientific Bulletin of Construction. Vol. No. 55 – Kharkiv, 2009. – P. 131–138.
38. Moschenok V. I. Increasing the operational properties of products: coll. of science works / V. I. Moschenok, D. B. Glushkova, V. P. Tarabanova // Bulletin of the Khnadu: coll. of science pr. – Kharkiv, 2006. – Issue 33. – pp. 54–56.
39. Moschenok V. I. Increasing the tribotechnical characteristics of gear friction: coll. scientific works / V. I. Moschenok, O. P. Lyubchenko, D. B. Glushkova, O. K. Oliynyk // Bulletin of the Khnadu: coll. of science pr. – Kharkiv, 2007. – Issue 33. – pp. 64–66.
40. D. B. Glushkova Application of the theory of mathematical planning in the selection of optimal modes of surface strengthening / D. B. Glushkova, Yu. V. Ryzhkov, V. A. Bagrov, A. I. Stepaniuk / Automotive transport : coll. of science pr. – Kharkiv, Khnadu, 2020. – Issue 46.
41. D. B. Glushkova Determination of optimal friction pairs using the thermoelectric motive force method of non-destructive control / D. B.

Glushkova, V. A. Bagrov // The 13 th International scientific and practical conference "Modern directions of scientific research development" (June 15–17, 2022) BoScience Publisher, Chicago, USA. 2022 – pp. 268–277.

42. S. M. Visokos Basics of materials science: a study guide / S. M. Vysokos, Yu. Yu. Glushko, M. V. Pekhovka, V. O. Sashko, T. M. Tereshchenko. - 2018. - 136 p.
43. Yu. V. Ryzhkov. Increasing the wear resistance of rubbing surfaces / S. M. Dub, A. N. Kovalchuk, Yu. V. Ryzhkov, D. B. Glushkova, V. P. Tarabanova // Bulletin of the Khnadu: coll. of science pr. – Kharkiv, 2009. – Issue 46. – P.39–42.
44. Bolshakov V. I. Stages of identification of multi-parameter technologies and ways of their implementation / V. I. Bolshakov, V. M. Volchuk, Yu.I. Dubrov // Bulletin of the National Academy of Sciences of Ukraine.– 2013. –No. 8. –P. 66 –72.
45. Hlushkova D. Studying the properties of steel for sidewalls of chute conveyors / Hlushkova D., Kalinin V., Stepanyuk A., Hnatyuk A., Serzhenko I. // International Science Group. – Boston : Primedia eLaunch, 2021. 758. Available at: DOI- 10.46299/ISG.2021.MONO.TECH.II – P. 560-564. (collective monograph).
46. Glushkova D. B., Bagrov V. A. Application of modern technologies to increase the wear resistance of volumetric hydraulic drive parts / Theoretical and practical aspects of modern scientific research : collective monograph, Sherman Oaks, California : GS Publishing Services, 2022. - P. 171 -178 (collective monograph).
47. Scientific and technological basis of improving the tribological characteristics of parts of mechatronic systems / Glushkova D. B., Ryzhkov Yu. V., Baidala. - Kharkiv, 2022. - 119 p.

48. Glushkova D. B. Increasing the reliability of working bodies of hydroficated special purpose machines :monograph. - Dnipro :Zhurfond, 2023. - 258 p.
49. Gluskova D., Volchuk V. Determination of the optimal parameters of laser boriding to improve the wear resistance of piston rings // New materials and technologies in metallurgy and mechanical engineering No. 2, 2022. P. 29-32.
50. Glushkova D. B., Kalinina N. E., Demchenko S. V., Nosova T. V. Increasing the corrosion resistance of welded joints ′as a result of heat treatment // Metallovedenie y thermal treatment of metals. - 2022. - #1. - P. 21-28.
51. Justification of the choice of scandium for microalloying of high-strength aluminum alloys / N. E. Kalinina, D. B. Glushkova, N. I. Tsokur, T. V. Nosova, V. A. Bagrov, S.V. Demchenko // Aviation and space technology and technology, 2022, No. 4 special issue 2 (182). P. 114-118.
52. Bagrov V. A., Glushkova D. B. Formation of the structure and phase composition of wear-resistant steels doped with titanium // KHNADU Herald, Vol. 97, 2022. - C. 30-33.
53. Bagrov V. A., Glushkova D. B. Properties of wear-resistant nickel-free secondary hardening steels for surfacing dies of hot metal processing // KHNADU Herald, Vol. 97, 2022. - C. 34-37.
54. Structure and properties of nickel-based gas plasma powder coatings / D. B. Glushkova, V. A. Bagrov, S. V. Demchenko, V. M. Volchuk, O. V. Kalinin, N. E. Kalinin // KHNADU Herald, Vol. 97, 2022. - C. 74-81.
55. Methods of obtaining a dispersed structure and increasing the strength of silicon-manganese steels / Bolshakov V.I., Kalinin O.V., Glushkova

D.B., Tokhtar G.I., Bagrov V.A., Hnatyuk A.A.// Visnyk I'm looking for - 2021. - No. 94. - P. 7-12.

56. Volchuk, V. M. Model for evaluating the hardness of cast iron rolls SPKHN-43 and SSKHNF-47 / V. M. Volchuk // Metal science and heat treatment of metals. – 2019. – No. 4. – P. 22–35. URL: https://doi.org/10.30838/J.PMHTM.2413.241219.22.597
57. D. B. Hlushkova. Improvement of the technological process of increasing the durability of the working tool of hydraulic hammers by detonation spraying/ D. B. Glushkova, V. A. Bagrov. // KHNADU Herald.-2021. - #94. - P. 39-46.
58. Increasing the wear resistance of units of a volumetric hydraulic drive // Glushkova D. B., Avrunin G. A., Ryzhkov Yu. V., Voronkov O. I., Stepaniuk A. I., Hnatyuk A. A. // Bulletin of the Khnadu.- 2021.-№94.- P. 80-84.
59. Influence of temperature of thermal processing on intercrystalline corrosion resistance of welding joints / Kalinina NE, Hlushkova D. B., Dzhur YO, Khodyrev S. Ya., Kalinin VT // Jornal of chemistry and technologies 2020.-28(1).-p. 34-41.
60. Spesial features of the phase composition and structure of aluminum alloys modified by refractory nanocompositions / Kalinina N. E., Nlushkova D. B., Voronkov AI, Sanin AF, Kalinin VT, Nosova T. V., Bondarenko O. V. // Functional materials. - 2020. - Vol. 27. - No. 3 (2020). - P. 508-512.
61. V. I. Bol'shakov, VM Volchuk. Materials science aspects of using wavelet-multifractal approach to an evaluation of structure and properties of low-carbon low-alloy steels // Metallofiz. Noveishie Tekhnol. 2011, vol. 33, No. 3, p. 347.

62. Volchuk VM, Uzlov OV, Puchikov OV, Ivantsov SV Fractals Theory Application for Evaluation of Influence of Non Metallic inclusions on Mechanical Properties of S355J2 Steel //IOP Conference Series: Materials Science and Engineering. – IOP Publishing, 2021. – T. 1021. – No. 1. – P. 012053. URL: https://iopscience.iop.org/article/10.1088/1757-899X/1021/1/012053/meta
63. Fractals and properties of materials: monograph / [V. Bolshakov, V. Volchuk, Yu. Dubrov]. - Saarbrucken : Lambert Academic Publishing, 2016. - 140 p.
64. Volchuk VM, Uzlov OV, Puchikov OV, Zotov DS, Sokoliuk V. I. Fractal model of mechanical properties evaluation of C-Mn-Al-Ti-N steel with acicular ferrite structure for railway freight cars. //AIP Conference Proceedings. – AIP Publishing LLC, 2021. – Vol. 2389. – No. 1. – P. 080002. URL: https://doi.org/10.1063/5.0063496
65. Vakhrusheva VS, Volchuk VM, Hruzin NV, Tiutiriev IA Fractal model of estimating quality of cold worked fuel cladding tubes //Voprosy Atomnoj Nauki i Tekhniki. – 2021. –Vol. 135. – No. 5. – P. 57-63. URL: https://doi.org/10.46813/2021-135-057
66. Volchuk VM, Uzlov OV, Puchikov OV, Ivantsov SV, Tiutiriev I. A. Fractal model of structure-properties effect of low carbon steel //IOP Conference Series: Materials Science and Engineering. - IOP Publishing, 2021. - T. 1100. - No. 1. – P. 012034. URL: https://iopscience.iop.org/article/10.1088/1757-899X/1100/1/012034/meta#references
67. Declaratory patent for an invention. 51439A of Ukraine, G06K9/00. The method of determining the fractal dimension of an image /V. I.

Bolshakov, Yu. I. Dubrov, F. V. Kriulin, V. M. Volchuk. –Register 02.04.02: Publ. 15.11.02, Bul. No. 11. –4 p.

68. Bausk EA, Volchuk VM, Uzlov OV Remaining Service Life Evaluation of Nuclear Power Plants Construction Steel Elements //Journal of Physics: Conference Series. - IOP Publishing, 2021. - Vol. 1926. - No. 1. – P. 012050. URL: https://doi.org/10.1088/1742-6596/1926/1/012050
69. Kroviakov S., Volchuk V., Zavoloka M. Fractal Model of the Influence of Expanded Clay Concrete Macrostructure on its Strength. *Key Engineering Materials* . –2020. –Vol. 864. –Pp. 43–52. URL: https://doi.org/10.4028/www.scientific.net/kem.864.43
70. Volchuk V. Method of material quality estimation with usage of multifractal formalism / V. Volchuk, I. Klymenko, S. Kroviakov, M. Orešković // Tehnički glasnik - Technical Journal. –2018. –Vol. 12. –No. 2. –P. 93 –97. URL: https://doi.org/10.31803/tg-20180302115027
71. Hlushkova D. B. Mathematical modeling of the structure and properties of low-carbon alloys / D. B. Hlushkova, V. M. Volchuk // Functional Materials. – 2024 - No. 31(3). - Year 391–395.
72. Hlushkova DB A study on the influence of composition and fractal structure of the Fe-Cr-Ni alloy on its properties / Hlushkova DB, Volchuk VM // Functional Material - 2024. - No. 31(2) - Pp.173–177.
73. Bolshakov VI Evaluation of High Strength Steel Fatigue / V. I. Bolshakov, VM Volchuk, OF Parhomenko // UDCS'19: Fourth International Iron and Steel Symposium, April 4-6, 2019, Karabuk University, Karabuk, Turkey . –2019. –Vol. 4. –Pr. 415 –417. URL: https://drive.google.com/open?id=1jfWwEhSuRl-3bGcv-dG7CzYnmMh7KcVT

74. Hlushkova DB, VM Volchuk, Pavlo Polyansky, VA Saenko and A. A. Efimenko. Fractal modeling of the mechanical properties of the metal surface after ion-plasma chrome plating. // Functional Materials , 2023, 30(2), pp. 275–281 .
75. Volchuk V. M. Evaluation of the effect of carbon on the structure of rolls / V. M. Volchuk, M. A. Kotov, A. S. Shtandenko // Metal science and thermal treatment of metals. – 2021. – No. 4. – P. 33–44. URL: https://doi.org/10.30838/J.PMHTM.2413.281221.33.822
76. Kroviakov S. Search for Ranking Approaches of Expanded Clay Concrete Quality Criteria / S. Kroviakov, V. Volchuk, M. Zavoloka, V. Kryzhanovskyi. In: *Materials Science Forum* . Trans Tech Publications Ltd. –2019.– Vol. 968.– P. 20-25. URL: https://doi.org/10.4028/www.scientific.net/MSF.968.20
77. Kalinina NE, Glushkova DB, Voronkov AI, Kalinin V.T. Influence of nanomodification on structure formation of multicomponent nickel alloys // Fu 1. Corrosion resistance of reinforced layers of 15X11MF steel steam turbine blades / Hlushkova D., Bagrov V., Stepaniuk A. , Hrinchenko ED, Hnatiuk AA, Kalinina N.E., Kalinin VT // VANT. - 2021. No. 2(132). - P. 136-141.
78. The method of assessing the quality and properties of products / Vol. S. Skoblo, S. O. Burtsev, O. Yu. Klochko [and others] // Patent of Ukraine UA No. 71815, IPC (2012.01) C21D5/00. - No. u 201200948; statement 30.01.2012; published 25.07.2012, Bull. No. 14. - 6 p.
79. The method of heat treatment of rolls made of high-alloy cast iron . / T. S. Skoblo, O. Yu. Klochko, V. Ya. Pogorelov [and others] // Patent of Ukraine UA No. 65602, IPC (2011.01) C21D5/00. - No. u2011006215; statement 18.05.2011; published 12.12.2011, Bull. No. 23. - 10 s.

80. Increasing fretting resistance of flexible element pack for rotary machine flexible machine flexible coupling. Part 1. Analysis of the reasons affecting fretting resistance of flexible elements fror expansion coupling / Tarelnyk V., Hlushkova D., Martsynkovskyy V., Dumanchuk M., Antoszewski B., Kundera Cz, Konopiianchenko Ie, Tarelnik, N., Hudkov S ., Zahorulko A. // Jornal of Physics: Conference Series. - 2021. - 1741. - 11 p.
81. Structural and phase composition features of titanium and chromium nitride coatings obtained by ion-plasma deposition / D. Hlushkova, A. Voronkov, N. Kalinina, V. Kalinin, L. Polonskyi, A. Stepaniuk // Functional Materials, 27, No. 4 (2020). - P. 710-715.
82. Materials are metal. Determination of hardness according to Brinell. Part 1 [Text] : DSTU ISO 6506-1:2007 . Test method (ISO 6506-1:2005, IDT). –Effective from 2009-01-01.– K.: Derzhspozhivstandard of Ukraine, 2010. –IV, 12 c. : tab. – (National Standard of Ukraine).
83. Metrology. State verification scheme for means of measuring the hardness of Shore D [Text]: DSTU. GOST 8.516:2003 / form. Sikorska; - Officer. rank. in Ukraine from 01.07.2004. - K.: Derzhspozhivstandard of Ukraine, 2004. - III, III, 3 p. – (National Standard of Ukraine).
84. Non-destructive testing . Ultrasonic control . Ch3. [Text]: DSTU EN 583-3-2005; Method of passage. (EN 583-1:1998, IDT) / trans. from English and science and technology ed. V. Troitsky [and others]; - Chin. from 01.01.2008. - K.: State Committee of Ukraine on Technical Regulation and Consumer Policy, 2007. - IV, 6 p. – (National Standard of Ukraine).
85. Indestructible CONTROL . CONTROL magnetoporoshkov y. Ch2. [Text]: DSTU EN ISO 9934-2:2005; Means of control (EN ISO 9934-

2:2002, IDT); . - Chin. dated 2008-01-01.- K.: Derzhspozhivstandard of Ukraine, 2007. - V, 16 p.- (National Standard of Ukraine).

86. Metrology. [Text] ; DSTU 5017:2008 ; State verification scheme for measuring instruments parameters roughness Ra, Rmax and Rz in the range from 0.025 μm to 1600 μm; - Chin from 2009-01-01. - K.: Derzhspozhivstandard of Ukraine, 2009. - III, 5 p. - (National Standard of Ukraine) .
87. TU U27.1-26524137-1291 :2007. Cast iron rolls for hot rolling of metals. – To replace TU U27.1-00190319-1291 -2002; Rank. from 01.02.2008. - Kh., 2007. - 29 p.
88. Use of detonation sputtering to increase the durability of hydraulic hammer critical parts / DB Hlushkova, IH Kirichenko, V. A. Bahrov, N. Ye. Kalinina, TV Nosova // PAST. 2021. No. 5 (135). pp. 139-145.
89. Transformation of structure and properties of structural steel during nanomodification and strengthening treatment / VI Bolshakov, A. V. Kalinin, D. B. Hlushkova, Y. V. Ryzhkov, V. A. Bagrov // Functional materials. 28, No. 3, 2021. p. 486-491.
90. V. I. Bolshakov, O. I. Kalinin, N. E. Kalinina, D. B. Hlushkova, O. I. Voronkov, YV Ryzhkov, AI Stepanyuk. Increasing the corrosion resistance of welded joints of heat-resistant nickel alloy with steel // VANT. 2022.-№1(37).- P. 195-198.
91. D. B. Hlushkova, OI Voronkov, YV Ryzhkov, NE Kalinin, T. V. Nosova. Pecularities of the formation of a hardened layer during laser boring of piston rings // VANT. 2022.-№1(37).- P. 199-201.
92. V. S. Vahrusheva, DB Hlushkova, VM Volchuk, TV Nosova, S. I. Mamhur, NI Tsokur, V. A. Bagrov, S. V. Demchenko, Yu. V. Ryzhkov, V. O. Scrypnikov. Increasing the corrosion resistance

of heat-resistant alloys for parts of power equipment // VANT. 2022. No. 4(140). - P. 137-140.

93. D. B. Hlushkova, V. A. Bagrov, S. V. Demchenko, V. M. Volchuk, O. V. Kalinin, N. E. Kalinina. Structure and properties of powder gas-plasma coatings based on nickel // VANT. 2022. No 4(140). - P. 125-130.

94. Bolshakov Vad. I. On the incompleteness of formal axiomatics in problems of identification of metal structure / Vad. I. Bolshakov, V. AND. Bolshakov, Yu.I. Dubrov // Bulletin of the National Academy of Sciences of Ukraine. –2014. –No. 4. - C. 55-59.

95. Bolshakov Vad. I. Partial compensation of the incompleteness of formal axiomatics in the identification of the metal structure / Vad. AND. Bolshakov, V. AND. Bolshakov, V. M. Volchuk, Yu. I. Dubrov // Bulletin of the National Academy of Sciences of Ukraine.– 2014.– No. 12. - pp. 45-48.

96. V. I. Bolshakov Scientific work "The method of forecasting and controlling the quality characteristics of rolled rolls in their production technology" / V. I. Bolshakov, V. M. Volchuk, Yu. I. Dubrov / Certificate of Ukrainian copyright registration for the work No. 54703 from 12.05.2014

97. D. B. Glushkova Research on the structure and phase composition of ion-plasma coatings / D. B. Glushkova, O. I. Voronkov, A. I. Stepaniuk, S. V. Demchenko, N. E. Kalinin, V. T. Kalinin / Bulletin of the Khnadu: coll. of science pr. – Kharkiv, 2020. – Issue 91. – pp. 122–129.

98. Development of a system of targeted selection of the most effective technology for improving the quality of babbit coatings of sliding bearings. Part 2. Mathematical model of wear of babbitt coatings. Criteria for choosing a technology for applying babbit coatings / V. B.

Tarelnyk, O. P. Gaponova, E. V. Konoplyanchenko, N. V. Tarelnyk, M. Yu. Dumanchuk, V. O. Pirogov, T. P. Voloshko, D B. Glushkova// Metallophysics and Advanced Technologies Metallophysics and the latest technologies . 2022, vol. 44, No. 12, pp. 1643–1659.

99. Influence of structure and phase composition on wear resistance of sparingly alloyed alloys/ D. B. Hlushkova, V. A. Bagrov, V. M. Volchuk, U. A. Murzakhmetova// Functional Materials, 30, No. 1 (2023), pp. 74-78. https://doi.org/10.15407/fm30.01.74

100. Study of wear of the building-up zone of martensite-austenitic and secondary hardening steels of the Cr-Mn-Ti system / D. B. Hlushkova, V. A. Bagrov, V. A. Saenko, V. M. Volchuk, A. V. Kalinin, N. E. Kalinina // Issues of atomic science and technology 2023, No. 2 (144). - pp. 105-109.

101. Study of nanomodification of nickel alloy GS3 with titanium carbide / D. B. Hlushkova, A. V. Kalinin, N. E. Kalinina, V. M. Volchuk, VA Saenko, AA Efimenko // Issues of atomic science and technology 2023, No. 2 (144). - p. 126-129.

102. Gödel K. Über formal unentscheidbare Sätze der Principia Mathematica und verwandter Systeme I . / K. Gödel // Monatshefte für Mathematik und Physik. –1931. –Vol. 38. –No. 1. –P. 173 –198.

103. Garashchenko Y. Fractal Analysis of Structural and Phase Changes in the Metal of Welded Steam Pipe Joints / Y. Garashchenko, A. Glushko, O. Kobets and O. Harashchenko // Design, Simulation, Manufacturing: The Innovation Exchange. – Springer, Cham. - 2021. - P. 31-40. URL: https://doi.org/10.1007/978-3-030-77719-7_4

104. Zhuravel' IM, Michuda, L. Z. Application of the Mandelbrot–Zipf Law for the Quantitative Evaluation of the Average Size of Steel Grains

/ I. M. Zhuravel', L. Z. Michuda // Materials Science –2021. –Vol. 57. –P. 80−85. URL: https://doi.org/10.1007/s11003-021-00517-2

105. Torop VM On the Causes of Fractures of Reinforcing Ropes of the Protective Shells of Power-Generating Units of Nuclear Power Plants / VM Torop, MD Rabkina, OO Shtofel, V. V. Usov, N. M. Shkatulyak, OS Savchuk //Materials Science. - 2018. - Vol. 54. - No. 2. - P. 240-249. URL: https://doi.org/10.1007/s11003-018-0179-y

106. Volchuk VM, Kotov MA Fractal express methods evaluation of a breaking stress of concrete //Journal of Physics: Conference Series. - IOP Publishing, 2021. - Vol. 1926. - No. 1. – P. 012023. URL: https://doi.org/10.1088/1742-6596/1926/1/012023

107. Quintana-Rodríguez JA, Doyle JF, Carrión-Viramontes F. J., Samayoa-Ochoa D. and López-López JA Material characterization for dynamic simulation of non-homogeneous structural members // Key Engineering Materials. –2010. –Vol. 449. –P. 46–53. URL: https://doi.org/10.4028/www.scientific.net/KEM.449.46

108. Hongchao X. et al. The influence of surfactant on pore fractal characteristics of composite acidized coal // Fuel. - 2019. - Vol. 253. - P. 741-753. URL: https://doi.org/10.1016/j.fuel.2019.05.073

109. Ţălu Ş., Bramowicz M., Kulesza S., Dalouji V., Solaymani S. and Valedbagi S. Fractal features of carbon–nickel composite thin films // Microscopy Research and Technique. - 2016. - Vol. 79. - no. 12. – P. 1208-1213. URL: https://doi.org/10.1002/jemt.22779

110. A. S. Kobets Abrasive and fatigue wear of rubber lining in the context of fractal analysis / A. S. Kobets, V. I. Dyrda, Ye. IN. Kalgankov, I. M. Tsanidi, O. A. Chernii // Geotechnical mechanics. –2019. –Issue 144. –P.103-110.

111. Nakano T. and Miyazaki J. Surface Fractal Dimensionality and Hygroscopicity for Heated Wood // Wood research and technology. –2003. –Vol. 57, no. 3 –P. 289-294. URL: https://doi.org/10.1515/HF.2003.043

112. Dubrov Yu. Ways of regularization of materials science ill-posed problems / Yu. Dubrov, V. Volchuk // Metallurgy and heat treatment of metals. – 2019. – No. 4. – P. 47 – 50. URL : https://doi.org/10.30838/J.PMHTM.2413.241219.47.600

113. Krovyakov S.O. The search for approaches to the ranking of expanded clay concrete quality criteria / S. O. Krovyakov, M. V. Zavoloka, V. O. Kryzhanovskyi, V. M. Volchuk // Actual problems of engineering mechanics: collection of theses VI International. science and practice conf. –Odessa: ODABA, 2019. –P. 166-168. URL : http://mx.ogasa.org.ua/handle/123456789/8254

114. Samayoa D. Fractal model equation for spontaneous imbibition / D. Samayoa, LA Ochoa-Ontiveros, L. Damián-Adame, E. Reyes de Luna, L. Álvarez-Romero, G. Romero-Paredes // *Revista mexicana de física* . –2020. –Vol. 66, no. 3. –P. 283-290. URL: https://doi.org/10.31349/revmexfis.66.283

115. D. B. Hlushkova, I. H. Kyrychenko, V. A. Bahrov, N. Yes. Kalinina, T. V. Nosova. Use of detonation sputtering to increase the durability of hydraulic hammer critical parts // *Problems of Atomic Science and Technology* . 2021, No. 5(135), p. 139-145 .

116. D. B. Hlushkova, V. A. Bahrov, O. D. Hrinchenko, A. A. Hnatiuk, N. E. Kalinina, V. T. Kalinin. Corrosion Resistance of Reinforced Layers of 15X11MF Steel Steam Turbine Blades // *Problems of Atomic Science and Technology* . 2021, No. 2(132), p. 136-141 .

117. C. Paul, P. Ganesh, S. Mishra. Investigating laser rapid manufacturing for Inconel-625 components // *Optics and Laser Technology.* 2007, N 39(4), p. 800-805.

118. G. Ram, A. Reddy, K. Rao. Microstructure and tensile properties of Inconel 718 pulsed Nd-YAG laser welds // *Journal of Materials Processing Technology.* 2005, N 167(1), p. 73-82.

119. Sidashenko OI, Luzan S. (2017). Study of the wear resistance of restorative coatings of the Ni-Cr-B-Si system, modified with mechano-activated SVS-materials. Design, production and operation of agricultural machines: general state. between science and technology coll. Kropyvnytskyi, vol. 47, part 1, pp. 221–229.

120. Paul C., Ganesh P., Mishra S. (2007). Investigating laser rapid manufacturing for Inconel-625 components. Optics and Laser Technology, no. 39 (4), pp. 800–805.

121. Hlushkova DB, Bahrov VA, Hrinchenko OD, Hnatiuk A. A., Kalinina N. E., Kalinin V. T. // Bulletin of the Khnadu, vol. 100, 2023 (2021). Corrosion Resistance of Reinforced Layers of 15X11MF Steel Steam Turbine Blades. Problems of Atomic Science and Technology, no. 2 (132), pp. 136–141.

122. Trembach BO, Sukov MG, Vynar VA, Trembach I. O., Subbotina V. V., Rebrov O. Yu., Rebrova OM, Zakiev VI (2022). Effect of incomplete replacement of Cr for Cu in the deposit-ed alloy of Fe–C–Cr–B–Ti alloying system with a medium boron content (0.5% wt.) on its corrosion resistance. Metallofiz. Noveishie Tekhnol, no. 4 (44), pp. 493–513.

123. Yanchuk V., Kruhlov I., Zakiev V., Lozova A., Trembach B., Orlov A., Voloshko S. (2022). Thermal and ion treatment effect on nanoscale

thin films scratch resistance. Metallofiz. Noveishie Tekhnol, no. 10 (44), pp. 1275–1292.

124. Murashov AP, Vigilyanska NV, Gryshchenko OP, Yushchenko AO, Gorban VF (2022). Study of mechanical properties and wear resistance of plasma coatings based on Fe-Al in-termetalide. Bulletin of the Vinnytsia Polytechnic Institute, no. 4, pp. 91–96.

125. Volchuk V., Kroviakov S., Kryzhanovskyi V. (2004). Strength assessment of lightweight concrete considering metric variance of the structural elements. Revista Română de Materiale / Romanian Journal of Materials, no. 2 (52), pp. 185–193

126. Mandelbrot BB, Evertsz CJ, Gutzwiller MC (2004). Fractals and chaos: the Mandelbrot set and beyond. New York: Springer, 2004, 308 p.

127. Baqir M.A. et al. (2021). ZrN fractal-graphene-based metamaterial absorber in the visible and near-IR regimes. Optik, 237, p. 166769.

128. Tieng S., Brinza O. et al. (2012). Nucleation and fractal growth of zirconium oxo-alkoxy nanoparticles at the induction stage of sol-gel process. Journal of Solgel Science and Technology, no. 1 (64), pp. 145–148.

129. Bolshakov VI, Glushkova DB (2015). Investigation of peculiarities of piston rings laser berat-ing. Bulletin of Prydniprovska State Academy of Civil Engineering and Architecture, no. 11, pp. 27–31.

130. Holyakevych A. A., Orlov LM, Pokhmur'ka HV, Student M. M. Chervins'ka N.R., Khyl'ko OV (2015). Influence of the Phase Composition of the Layers Deposited on the Rods of Hydraulic Cylinders on Their Local Corrosion. Materials Science, no. 5(50), pp. 740–747.

131. Raoufi D., Fallah HR, Kiasatpour A., Roza-tian ASH (2008). Multifractal analysis of ITO thin films prepared by electron beam deposition method. Applied Surface Science, no. 7 (254), pp. 2168–2173.
132. Rényi A. (1970). Probability Theory. Amsterdam: North-Holland, pp. 301–367.
133. Hausdorff F. (1919). Dimension und äusseres Mass. Math. Ann., no. 79, pp. 157–179.